Mitochondrial Biology: RNA Import and Xenomitochondrial Compensatory Mechanisms

by

Matthew V. Cannon

A dissertation submitted to the Graduate Faculty of
Auburn University
in partial fulfillment of the
requirements for the Degree of
Doctor of Philosophy

Auburn, Alabama
May 9, 2011

Approved by

Carl A. Pinkert, Chair, Professor of Pathobiology
Frank F. Bartol, Alumni Professor of Anatomy, Physiology and Pharmacology
R. Curtis Bird, Professor of Pathobiology
Paul A. Cobine, Assistant Professor of Biological Sciences
Michael H. Irwin, Associate Research Professor of Pathobiology
Jay E. Reeder, Assistant Professor of Urology, SUNY Upstate

Abstract

Deficiencies or alterations in mitochondrial function can cause or exacerbate many human diseases, including metabolic and developmental disorders. The first experiments described herein were conducted to study compensatory mechanisms for mitochondrial inefficiencies. Xenomitochondrial mice, harboring evolutionarily divergent *Mus terricolor* mitochondrial DNA (mtDNA) on a *Mus musculus domesticus* nuclear background, were characterized phenotypically. Lack of *in vivo* phenotype indicative of mitochondrial dysfunction in xenomitochondrial mice contrasted mitochondrial dysfunction observed in *in vitro* xenomitochondrial cybrid studies. Genetic studies revealed that the only genes involved in energy production with expression changes in xenomitochondrial mice were encoded by the mtDNA. Results illustrate that compensatory mechanisms for mild mitochondrial inefficiencies alter mtDNA gene expression without altering expression patterns of nuclear encoded genes involved in mitochondrial energy production. Understanding these mechanisms will facilitate development of therapeutic interventions for mitochondrial disorders. Experiments described subsequent to xenomitochondrial characterization explored mechanisms whereby specific RNAs are imported into mitochondria. Characterization of mitochondrial RNA import mechanisms may allow development of gene therapy to treat devastating mitochondrial diseases. RNA affinity purification identified proteins that interact selectively with imported RNAs from both cellular and mitochondrial lysates. RNA immunoprecipitation (RIP) did not confirm protein:RNA interactions due to large variability in results. The cytoplasmic roles of proteins identified by RNA affinity purification studies shed light on specific mechanisms of mitochondrial RNA import. Additionally, sequencing of

mitochondrial RNA revealed several novel RNAs associated with mitochondria. These RNAs are uncharacterized and future studies will reveal the biological significance of their association with mitochondria.

Acknowledgments

I gratefully acknowledge Drs. Frank F. Bartol, R. Curtis Bird, D. Mark Carpenter, Paul A. Cobine, Michael H. Irwin, Jay E. Reeder, and Jacek Wower for insightful comments, discussion and assistance and Dr. David Dunn, Dr. Kodeeswaran Parameshwaran and Dr. Matthew Schoell for helpful discussion. This work was supported in part by grants from NIH, NSF, AAES and Auburn University.

Dedication

I dedicate this work to my family.

To my grandfather, for inspiring me to work in science.

To my father for teaching me how to think and encouraging me to strive for my best.

To my mother for pushing me to work hard and for sacrifices made during my childhood.

To my stepmother for looking after me and taking such great care of me.

And to the rest of my family for their love, encouragement and support.

Table of Contents

List of Tables

List of Figures

List of Abbreviations

129S6 – 129S6/SvEvTac

ATP – Adenosine-5'-triphosphate

BN-PAGE – blue native polyacrylamide gel electrophoresis

CAP^R – Chloramphenicol resistant

CS – citrate synthase

DDM – dodecyl maltoside

ETC – electron transport chain

FKPM – Isoform-level relative abundance in fragments per kilobase of exon model per million mapped fragments

H1 RNA – RNase P RNA subunit

IACUC – Institutional Animal Care and Use Committee

IGV – Integrative Genomics Viewer

LC-MS/MS – liquid chromatography tandem mass spectroscopy

LF – left fore paw

LH – left hind paw

mitoplast – mitochondria lacking outer membrane

MPTP – 1-methyl-4-phenyl-1,2,3,6-tetrahydropyridine

mtDNA – mitochondrial DNA

O_H – mtDNA heavy strand origin of replication

O_L – mtDNA light strand origin of replication

OLAW – Office for Laboratory Animal Welfare

SDS-PAGE – sodium dodecyl sulfate polyacrylamide gel electrophoresis

qPCR – quantitative PCR

qRT-PCR – quantitative reverse transcriptase PCR

RF – right fore paw

RH – right hind paw

RIC – RNA import complex

RIP – RNA immunoprecipitation

RT+ – Reverse transcriptase positive

RT- – Reverse transcriptase negative

Th RNA – RNase MRP RNA subunit

TIM – translocase of the inner mitochondrial membrane

TOM – translocase of the outer mitochondrial membrane

VDAC – voltage-dependant anion channel

VRC – vanadyl ribonucleoside complexes

Foreword

Pole, Gait, Rota-Rod, Beam and Wire Hang analyses were conducted by Dr. David Dunn and Jeffrey DeFoor. Dr. David Dunn performed oxygen consumption measurements. Matthew Cannon was assisted with lactate measurement, exercise testing and mouse husbandry by Carolyn Cassar, Dr. James Corsetti, Katie Donegan, Dr. David Dunn, Dr. Rob Howell, Dr. Chris Ingraham, Dr. Michael Irwin, Chad Lerner, Jamie Littleton, Dr. Michael Massett and Dr. Carl Pinkert. Axel Dessal performed the first Barnes maze experiment, with subsequent experiments performed by Matthew Cannon. Mass spectroscopy analyses were performed at facilities at both the University of Alabama at Birmingham and the University of Rochester. Following preparation of RNA by Matthew Cannon; Drs. Andrew Brooks and Qi Wang performed microarray analyses at Rutgers University EOHSI Binomics Research and Technology Center. Dr. Shawn Levy and Braden Boone performed RNA sequencing at the HudsonAlpha Institute for Biotechnology's Genomic Services Lab on samples prepared by Matthew Cannon. Braden Boone gave instruction on basics of RNA sequence data analysis. Dr. Mark Carpenter provided statistical analysis assistance on RNA immunoprecipitation data. The Auburn University College of Veterinary Medicine Clinical Pathology Lab performed cytological analysis following blood isolation by Matthew Cannon.

Chapter 1 – Literature review

Section 1 – Mitochondrial biology

The second law of thermodynamics states that in a closed system, entropy causes a tendency towards disorder. The battle against entropy is a major reason that non-photosynthetic organisms require energy intake in the form of food. This energy supports growth and maintenance of homeostasis within the organism. Organismal conversion of nutrients into amino acids, lipids, nucleotides and high-energy adenine triphosphate (ATP) molecules involves a highly complex system of enzymes and transport complexes.

The manner in which most organisms form the high-energy molecules required to maintain the organization inherent to life is through the breakdown of glucose. Glycolysis converts glucose into two molecules of pyruvate and produces ATP. Pyruvate molecules formed through glycolysis can be shuttled into the Krebs cycle or converted into lactic acid to produce energy. In the Krebs cycle, the enzyme pyruvate dehydrogenase converts pyruvate into acetyl-CoA, which is joined with a four-carbon molecule, oxaloacetate, forming citrate. Citrate is broken down into oxaloacetate, producing NADH and reducing FAD to $FADH_2$. The electron transport chain (ETC) uses energy stored in NADH and $FADH_2$ to shuttle electrons through ETC complexes I-IV, pumping protons out of the mitochondrial matrix to create a proton gradient across the inner mitochondrial membrane. This gradient is then used by complex V of the ETC to convert ADP into ATP (Wallace, 2007).

Inhibition or inefficiencies in energy production can have highly deleterious effects on cellular and organismal homeostasis. Many diseases result from mitochondrial dysfunction and these diseases lead to phenotypes ranging from mild lactic acidosis to blindness in adults, or even infant mortality. These diseases are associated with mutations in either nuclear or mitochondrial

genomes and studies have revealed many distinct mutations. For mutations in mitochondrial DNA (mtDNA), the severity of the disease varies with the level of heteroplasmy (ratio of mutated to total mtDNA molecules.) Treatment options for mitochondrial disorders are limited, generally involving alterations in patient diet, use of dietary supplements and avoidance of conditions leading to metabolic stress (Debray et al., 2008; DiMauro and Schon, 2001; Thorburn and Dahl, 2001; Wallace, 1999).

The mammalian mitochondrial genome is a circular double stranded DNA molecule roughly 16.5 kilobases in length. The gene content and organization is highly conserved among mammals. The mtDNA is present in hundreds to hundreds of thousands of copies per cell and encodes 13 proteins, 22 tRNAs and two ribosomal RNAs. The tRNAs and rRNAs function in translation within the mitochondria to produce the 13 protein subunits of the ETC encoded by the mtDNA. Production and processing of mitochondrial RNAs occurs by a process distinct from nuclear RNA processing. The control region of mtDNA, termed the D-loop, encodes three promoters (two heavy strand promoters and one light strand promoter) that signal initiation of transcription of large polycistronic RNAs in both directions from the promoter. The polycistronic RNAs are processed into individual tRNAs, rRNAs and mRNAs (Fernandez-Silva et al., 2003; Taanman, 1999; Wallace, 2007).

mtDNA replication is initiated in the D-loop region at the heavy strand origin of replication (O_H) and polymerization by DNA polymerase γ proceeds along the circular DNA molecule. DNA production is single stranded until replication machinery passes the light strand origin of replication (O_L), which is located outside the D-loop region between the coding regions of mt-CoI and mt-Nd2. After the replication machinery passes the O_L, RNase MRP ribonucleoprotein complex produces a short RNA primer at the O_L. This allows DNA replication in the opposite direction, producing double stranded DNA. When both strands are

complete,DNA replaces the RNA primer and ligation of the ends of both heavy and light strands completes mtDNA replication (Fernandez-Silva et al., 2003; Taanman, 1999).

Section 2 – Animal models of mitochondrial disease

History of xenomitochondrial mice

Animal models of mitochondrial dysfunction would enable studies designed to explain how specific mtDNA mutations and polymorphisms cause and/or affect the pathological progression and severity of metabolic disorders and related disease. Unfortunately, several factors prevent direct engineering of mtDNA in live mitochondria or cells needed to develop mammalian animal models of mitochondrial disease. The following biological and biotechnological barriers deny researchers the opportunity to study a wide variety of known mtDNA mutations in an *in vivo* model system in order to characterize pathologies and test therapeutic strategies:

1) Lack of mitochondrial recombination. (Eyre-Walker and Awadalla, 2001; Howell, 1997).

2) Alteration of the hundreds to hundreds of thousands of mtDNA molecules per cell (Wallace, 1999).

3) Introduction of DNA into mitochondria or alteration of mitochondrial genomes within dual mitochondrial membranes while preserving mitochondrial viability (Khan et al., 2007).

4) Preservation of altered mtDNA population despite selective pressure and genetic drift, possibly through elimination of endogenous mtDNA (Pinkert and Trounce, 2002).

Due to the lack of animal models harboring engineered mtDNA mutations, innovative approaches are necessary to study the association of mtDNA mutations with disease (Cannon et al., 2004). The chloramphenicol resistant (CAP^R) mouse model was produced from cells found to

have a cytoplasmically conferred resistance to the antibiotic chloramphenicol. This phenotype was attributed to a mtDNA mutation in the 16S rRNA gene (Bunn et al., 1974; Wallace, 1999). The CAP^R mouse, which exhibited mitochondrial dysfunction, enabled studies of a mtDNA mutation at tissue and organismal levels (Levy et al., 1999; Sligh et al., 2000).

Cytoplasmic hybrid or "cybrid" cell lines provide another method with which to model mitochondrial disease. A cybrid cell is created through the fusion of an enucleated cell and an intact cell (generally devoid of mtDNA – ρ^0 cells) to produce a single cell with mixed mitochondrial populations (Bunn et al., 1974; King and Attardi, 1989). Production of cybrid cell lines using an immortalized cell line allows for easy propagation (Khan et al., 2007; Trounce and Pinkert, 2007). The fusion of cytoplasm from patients with mitochondrial dysfunction with immortalized cell lines allows characterization of the biochemical phenotype of cell lines containing specific mtDNA mutations. This approach also provides a uniform nuclear background for studies using cytoplasts made from different individuals, thereby eliminating confounding nuclear variables (Swerdlow, 2007).

Xenomitochondrial cybrid cell lines are a sub-type of cybrid cell line. Xenomitochondrial cybrids allow study of mitochondrial dysfunction caused by mitochondrial polymorphisms instead of a specific mtDNA mutation. Creation of xenomitochondrial cybrids harboring mitochondrial genomes derived from an evolutionarily divergent source compared to the nuclear genome leads to suboptimal binding of ETC subunits encoded by the introduced mtDNA with ETC subunits encoded in the nucleus. Proof of concept experiments included production of xenomitochondrial cybrids derived from human cells supplemented with mitochondria from gorilla, chimpanzee or pygmy chimpanzee cytoplasmic donors. These studies revealed that xenomitochondrial cybrids exhibited mitochondrial deficiencies in complex I activity (Barrientos et al., 1998; Kenyon and Moraes, 1997). Work with *Mus musculus domesticus (M.m. domesticus)* cybrids containing *Rattus norvegicus (R. norvegicus)* mtDNA demonstrated severely impaired

mitochondrial function, including elevated lactate production, impaired state III respiration and ETC complex deficiencies (McKenzie and Trounce, 2000). Study of xenomitochondrial cybrid cell lines demonstrated viability of xenomitochondrial cybrids as models of mitochondrial dysfunction and provided insight into the biochemical pathology of mitochondrial dysfunction. The cybrid approach did not, however, provide a model for the study of disease progression at the tissue or organismal level (Khan et al., 2007).

Xenomitochondrial cybrids with *Mus terricolor* (*M. terricolor*) mitochondria within *M.m. domesticus* cells should exhibit a deficit in mitochondrial function similar to that seen in the previous xenomitochondrial studies, though less extreme, as *M. terricolor* only diverged from the lab strain six million years ago (Barrientos et al., 1998; Kenyon and Moraes, 1997; Pinkert and Trounce, 2002; Pogozelski et al., 2008). Sequencing of the *M. terricolor* mtDNA revealed 159 amino acid changes in *M. terricolor* compared to *M.m domesticus.* The 12S and 16S rRNAs had 31 and 124 changes, respectively, as well as insertion/deletion mutations. tRNAs had homology ranging from 93%-100% (Pogozelski et al., 2008). Early *in vitro* studies showed increased lactate production, which is indicative of impaired mitochondrial function, correlated to increasing evolutionary distance of introduced mtDNA in xenomitochondrial cells (McKenzie et al., 2003; Trounce and Pinkert, 2007).

The potential to provide inroads into the study of mitochondrial disease *in vivo* encouraged production of a murine xenomitochondrial model (B6NTac(129S6)-mt$^{M.\ terricolor}$/Capt; line D7). Injection of female *M.m domesticus* cybrid embryonic stem cells containing mitochondria derived from an evolutionarily divergent murine species into blastocyts lead to the creation of chimeric founder xenomitochondrial mice (McKenzie et al., 2004; Pinkert and Trounce, 2007; Trounce et al., 2004). Subsequent breeding resulted in a homoplasmic xenomitochondrial mouse line derived from cybrid cells which was used in preliminary phenotypic characterization (Pinkert and Trounce, 2002; Trounce et al., 2004).

Studies of xenomitochondrial mice have not revealed an overt phenotype (Pinkert, 2005).. Xenomitochondrial mice were produced by injection of mouse 129S6/SvEvTac (129S6) ES cells harboring *M. terricolor* mtDNA into host mouse C57BL/6NTac blastocysts, followed by breeding chimeric xenomitochondrial females to C57BL/6NTac males (Pinkert and Trounce, 2002). Fourth generation offspring were originally assessed in Barnes maze behavioral studies. Initial experiments revealed a deficit in spatial memory in xenomitochondrial mice, though the deficit diminished with subsequent experiments. Parental background strain of xenomitochondrial mice was established as a confounding factor after both 129S6/SvEvTac and C57BL/6NTac controls were included in analyses(data not shown). Differences initially observed between xenomitochondrial mice and C57BL/6NTac controls were attributed to partial 129S6 ancestry. This agreed with research by others demonstrating that 129S6 mice performed poorly in certain tests compared to C57BL/6NTac mice (Crawley et al., 1997). Backcrossing of the xenomitochondrial lineage to C57BL/6NTac males for a minimum of ten generations produced the required homogeneous nuclear background required for further phenotypic evaluation.

Section 3 – RNA import into mitochondria

In order to understand the pathology of diseases associated with altered mitochondrial function, a thorough understanding of basic mitochondrial biology is essential. A growing body of evidence supports the theory that mitochondria import specific RNAs from the cytoplasm (Adhya, 2008; Dorner et al., 2001; Entelis et al., 2001a; Entelis et al., 2001b; Wang et al., 2010). Research on the import of nuclear encoded RNAs into mitochondria is providing a greater understanding of how and when import occurs. Additionally, gene therapy approaches could utilize the RNA import pathway to direct engineered RNAs into the mitochondria, compensating for mtDNA mutations.

The first report of RNA import into mitochondria described experiments involving protozoans as an experimental model. Hybridization experiments showed that tRNAs present

within mitochondria did not all hybridize to the mtDNA, suggesting that some were imported from nuclear encoded genes (Suyama, 1967). Subsequent research showed that RNA import was common to many species including protozoa, plants, yeast and mammals (Dorner et al., 2001; Li et al., 1994; Marechal-Drouard et al., 1988; Martin et al., 1977; Martin et al., 1979; Simpson et al., 1989). Sequencing of mitochondrial genomes from a variety of organisms provided some of the most dramatic and convincing evidence for mitochondrial RNA import. Studies revealed that, in some species, the entire set of tRNA genes was missing from mtDNA (Gray et al., 1998; Janke et al., 1997; Schneider and Marechal-Drouard, 2000; Unseld et al., 1997). Given that tRNAs were essential for support of the mitochondrial translation process, it became clear that the mitochondrial tRNA pool was supplemented by nuclear encoded tRNAs. A large portion of work done to date investigating RNA import into mitochondria stemmed from this research, and provided insights into the specifics of when, how and which RNAs enter the mitochondria (Entelis et al., 2001a; Rubio et al., 2008; Wang et al., 2010).

Protists

The most extensive research on tRNA import has involved study of protists, eukaryotic organisms that are primarily single celled. In the protozoans *Trypanosoma* and *Leishmania*, all mitochondrial tRNAs are imported from the cytoplasm (Gray et al., 1998). In *Tetrahymena*, the majority of tRNAs are imported (Gray et al., 1998). The large number of imported tRNAs has provided excellent opportunities for investigating the specifics of RNA import into mitochondria. Regions of tRNA involved in import vary among different protozoa. However, the anticodon, D-domain and T-domain have all been implicated (Bhattacharyya and Adhya, 2004a; Crausaz Esseiva et al., 2004; Entelis et al., 2001b; Schneider and Marechal-Drouard, 2000).

An important discovery in protozoa was the report of a protein complex responsible for RNA import. Isolated from *Leishmania,* this 620 kDa RNA import complex (RIC) was purified from the inner mitochondrial membrane using affinity chromatography and was found to function

in the ATP dependent import of tRNAs into phospholipid vesicles (Bhattacharyya and Adhya, 2004b; Bhattacharyya et al., 2003). Further work by this group revealed that many proteins associated with the RIC complex had other functions within the cell. One protein, RIC1, functioned not only to import tRNAs, but also as the α subunit of the F1 ATP synthase molecule (Goswami et al., 2006). Other subunits within the RIC include complex III subunits and subunit VI of complex IV (Home et al., 2008; Mukherjee et al., 2007). These studies raised interesting questions about the association of ATP production and tRNA import.

Study of the RIC complex led to investigations of the therapeutic potential of RNA import into mitochondria. RIC from *Leishmania* was incubated with human mitochondria harboring mtDNA mutations (Mahata et al., 2005). Functional assays demonstrated not only the import of tRNAs but improvement of mitochondrial translation. Results showed that tRNAs imported by this method could function within the mitochondrial tRNA pool (Mahata et al., 2005). Excellent reviews on RNA import in protists were published recently (Adhya, 2008; Duchene et al., 2009)

Plants

In plants, import of tRNAs into mitochondria is common (Marechal-Drouard et al., 1993). Research has produced insight into the regions of imported tRNAs responsible for directing import and, while no specific "import signal" has been found, regions determined to be involved in specification of importability include the anticodon and both D and T arms (Delage et al., 2003; Duchene et al., 2009; Laforest et al., 2005; Salinas et al., 2005). In addition, tRNA aminoacylation is believed to be involved in tRNA import (Bhattacharyya and Adhya, 2004a; Delage et al., 2003; Laforest et al., 2005; Salinas et al., 2005). Research aiming to elucidate the proteins involved in tRNA import in plants found that the voltage-dependant anion channel (VDAC) was involved, and that TOM20 and TOM40, which play roles in protein import into the

mitochondria, may also be involved (Salinas et al., 2006). Future research should shed light on the mechanisms by which RNAs cross into the mitochondrial matrix of plants.

Yeast

In yeast, two-dimensional gel electrophoresis demonstrated that only $tRNA^{Lys}$ was imported into mitochondria (Martin et al., 1977; Martin et al., 1979). Further experiments showed that tRNA import was ATP dependent and, required aminoacylation, the Lys^{CUU} tRNA synthetase and the protein import machinery (Kamenski et al., 2007; Tarassov et al., 1995a; Tarassov et al., 1995b). The anticodon of tRNA and a portion of the acceptor stem are critical for the import of $tRNA^{Lys}$ into the mitochondrion (Entelis et al., 1998). Involvement of protein import machinery in this instance is interesting as it differs from the import machinery of protozoa, which have a distinct RNA import complex in the inner mitochondrial membrane.

The Th RNA of RNase MRP was shown to be imported into yeast mitochondria selectively (Lu et al., 2010). Additionally, research revealed the substrate specificity, distinct biochemical characteristics and distinct protein subunits of mitochondrial RNase MRP in yeast. The results indicated that the RNase MRP activity within the mitochondria is not contamination of nuclear RNase MRP (Lu et al., 2010).

Different requirements for mitochondrial RNA import suggest that this process may have evolved independently at least twice (Schneider and Marechal-Drouard, 2000). Because mammals are more closely related to yeast than protists, they are more likely to share mechanisms of RNA import with yeast than protists. The mammalian mechanisms could also be unique if their RNA import mechanism emerged after the lineage diverged from yeast. Import mechanisms may have evolved separately as critical tRNAs or enzymatic RNAs were lost from the mtDNA and their nuclear counterparts were required within the mitochondria.

Characterization of RNA import mechanisms in more organisms will allow definitive statements regarding the evolution of RNA import systems.

Mammals

That RNAs are imported into mitochondria has been disputed to a greater extent in mammals. Import of tRNA is an obvious requirement if an incomplete set of tRNAs is encoded by the mtDNA, however similar evidence is not applicable to imported enzymatic RNAs. Early publications discussing mammalian mitochondrial RNA import described imported enzymatic RNAs including the RNA subunits of RNase MRP (Th or 7-2 RNA), RNase P (H1 or 8-2 RNA), 5S rRNA and 5.8S rRNA (Chang and Clayton, 1987; Doersen et al., 1985; Wong and Clayton, 1986; Yoshionari et al., 1994). There was debate over whether the RNAs were imported or if experiments were detecting cytoplasmic contamination in mitochondrial RNA samples. The debate stemmed from low quantities of RNA molecules detected within mitochondria and the argument that these enzymes had lost their RNA subunit evolutionarily and no longer needed an RNA component (Kiss and Filipowicz, 1992; Rossmanith and Potuschak, 2001; Topper et al., 1992).

Controversy surrounding mammalian mitochondrial RNA import relates to the technical difficulty of isolating a pure sample of mitochondrial RNAs that are devoid of cytoplasmic RNAs. It is impossible to eliminate all cytoplasmic RNAs from a mitochondrial sample. Therefore, an assay to detect mitochondrial import of RNA needs carefully designed and rigorously tested controls to show that the imported RNAs are a legitimate portion of the mitochondrial RNA pool and play an active role in mitochondrial metabolism.

H1 RNA component of RNase P

The first reports of import of H1 RNA of RNase P into mitochondria and the first observation of nuclear RNA within mitochondria occurred in 1985 and research has continued to

support the import of the H1 RNA into mitochondria (Doersen et al., 1985; Puranam and Attardi, 2001). Doersen and co-workers reported that protein fractions isolated from nuclease-treated mitochondria had RNase P activity, which was abolished by addition of micrococcal nuclease (Doersen et al., 1985). Puranam and Attardi demonstrated the presence of H1 RNA in highly purified, digitonin- and micrococcal nuclease-treated mitoplasts (mitochondria with the outer membrane removed) (Puranam and Attardi, 2001).

A 1997 study provided experimental evidence for import of the H1 RNA into mitochondria while investigating nuclear localization of the H1 RNA (Jacobson et al., 1997). Investigators used injection of fluorophore-conjugated RNAs and *in situ* hybridization to localize both the H1 and Th RNA within cells (Jacobson et al., 1997). Interestingly, both H1 and Th RNAs localized to the cytoplasm with punctate, perinuclear staining indicative of mitochondria, (Jacobson et al., 1997). Additionally, in the same study, injection of truncated H1 RNA, which lacks the To antigen binding domain, showed that nucleolar localization of these RNAs was abolished and the RNAs localized instead in a perinuclear, punctate pattern indicative of mitochondria. This suggests that the To antigen binding domain is unnecessary for H1 RNA import into mitochondria (Jacobson et al., 1997).

An interesting addendum to the concept of mitochondrial H1 RNA import pertains to the function of this RNA within mitochondria. It would be plausible to assume that, because H1 RNA is imported into mitochondria and mitochondria have RNase P activity, H1 RNA is involved with mitochondrial RNase P activity. However, studies aimed at identifying complexes responsible for RNase P activity in the mitochondria have not shown the necessity for the H1 RNA (Holzmann et al., 2008; Rossmanith and Karwan, 1998; Rossmanith and Potuschak, 2001). Evidence currently points towards a RNase P activity within mitochondria independent of any RNA subunits which, instead, requires three core proteins (Holzmann et al., 2008). This raises questions about the function of mitochondrial H1 RNA. Two possibilities seem likely. First, H1 RNA could be

functioning in a capacity distinct from the protein-only RNase P enzyme, perhaps in another facet of RNA processing within the mitochondria. Alternatively, H1 RNA may be imported due to evolutionarily conserved sequence similarity with the Th RNA; possessing no function within the mitochondria as a biologically irrelevant molecule. If the region of H1 RNA directing import into mitochondria is homologous to that of Th RNA and evolutionarily conserved due to a cytoplasmic role, RNA may occur without a functional role within the mitochondria. If there were no negative consequence of the H1 RNA import, there would be no evolutionary pressure to prevent its import.

Th RNA component of RNase MRP

Import of the Th RNA subunit of MRP was first reported in 1987 (Chang and Clayton, 1987). Purification of mitochondria followed by northern blots and sequencing demonstrated the presence of Th RNA in mitochondria. Further work by another group involved purification steps as well as *in situ* hybridization to provide further evidence for this process (Li et al., 1994). This work further described regions of Th RNA responsible for directing import. Authors found that expression of a mutated form of Th RNA, lacking 57 central nucleotides, impaired mitochondrial import, while deletions at the beginning and end of the Th RNA molecule did not affect import. These data illustrated that the central region of Th RNA is necessary for mitochondrial import, but did not show that this sequence is sufficient for import. Sequence deletions in Th RNA could alter secondary structure in remaining regions of altered RNAs, hindering interactions with proteins directing mitochondrial import. Thus, the impaired import of RNAs lacking the inner region could be due to alterations of secondary structure of RNA molecules.

The import status of Th RNA is still debated due to the low number of molecules estimated to be present in mitochondria (Kiss and Filipowicz, 1992; Puranam and Attardi, 2001). An estimated 6 to 15 molecules per cell associate with mitochondria. This number was obtained by quantification using Northern blots and, therefore, may not be as accurate as qPCR-based

assays (Puranam and Attardi, 2001). Further studies are needed to determine whether Th RNA represents a RNA imported into mitochondria in minimal numbers or if such observations represent cytoplasmic contamination of mitochondrial fractions.

5.8S rRNA

The 5.8S rRNA, which was suggested in 1986 to be present within the mitochondrial compartment, presents an interesting case in the history of RNA import into mitochondria (Wong and Clayton, 1986). Wong and Clayton (1986) identified primase activity in a cytoplasmic protein fraction that could be abolished by treatment with nuclease. Upon isolation of RNA from this fraction it was noted that 5.8S rRNA was present (Wong and Clayton, 1986). Addition of purified 5.8S rRNA to the nuclease-treated protein fraction restored primase activity. Results indicated that 5.8S rRNA was present within the mitochondrial compartment.

A 1983 paper describing a protocol for purification of mitochondrial RNA and DNA demonstrated the presence of 5S rRNA and 5.8S rRNA and the absence of the cytoplasmic 18S rRNA in mitochondrial RNA (Tapper et al., 1983). However, mitochondrial samples were not treated with a nuclease prior to isolation of RNA, so cytoplasmic RNAs may have contaminated the sample. The high abundance of both 5S rRNA and 5.8S rRNA within mitochondrial RNA, combined with the absence of 18S rRNA lends credence to the idea that these RNAs specifically associated with the mitochondrial compartment.

Some studies contest the import of 5.8S rRNA into mitochondria. The 5.8S rRNA was used as a "non-imported" negative control RNA in a study designed to characterize the presence of 5S rRNA within mitochondria (Magalhaes et al., 1998). An investigation of 5S rRNA import into mitochondria also used the 5.8S rRNA as a negative control "non-imported" RNA. In this case, authors showed that, in contrast to 5S rRNA, 5.8S rRNA was not imported, (Entelis et al.,

2001a). These contradictory reports leave no clear answer to the question of 5.8S rRNA import into mitochondria.

5S rRNA

A number of studies showed the import of 5S rRNA into mammalian mitochondria. The 5S rRNA was detected by northern blot in RNA isolated from RNase treated mitoplasts derived from cows, rabbits and chickens (Yoshionari et al., 1994). Other publications presented data suggesting import of 5S rRNA into mitochondria (King and Attardi, 1993; Tapper et al., 1983; Wong and Clayton, 1986).

Methods for isolation of pure populations of mitochondrial RNAs involved sucrose gradient centrifugation to separate mitochondria from cells and used phenol to extract RNA (Tapper et al., 1983). Interestingly, the sucrose gradient purified mitochondria contained substantial amounts of 5S rRNA and 5.8S rRNA. Authors described these RNAs as contaminants from the cytoplasm. However, it was of interest that these RNAs were selectively contaminating mitochondrial RNA samples in high abundance while other cytoplasmic RNAs such as 18S rRNA were not identified.

Further evidence for mitochondrial import of 5S rRNA can be found in results from experiments investigating mitochondrial primase activity (Wong and Clayton, 1986). As part of their experiments, the authors isolated RNA from mitochondria or digitonin treated mitoplasts and ran the samples on a polyacrylamide gel. The resulting gels are similar to those reported by Tapper et al (1983). Both 5.8S and 5S rRNAs were present within RNA samples derived from isolated mitochondria. Because authors did not treat mitochondria with a nuclease, some of the RNA detected could represent cytoplasmic RNA contamination. Nevertheless, these data support the idea that both 5.8S and 5S rRNA associate with mitochondria.

In other research, bands corresponding to 5S rRNA were present on polyacrylamide gels used to separate radioactively labeled mitochondrial RNA samples (King and Attardi, 1993). The authors made note of additional high molecular weight bands on a polyacrylamide gel, including 5S rRNA, which they regarded as cytoplasmic contamination, contradicting a later statement noting the absence of cytoplasmic tRNAs as indicative of a highly pure sample of mitochondrial RNA (King and Attardi, 1993). Northern blots further supported the idea that 5S rRNA is imported into mitochondria by demonstrating the presence of 5S rRNA in carefully purified RNase-treated human mitoplasts (Magalhaes et al., 1998). A different report described the requirement of ATP and soluble proteins for 5S rRNA import (Entelis et al., 2001a). Furthermore, when a protein forming a stable beta-barrel with an attached mitochondrial import signal blocked protein import, 5S rRNA import was also inhibited (Entelis et al., 2001a). Inhibition of RNA import into mitochondria by blocking the protein import pathway lends credence to the premise that the protein import complexes, specifically the Translocase of the Outer Mitochondrial Membrane (TOM) complex, are involved in RNA import. The possibility exists that blocking protein import by this method may indirectly influence RNA import. Blockage could alter the mitochondrial proton gradient or other biological parameters, interfering with RNA import indirectly and thus the protein import machinery may not play a direct role in RNA import into mitochondria.

Further research identified regions altering the efficiency of import in an *in vitro* system including helix IV and five nucleotides at the base of helix I (Smirnov et al., 2008).

tRNA

The first report of naturally occurring tRNA import into mammalian mitochondria was in marsupials, whose mtDNA encodes a unique non-functional $tRNA^{Lys}$ (Janke et al., 1997). Sequencing the mitochondrial genome of the walaroo revealed mutations in $tRNA^{Lys}$ that prevented it from functioning normally within the mitochondrial compartment. Subsequent

analysis of several other marsupial species revealed commonality of the mutation, and the presence of a compensating nuclear-encoded tRNA within the mitochondrial tRNA pool (Dorner et al., 2001).

Mitochondrial import of a tRNA in a species so closely related to humans begs the question of whether human mitochondria maintain the machinery to import tRNAs. In 2001, Entelis and coworkers (Entelis et al., 2001a) demonstrated import of yeast $tRNA^{Lys}$ and *in vitro* transcribed human $tRNA^{Lys}$ into human mitochondria using an *in vitro* system. A later report by the same group demonstrated import of yeast $tRNA^{Lys}$ into human cells and showed functional rescue of cybrid cells harboring a mtDNA mutation (Kolesnikova et al., 2004). This paper included a description of changes in membrane potential and oxygen consumption in cybrid cells transfected with a gene encoding the yeast $tRNA^{Lys}$ gene, suggesting that the tRNAs were imported by mitochondria and able to function in mitochondrial translation (Kolesnikova et al., 2004).

Import of $tRNA^{Lys}$ into human mitochondria in conjunction with the RNA import complex from *Leishmania* was reported in 2005 (Mahata et al., 2005). Subsequent work suggested that $tRNA^{Gln}$ is imported naturally into both human and rat mitochondria (Rubio et al., 2008). This publication showed *in vitro* import of specific tRNAs into isolated human and rat mitochondria. The authors further suggested that earlier work demonstrating tRNA import in conjunction with the RIC in isolated human mitochondria could have resulted from indirect effects of the RIC on mitochondria function.

Section 4 – Mechanism of mitochondrial RNA import in mammals

Comparison of mitochondrial RNA import systems between species can provide important insights into the evolution of such systems. Identification of a distinct RNA import complex in protists with several multifunctional protein subunits demonstrates that protein

complexes with the sole purpose of importing RNAs into mitochondria do exist (Home et al., 2008). Unfortunately, for many of the unique subunits of the protist RIC, no homologues exist in mammals. This does not preclude the presence of a RIC homologue within mammalian mitochondria, but makes such searches difficult. Also going against the theory that a protist RIC homologue could exist in mammalian mitochondria is the fact that such a complex does not seem to exist in more closely evolutionarily related yeast. tRNA import into mitochondria seems to utilize the protein import complex, unlike protists (Brandina et al., 2007; Salinas et al., 2008).

The process by which RNAs enter the mitochondria likely occurs in distinct steps. The RNA to be imported must first move to the mitochondrial surface; this process likely involves cytoplasmic chaperones. In the literature, the only protein suggested to play this role is rhodanese. This enzyme can bind to 5S rRNA in its unfolded state immediately following translation. When rhodanese enzyme expression was silenced using siRNA, 5S rRNA import was impaired (Smirnov et al., 2010). Together, data strongly support the role of rhodanese in directing 5S rRNA to the mitochondrial surface. Binding of rhodanese to other imported RNAs is unknown however, leaving the role of rhodanese in the import of other RNAs uncertain.

The second stage of RNA import likely involves transfer of RNA from the chaperone to a membrane bound complex in the outer mitochondrial membrane to allow import across this membrane. In this role, mammalian mitochondria may import RNAs through a mechanism involving the protein import complex. Some evidence supports this theory, though there is evidence to the contrary (Entelis et al., 2001a; Rubio et al., 2008). Blockage of the protein import complex with a beta barrel protein impaired 5S rRNA import into mammalian mitochondria (Entelis et al., 2001a). A later report investigating tRNA import in mammals indicated that collapse of the mitochondrial proton gradient, required for protein import, did not impair import of tRNAs (Rubio et al., 2008). These contradicting reports could be consolidated in various ways. Blockage of the protein import pathway using a beta barrel could impair transport through the

TOM complex. Thus, the experiment using the beta barrel only implicates the TOM complex in RNA import and does not indicate a role for the Translocase of the Inner mitochondrial Membrane (TIM) complex. In the latter experiment by Rubio and collegues, collapsing the proton gradient would have only affected the TIM complex, as the proton gradient is required for TIM function (Rubio et al., 2008). Differing systems for import of 5S rRNA and tRNAs could also exist, or subtle differences in experimental systems could have led to different conclusions in different labs. In addition, it is possible that the TIM complex could be involved, but has differing requirements for RNA import and protein import. It is also possible that protein import complexes are not involved in mammalian RNA import into mitochondria and that a separate system has evolved.

A mitochondrial import signal for proteins is well characterized (Devaux et al., 2010; Schmidt et al., 2010). The RNA sequence responsible for directing mitochondrial RNA import is largely uncharacterized. Some research has begun to reveal which regions of imported RNAs act to direct import into mitochondria in mammals. A study investigating the Th RNA showed that deletion of the central region of this RNA from nucleotide 118 to 175 abolished mitochondrial localization (Li et al., 1994). This suggests that some portion of this region is involved in directing the RNA into mitochondria. However, since deletion would affect the secondary structure of the RNA, further experiments are needed to determine what role, if any, the central region of the Th RNA plays in directing import. Additionally, in order to demonstrate that a particular sequence of RNA acts as an import signal, it would be necessary to show that the sequence alone is sufficient to drive import into mitochondria. Interestingly, another report supports the presence of the mitochondrial localization signal in this region. A hairpin loop from the Th RNA region 149-170 was attached to $tRNA^{Trp}$ or GAPDH mRNA and imported into human or yeast mitochondria, respectively (Wang et al., 2010). That such a short RNA segment is

sufficient to direct RNA import into mitochondria in two diverse species is good evidence to suggest that this sequence represents a legitimate RNA import signal.

Additional evidence for a mitochondrial RNA targeting signal comes from a study investigating $tRNA^{Lys}$ import into yeast and human mitochondria. Authors used an *in vitro* selection (SELEX) process to mutate the tRNA and then screen mutants retaining import ability. Several stages of this selection followed by sequencing of the final products revealed a set of altered tRNA-like sequences capable of import into both yeast and human mitochondria. Interestingly, these RNAs had lost the normal secondary structure of a tRNA and the D arm and T loop were the primary regions conserved. These regions of the targeted RNA molecules are important determinants of importability (Kolesnikova et al., 2010). Further experiments along these lines with different imported RNAs could provide a generalized consensus sequence necessary and sufficient to import RNAs into mitochondria.

The H1 RNA subunit of RNase P localizes to the nucleus as well as to mitochondria. Research investigating regions of RNA acting as a signal for nuclear localization includes data of interest with respect to mitochondrial localization. This study was investigating a portion of the H1 RNA subunit of RNase P bound by the To-antigen, a protein involved in autoimmune disorders in human patients. In order to determine if the To-antigen binding site (21-64 of human MRP RNA) of the H1 RNA is important for nuclear localization, truncated RNAs lacking the To antigen binding site were produced, labeled fluorescently and injected into the nucleus of cells. The injected RNA did not localize within the nucleus when the To region of the RNA was removed, but rather diffused out and formed a punctate, perinuclear pattern around the nucleus, which the authors suggested could be mitochondria (Jacobson et al., 1997). This indicated that the first 70 nucleotides, which includes the To antigen binding site, are dispensable for mitochondrial localization. Results hinted that competition between proteins localizing RNAs to the nucleus and proteins directing import into the mitochondria may control the amount of RNA imported into

mitochondria. Further insight into the regions of the H1 RNA directing import came from a report characterizing the role of polynucleotide phosphorylase (PNPase) in mitochondrial RNA import. A series of experiments with truncated H1 RNAs revealed that a central 20 nucleotide hairpin was capable of directing the import of RNA into both yeast and human mitochondria (Wang et al., 2010). If confirmed by further study, this report would represent the first identification of a RNA import signal sufficient to direct import of RNAs into the mitochondria.

A study designed to determine the necessary conditions for import of 5S rRNA into human mitochondria revealed that both ATP and a soluble protein fraction were required for import *in vitro* (Entelis et al., 2001a). Treatment of mitochondria with protease impaired RNA import, suggesting that protease-sensitive surface proteins were required. Blockage of the protein import pathway interfered with RNA import *in vitro*, and collapse of the mitochondrial hydrogen ion gradient impaired import of the 5S rRNA (Entelis et al., 2001a; Rubio et al., 2008). Together, these factors begin to reveal aspects of the mechanisms of RNA import into mitochondria, but do not fully define the ways in which RNAs are imported.

Another set of experiments were aimed at determining which regions of the 5S rRNA are necessary for directing mitochondrial import through two different approaches. In the first approach, the authors deleted large regions of the 5S rRNA, based on secondary structure, to determine if the separate regions were able to be imported independently (Smirnov et al., 2008). Results indicated that the β-domain was imported poorly, while the γ-domain was imported well. This suggested that the γ-domain contains a mitochondrial localization signal. The second approach took advantage of the fact that yeast 5S rRNA is poorly imported. Substitutions were made in the yeast 5S rRNA with human 5S rRNA domains and import of hybrid RNAs was tested. Results were less definitive, indicating that both β and γ-domains improved importability of the yeast 5S rRNA, with the β-domain being most effective (Smirnov et al., 2008). Individual mutations of 5S rRNA were designed and their importability was tested. Overall, data from these

experiments showed that two regions of the 5S rRNA affect importability the most. The γ-domain and two G-U pairs in the α-domain, when deleted and mutated, respectively, ablated 5S rRNA mitochondrial importability. Alteration of one or the other of these domains does not affect import as dramatically (Smirnov et al., 2008). Subsequent studies support these observations and reveal that the enzyme rhodanese binds to these regions and is involved in directing the import of the 5S rRNA into the mitochondria, supporting the importance of these regions as a localization signal (Smirnov et al., 2010).

Smirnov and co-workers (2008) observed that imported RNAs "run the gauntlet" to get imported into mitochondria (Smirnov et al., 2008). The increased rate of import of the 5S rRNA when the β-domain is mutated is likely because this region is critical for the binding of the L5 protein, which is responsible for transport of the 5S rRNA into the nucleus (Allison et al., 1993; Smirnov et al., 2008). By preventing binding of L5 and import into the nucleus, RNA localizes to the cytoplasm where it is more likely to enter the mitochondria. The increase in importability of 5S rRNA β-domain mutants suggests that the limiting factor in the quantity of 5S rRNAs imported into mitochondria is the number of available RNAs, and not the activity or quantity of proteins involved in RNA import into mitochondria. Thus, under normal circumstances, competition between nuclear localization and mitochondrial localization likely controls the amount of 5S rRNA that is imported into mitochondria.

The study of RNA import in the mammalian system has revealed enough information to begin to demonstrate how little we truly know about this aspect of mitochondrial biology. Current understanding of mechanisms of mitochondrial RNA import, biological implications of this process for human disease, potential for therapeutic use and even full characterization of which RNAs are imported are lacking. The goal of many of the experiments outlined in this dissertation is to add knowledge to our understanding of mitochondrial RNA import and advance this nascent field of life science research.

Chapter 2 – Compensatory mechanisms in xenomitochondrial mice

Section 1 – Introduction

Gaining a thorough understanding of the pathological mechanisms behind mitochondrial disorders is paramount to developing therapeutic approaches. Clinical studies and experimental models such as cell lines harboring mitochondrial mutations can provide invaluable information regarding the cellular pathways involved in disease progression, but for a view of the pathways acting at the tissue or systemic level, an animal model is invaluable. Such a model allows manipulation and investigation of mitochondrial disease in a manner not possible with clinical or cell culture studies. Currently, due to limitations in the ability to engineer mtDNA mutations, animal models of specific mtDNA mutations are lacking. To address the need for an animal model of mitochondrial disease, alternate approaches are required to model diseases associated with mtDNA mutations. Xenomitochondrial mice, mice engineered with mtDNA derived from evolutionarily divergent species, allow study of mitochondrial dysfunction due to mtDNA polymorphisms. Following production of mice, preliminary phenotypic studies explored the effects of evolutionarily divergent mitochondria. We hypothesize that xenomitochondrial mice should exhibit neuromotor or muscular deficiencies. Additionally, we hypothesize that relatively normal phenotype uncovered in preliminary studies may be due to compensatory mechanisms acting at the genetic level. The following experiments continue phenotypic evaluation of xenomitochondrial mice and explore the compensatory mechanisms that allow normal cellular function in the face of polymorphic mtDNA.

Section 2 – Materials and methods

Mice

Three-week-old sex matched (three male and two female from each group) xenomitochondrial and control C57BL/6NTac mice were sacrificed for gene expression and mtDNA content analysis. Aged and young (9-14 months, 3-5 months respectively) male xenomitochondrial and C57BL/6NTac mice were subjected to a battery of neuromotor and muscular tests. Ten aged mice (five of each genotype) and seven young mice (four xenomitochondrial and three C57BL/6NTac) were used in all behavioral analyses. All mice were maintained in an AAALAC-accredited specific pathogen-free barrier facility with *ad libitum* access to water and feed on a 14:10 light:dark cycle. All mouse procedures including euthanasia conformed to Institutional Animal Care and Use Committee (IACUC) guidelines and the Guide for the Care and Use of Laboratory Animals, under Office for Laboratory Animal Welfare (OLAW) assurance #A3152-01.

Microarray

Agilent murine whole genome microarray chips were used to quantify gene expression in total brain RNA isolated from three-week-old xenomitochondrial and C57BL/6NTac control mice (N=5 per group). Data were analyzed using the ArrayAssist program (Stratagene, La Jolla, CA). Normalized data from xenomitochondrial and C57BL/6NTac control samples were compared to calculate fold change in gene expression.

qRT-PCR

MtDNA and RNAs from brain, heart and liver of three week old xenomitochondrial and control mice were quantified by qPCR and qRT-PCR using the ΔΔCt method with the assistance of the REST program (Livak and Schmittgen, 2001; Pfaffl et al., 2002).

Standard qRT-PCR was unsuitable to quantify mtDNA level and expression of mtDNA encoded transcripts. Due to sequence divergence between *M. m. domesticus* and *M. terricolor*, a carefully designed quantitative real-time PCR assay was required to avoid data artifacts resulting from sequence dissimilarities (Pogozelski et al., 2008). PCR primers were designed to amplify identical regions of *M. m. domesticus* and *M. terricolor* mtDNA and mtDNA transcripts; each primer sequence recognized given polymorphisms. If primers specific to each species amplify with comparable efficiencies, then the two primer sets can be treated as one primer set for the purposes of this analysis, allowing the quantification of expression of Mt-Co2 from mtDNA. Table 1 contains primer sequences. Underlined nucleotides denote species-specific sequence differences.

q-PCR was performed using SYBR green mastermix on DNA isolated from three week old xenomitochondrial and control tissues. DNA (50ng) from each sample was amplified in triplicate.

For qRT-PCR, 4µg of RNA were treated with DNase (Applied Biosystems Turbo DNA-free kit) to eliminate contaminating genomic and mitochondrial DNAs. After DNase inactivation, samples were split into RT positive (RT+) and RT negative (RT-) samples. Promega M-MLV reverse transcriptase was used to produce cDNAs in RT+ samples. RT- samples were treated identically to RT+ samples, but without M-MLV enzyme. qPCR of all RT- samples confirmed absence of contaminating DNA. Samples were adequately DNA-free if Ct values from RT- samples were at least 10 cycles higher than Ct values from corresponding RT+ samples. All samples were analyzed in triplicate using SYBR green master-mix.

Table 1: Primer sequences used to measure Mt-Co2 and β-actin DNA and cDNA.

• AGTCGTTCTGCCAATAGAACTTCCAATCCGT	Mt-Co2 *M.m.domesticus*	423F
• AGTCGTCCTACCAATGGAACTCCCAATCCGT	Mt-Co2 *M.terricolor*	423F
• TTAGATCCACAAATTTCAGAGCATTGGCCA	Mt-Co2 *M.m.domesticus*	608R
• TTGGAGCCGCAAATTTCGGAGCATTGACCA	Mt-Co2 *M.terricolor*	608R
• GAAATCGTGCGTGACATCAAAG	β-actin	619F
• TGTAGTTTCATGGATGCCACAG	β-actin	834R

Efficiency of PCR reactions was calculated as outlined elsewhere (Liu and Saint 2002). The efficiencies of Mt-Co2 primer sets were 90.0% for *M. m. domesticus* primers and 93.9% for *M. terricolor* primers in qRT-PCR of Mt-Co2 RNA and 95.8% for *M. m. domesticus* primers and 96.9% for *M. terricolor* primers for q-PCR of Mt-Co2 DNA and were therefore calculated together for qRT-PCR and q-PCR. Data were analyzed using the REST program, averaging replicates of each sample (Pfaffl et al., 2002).

In order to validate microarray data, RNA was isolated from brain tissue of three-week-old xenomitochondrial and C57BL/6NTac mice and analyzed by qRT-PCR. 4µg RNA samples were treated with Promega DNase for 15 minutes, inactivated, then split into RT+ and RT- samples. RT+ samples were treated with Promega M-MLV reverse transcriptase enzyme to produce cDNAs. RT- samples were treated identically, but without M-MLV enzyme. RT- samples were all amplified to confirm absence of contaminating DNA. qRT-PCR was then performed on all samples in triplicate using SYBR green mastermix. The Vector NTI program was used in design of primers. Data analyses were performed using the REST program (Pfaffl et al., 2002). Primer sequences are presented in Table 2.

Table 2: Primer sequences used to confirm microarray results.

CAGGGGTGAGCTGAAGCCACAAA	Arc 1936F
CCATGTAGGCAGCTTCAGGAGAAGAGAG	Arc 2249R
GTGTGGCCCCTGAGGAGCAC	β-actin 364F
AGGGACAGCACAGCCTGGAT	β-actin 505R
GATGTTCTCGGGTTTCAACGCCGACTA	Fos 142F
GCCCCTTCTGCCGATGCTCTG	Fos 520R
GCGCGCTCCACTCAAGTCTTCTTTC	Dusp1 475F
CCAGCATCCTTGATGGAGTCTATGAAGTCA	Dusp1 890R
AAGAAGCCAACAACTTGGTTGCTAGTTTTATTTCTG	Egr-2 134F
TTGCCCATGTAAGTGAAGGTCTGGTTTCTA	Egr-2 527R
GCCGCGTATCCTGGAGGCGA	Egr-4 263F
TCCGGCAGCAAGGCATCGGG	Egr-4 558R
AGGGAAGCGACGCCGAGAAA	Jun 86F
GTGTAGAGACAGGCTGCCAGGG	Jun 409R
TTGGGGGAGTGTGCTAGAAGGACTG	Nr4a1 12F
TGAGGAGCACGGCTGGGT	Nr4a1 351R

Muscular/neuromotor analyses

A Rota-Rod treadmill (Med Associates Inc., Georgia, Vt) was used to test motor coordination and endurance. Latency to fall from the Rota-Rod was measured both at 24rpm constant rotational velocity and at an accelerating rotational velocity of 4-40rpm. Mice were removed after 240 seconds (24rpm) and 300 seconds (4-40rpm acceleration) if no fall occurred.

Balance Beam experiments tested motor coordination and balance (Carter et al., 1999). Wooden beams used were 1 meter in length and of various shapes and sizes (Square: 28mm, 12mm, 5mm; Round: 28mm, 17mm, 11mm). Latency of mice to traverse the beam and reach an enclosed escape box and total number of foot slips were measured.

A Pole test analyzed motor function. Mice were placed upright at the top of a 50cm gauze-wrapped pole (1cm in diameter) topped with a rubber ball. Latency to turn around and descend was measured (Sedelis et al., 2000). Mice were removed from the apparatus after four minutes if descent was not completed.

A Wire Hang test was performed to examine muscle strength. Latency of a mouse to fall 50 cm into bedding from an inverted wire cage top was measured, with the mouse returned to its cage after four minutes if no fall occurred (Paylor et al., 1998).

Gait was analyzed using footprint measurements (Klapdor et al., 1997). A corridor leading to a darkened escape box was constructed and floored with white paper. After application of nontoxic paint of differing colors to fore and hind feet, mice ran along the corridor into the escape box. Distances measured between resultant footprints included: left-fore paw to left-fore paw (LF-LF), left-hind paw to left-hind paw (LH-LH), right-fore paw to right-fore paw (RF-RF), right-hind paw to right-hind paw (RH-RH), left-fore paw to right fore paw (LF-RF), left-hind paw to right-hind paw (LH-RH), right-fore paw to right hind paw (RF-RH), and left-fore paw to left-hind paw (LF-LH).

Mitochondrial respiration

Mitochondrial oxygen consumption was measured using a Clark-type oxygen electrode as described elsewhere (Tompkins et al., 2006). Mitochondria were isolated from skeletal muscle of 5-6 month old male xenomitochondrial and control mice by standard differential centrifugation following mechanical dissociation of tissue (Graham, 2001b). A 0.25ml mitochondrial suspension, diluted to 1.0 mg/ml in respiration buffer (300mM sucrose, 50mM KCl, 5mM KH_2PO_4, 1mM $MgCl_2$, 5mM EGTA, and 20mM Tris-HCl, pH 7.35) was incubated in a sealed bottle on a magnetic stir assembly at 37°C. Complex I-linked state 4 respiration was induced by adding 2.5mM malate and 10mM glutamate follow shortly by 100µM ADP to stimulate state 3. Respiration data are normalized to citrate synthase activity. Citrate synthase (CS) activity is measured spectrophotometrically (Trounce et al., 1996). Respiration values are reported as nmoles of oxygen consumption per minute per unit of citrate synthase activity ($nmolO_2$/min/CS).

Statistical analyses

qPCR data were statistically analyzed using the REST program (N = 5 for each group) (Pfaffl et al., 2002). Hazard ratios with 95% confidence intervals were generated for motor assays that produced censored values by Cox regression analysis using PROC PHREG in SAS Version 9.1 (N= 5 each for aged animals, N = 4 for young xenomitochondrial mice, N = 3 for young control mice) (SAS Institute, Inc., Cary, NC) (Cox, 1972). Statistical testing of Gait measurements and respiration (no censored values) was conducted with repeated measures analysis of variance using PROC MIXED in SAS. All statistical models considered variation due to genotype.

Section 3 – Results

Microarray analysis of whole genome gene expression

Microarray analysis identified seven genes for which expression was altered more than two-fold (Table 3). Identified genes all belong to the immediate-early response gene superfamily, primarily representing transcription factors. Microarray data showing potential expression changes for mtDNA-encoded genes were disregarded due to sequence divergence between *M. m. domesticus* and *M. terricolor*, which likely produced artifactual decreases in gene expression in xenomitochondrial mice. Microarray measurements of mtDNA-encoded transcripts from xenomitochondrial mouse tissue were near or at background levels (data not shown). Differential expression of genes associated directly with mitochondrial energy production was not observed. A single xenomitochondrial sample was excluded as an outlier during data analysis due to lack of correlation with other xenomitochondrial samples. Xenomitochondrial samples 1 through 4 had intra-group correlation coefficients greater than 0.9, while sample 5 had intra-group correlation coefficients between 0.78-0.8 indicating a lack of similarity with other xenomitochondrial samples. Heat Map analysis also identified sample 5 as an outlier.

qRT-PCR analysis

No differences were observed in mtDNA content between xenomitochondrial and control brain, liver or heart tissues (data not shown). Experiments validating microarray results confirmed down regulation of Fos, Egr2, and Egr4 in brain (Figure 1; p=0.039, 0.008 and 0.006, respectively). qRT-PCR did not show significant down regulation of Arc, Dusp1, Jun and Nr4a1 (P> 0.05). Expression of Mt-Co2 RNA in brain was up regulated 5.6 fold over controls (Figure 1; p=0.003).

Table 3: Genes identified by microarray as differentially expressed between control and xenomitochondrial samples.

Genes with more than two fold gene expression changes are identified.

Fold change	Gene	Function	Citation
-4.34	Activity-regulated cytoskeleton-associated (Arc)	Involved in memory and long term potentiation through a role in endocytosis of AMPA-R	(Bramham et al., 2008)
-3.69	Fos	Transcription factor, part of activator protein 1 (AP-1) complex, apoptosis, control of cell cycle and differentiation	(Verde et al., 2007)
-2.65	Dual specificity phosphatase 1 (Dusp1)	Innate immune control	(Bermudez et al., 2010)
-4.42	Early growth response 2 (Egr2, Krox20)	T-lymphocyte development, control of Schwann cell myelination, breathing pattern and early brain development	(Chatonnet et al., 2007; Desmazieres et al., 2009; Jang and Svaren, 2009; Lawson et al., 2010)
-2.56	Early growth response 4 (Egr4)	Transcription factor - male fertility, regulation of neuron-specific K+/Cl– cotransporter	(Tourtellotte et al., 1999; Uvarov et al., 2006)
-2.96	JUN proto-oncogene homolog B (Jun)	Transcription factor, part of AP-1 complex, control of cell cycle and differentiation, apoptosis, synaptic plasticity	(Verde et al., 2007)
-3.69	Nuclear receptor subfamily 4, group A, member 1 (Nr4a1)	Transcription factor, dopaminergic neuron function, possible role in insulin resistance, thymocyte selection	(He, 2002; No et al., 2010; Zhao and Bruemmer, 2010)

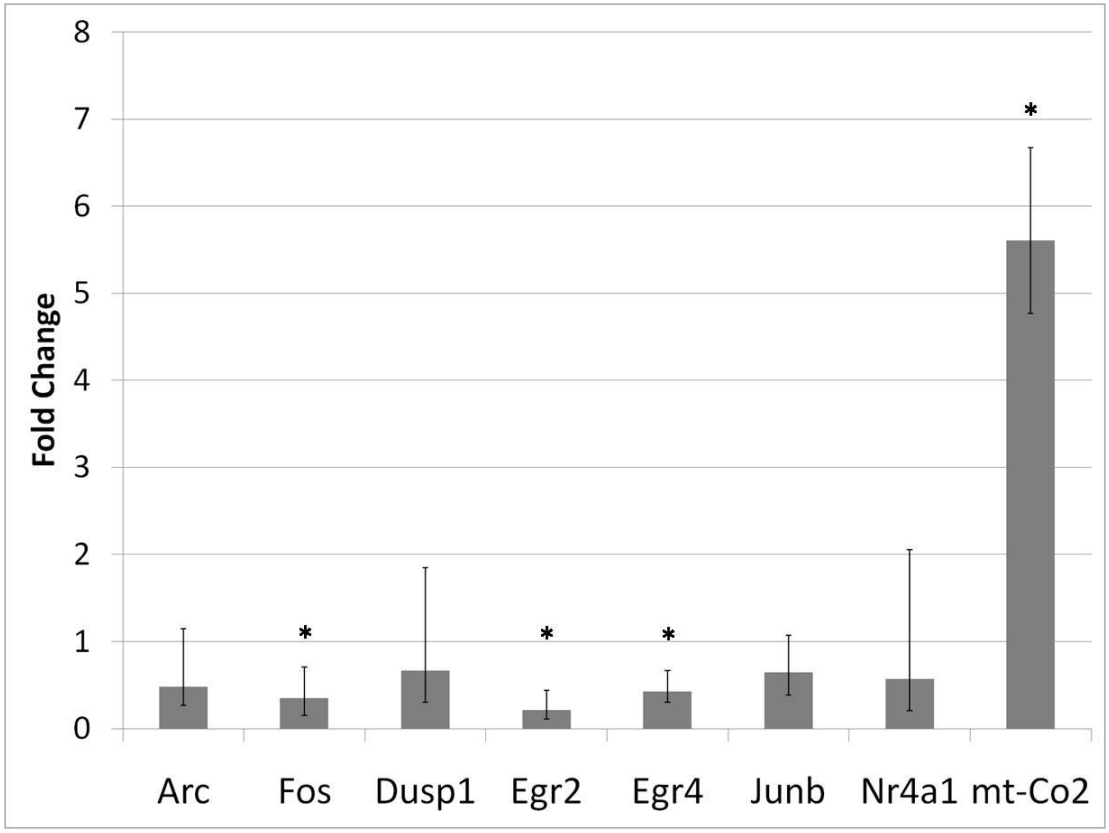

Figure 1: qRT-PCR measured fold change of mtDNA encoded mt-Co2 and genes identified by microarray as differentially expressed between xenomitochondrial and control samples.

Histogram represents the fold-change in gene expression of xenomitochondrial over control in brain tissue. A value of one represents no change. Error designated as +/- SE. Columns marked with an asterisk represent significant fold changes over control ($p<0.05$). Fos had a fold change of 0.4 ($p<0.001$), Egr2 had a fold change of 0.2 ($p<0.001$), Egr4 had a fold change of 0.4 ($p=0.006$) and mt-Co2 had a fold change of 5.6 ($p=0.003$). Error bars are asymmetrical due to mathematical transformation of data to fold change.

Motor analyses

Table 4 and Table 5 summarize data for all motor tests. Gait measurements in xenomitochondrial mice were comparable to controls in all measurements except the distance between left and right forefeet when both young and aged mice were grouped, with a p-value of 0.047.

Young xenomitochondrial mice were less likely to fall off a 24 rpm Rota-Rod than wild-type mice ($p<0.0001$). While older xenomitochondrial mice and their controls did not display any difference on the Rota-Rod ($p>0.05$), a difference remained when all mice were compared ($p=0.02$). Similarly, young xenomitochondrial mice performed better than control on accelerod ($p=0.001$), while no difference was seen in their aged counterparts ($p=0.9871$).

For the most part, no differences were seen in Balance Beam analysis. The only exception occurred among the older mice on the 17mm round beam and the 5mm square beam. Aged xenomitochondrial mice crossed the 17mm beam faster than control mice ($p=0.04$), while wild-type mice performed better ($p<0.0001$) on the 5mm beam. The results for the 5mm beam reflect the extreme difficulty all older mice had in crossing the 5mm beam – it was only successfully traversed three times, each time by a control mouse. As no xenomitochondrial mice crossed the beam in this particular test, no hazard ratio could be calculated. This is denoted by "***" in Table 5.

Table 4: Least square means and p-values for behavioral and motor tests performed on aged and young mice: Gait Analyses.

Distances were measured between pawprints to investigate quantitative differences in animal mobility. LF- left fore, LH- left hind, RF- right fore, RH- right hind. (Xeno – experimental xenomitochondrial mice, Control – C57BL/6). Units are cm ±SE.

		Gait LFLF	Gait LFLH	Gait LFRF	Gait LHLH	Gait LHRH	Gait RFRF	Gait RFRH	Gait RHRH
Aged Mice	**Control**	6.80 ± 0.30	0.84 ± 0.15	1.51 ±0.09	6.72 ± 0.28	2.84 ± 0.13	6.73 ± 0.39	0.99 ± 0.14	6.28 ± 0.32
	Xeno.	7.00 ± 0.30	0.86 ± 0.15	1.34 ± 0.09	6.85 ± 0.28	2.96 ± 0.13	6.93 ± 0.39	0.88 ± 0.14	6.81 ± 0.32
p-value		0.644	0.928	0.223	0.758	0.580	0.719	0.585	0.294
Young Mice	**Control**	7.90 ± 0.37	0.88 ± 0.10	1.63 ± 0.07	7.92 ± 0.37	3.26 ± 0.20	8.30 ± 0.43	0.96 ± 0.14	8.09 ± 0.51
	Xeno.	9.10 ± 0.33	0.79 ± 0.09	1.45 ± 0.06	8.99 ± 0.33	3.10 ± 0.18	8.70 ± 0.39	1.00 ± 0.12	8.52 ± 0.45
p-value		0.066	0.522	0.107	0.083	0.564	0.520	0.865	0.554
Combined	**Control**	7.30 ± 0.40	0.86 ± 0.90	1.56 ± 0.06	7.23 ± 0.41	3.02 ± 0.12	7.40 ± 0.43	0.98 ± 0.09	7.06 ± 0.44
	Xeno.	8.00 ± 0.38	0.83 ± 0.80	1.39 ± 0.05	7.92 ± 0.39	3.02 ± 0.12	7.80 ± 0.40	0.93 ± 0.09	7.66 ± 0.42
p-value		0.198	0.814	**0.047**	0.249	0.975	0.496	0.703	0.338

Table 5: Hazard ratios (with 95% confidence intervals) and p-values for behavioral and motor tests performed on aged and young mice: Pole, Rota-Rod, Accelerod, Beam tests and Wire Hang.

The symbol * denotes inability to calculate hazard ratio. A hazard ratio of 1 indicates no difference between xenomitochondrial and control. A hazard ratio of greater than 1 indicates that the xenomitochondrial mice were X times more likely to register an event (ie: finish pole test or fall off Rota-Rod) than control. Results demonstrate that xenomitochondrial mice do not exhibit muscular or neuromotor deficiencies as anticipated.**

	Pole-test	**Rota-Rod**	**Accel-erod**	**Beam (Sq28)**	**Beam (Sq12)**	**Beam (Sq5)**	**Beam (Rd28)**	**Beam (Rd17)**	**Beam (Rd11)**	**Wire Hang**
Aged Mice	0.993 (0.683-1.443)	1.163 (0.802-1.685)	0.996 (0.591-1.677)	1.404 (.523-3.765)	1.945 (0.566-6.683)	***	1.658 (0.648-4.245)	2.873 (1.050-7.866)	1.447 (0.558-3.748)	1.120 (0.785-1.597)
p-value	0.969	0.426	0.987	0.5	0.291	**<0.0001**	0.292	**0.04**	0.447	0.533
Young Mice	0.823 (0.511-1.311)	0.384 (0.249-0.592)	0.316 (0.164-0.608)	2.493 (0.770-8.076)	1.765 (0.481-6.472)	0.907 (0.281-2.928)	0.841 (0.265-2.664)	0.539 (0.140-2.081)	0.490 (0.139-1.726)	0.484 (0.298-0.788)
p-value	0.413	**<.0001**	**0.001**	0.128	0.391	0.871	0.768	0.37	0.267	**0.004**
All	0.893 (0.667-1.196)	0.717 (0.537-0.958)	0.597 (0.393-0.908)	1.94 (0.92-4.091)	1.933 (0.832-4.492)	0.523 (0.172-1.588)	1.311 (0.648-2.650)	1.796 (0.872-3.699)	1.105 (0.543-2.250)	0.730 (0.551-0.968)
p-value	0.577	**0.025**	**0.016**	0.082	0.126	0.253	0.451	0.112	0.783	**0.029**

Pole and Wire hang tests were used as additional indicators of neuromotor function. No differences were seen at any age in Pole test analyses ($p>0.05$). However, the Wire Hang testing of young mice indicated that xenomitochondrial mice were less likely to fall than controls ($p=0.0035$). No difference was seen between groups of aged mice ($p>0.05$).

Oxygen consumption

Complex I linked respiration of mitochondria isolated from skeletal muscle of xenomitochondrial mice was 21.3±8.1 nmolO_2/min/CS vs. 23.7±8.1 nmolO_2/min/CS for controls. Xenomitochondrial respiration values were not different from controls ($p>0.05$).

Section 4 – Discussion

In phenotypic characterizations of xenomitochondrial mice, we hypothesized that mitochondrial energy production and, in turn, neuromotor activity might be altered. To test mitochondrial function, we examined oxygen consumption and motor function of xenomitochondrial mice. Respiration studies found no differences between xenomitochondrial and control mice. Neuromotor and muscular analyses involved both young (3-5 months of age) and older (9-14 months of age; equivalence to "middle aged" adult humans) xenomitochondrial mice. Few differences were detected between xenomitochondrial and control mice. Unexpectedly, young mice displayed the most differences. Perhaps more surprisingly, in tests where phenotypic differences were noted, xenomitochondrial mice exhibited superior performance. Compensatory changes in mitochondrial function to the point of superior function in response to mtDNA polymorphisms might explain these results. Alternatively, the mixture of 129S6 and C57BL/6NTac nuclear backgrounds of xenomitochondrial mice may play a role in apparent superior performance, even after more than 10 generations of backcrossing our xenomitochondrial maternal lineage with C57BL/6NTac males.

Given that several early *in vitro* experiments demonstrated varying levels of mitochondrial dysfunction in xenomitochondrial cells containing chimpanzee, gorilla, *R. norvegicus or M. terricolor* mtDNA, the absence of detectable phenotype in xenomitochondrial mice is noteworthy (Kenyon and Moraes, 1997; McKenzie and Trounce, 2000; McKenzie et al., 2004). It is clear that the specifics of cellular metabolism are altered in xenomitochondrial mice compared to cells studied *in vitro*, allowing relatively normal function despite presence of divergent mtDNA. These cellular conditions act as a compensatory mechanism, influencing *in vivo* development and mitochondrial function in xenomitochondrial mice. Identification and exploitation of this compensatory mechanism could reveal the specifics of the pathology of metabolic disorders and provide a valuable inroad to treatments for patients lacking many treatment options.

Our initial hypothesis was that genetic compensatory mechanisms in xenomitochondrial mice masked the defect seen in early *in vitro* experiments. The compensatory mechanisms were hypothesized to function primarily through alteration of expression of genes involved in mitochondrial biogenesis and function, allowing normal function of mitochondria in xenomitochondrial mice.

To test the genetic compensatory mechanism hypothesis, a full genome microarray was employed to analyze brain gene expression in three week old xenomitochondrial and control mice. Young mice were evaluated due to rapid growth; indicative of high rates of ATP utilization. RNA from brain was chosen for analysis due to the high metabolic requirements of this tissue. Due to the commonality of basic mechanisms of mitochondrial function between cells and tissues, basic compensatory mechanisms should be common as well, with tissues utilizing the most energy showing more pronounced responses due to rapid production of ATP. Given the high metabolic rate of neurons, it seems unlikely that genetic compensatory mechanisms would not be present in brain tissue while occurring in other tissues.

Genes identified by microarray as differentially expressed belonged to a family of immediate-early response genes; representing primarily transcription factors. qRT-PCR data validated down regulation of cFos, Egr2 and Egr4 while expression of other genes was not different than control. Considering the down regulation of these transcription factors, it is interesting that putative downstream targets were unaltered in their expression profiles. Down regulation of these transcription factors in xenomitochondrial mice could represent a lower baseline ability to alter expression of target genes when appropriate molecular signals are received. These changes in gene expression patterns could result in experimental mice less able to respond to cellular stress. Down regulation of proto-oncogenes could implicate mild mitochondrial dysfunction as a causative factor in oncogenesis if supported by other models (Gogvadze et al., 2008).

mtDNA-encoded transcript quantification proved much more difficult than initially expected due to mtDNA sequence divergence between xenomitochondrial and control samples. Microarray analysis identified massive down regulation of mtDNA-encoded genes in xenomitochondrial samples. These data turned out to be artifactual, as the signal in xenomitochondrial samples was at or near background levels for all mtDNA encoded genes. Sequence divergence between xenomitochondrial and control samples was such that control transcripts bound well to microarray probes for mtDNA genes, while xenomitochondrial transcripts bound very weakly. This sequence divergence also prohibited use of northern blot to quantify mtDNA-encoded transcripts, as differential probe affinity would lead to inaccurate data.

The PCR assay designed to measure Mt-Co2 expression was suboptimal due to the use of separate primer sets for xenomitochondrial and control samples. However, given the constraints of the model system, namely the sequence divergence present between xenomitochondrial and control mice, no other approach would have given better results. While this assay is only capable of approximating expression differences between groups, the approximation should be quite

accurate given that the efficiencies of the PCR primer sets used were so similar. PCR efficiency is a primary concern in this instance because the primers had slightly differing sequence. The amplified region of the mtDNA also has polymorphisms. This can lead to differing amplification efficiencies caused by different primer binding affinity or different amplicon melting or annealing temperatures. If the primers had amplified differently, the data would have been skewed toward an artifactual up regulation of the more efficient primer set.

Elimination of mtDNA contamination was difficult in qRT-PCR assays of Mt-Co2 gene expression due to lack of intron sequence in mtDNA encoded transcripts. Extensive DNase treatment was required to reduce mtDNA contamination to acceptable levels. In final analyses, Ct values from RT- samples were 10 or more cycles greater than corresponding RT+ samples. This difference indicates that mtDNA contamination levels represent less than $1/1024^{th}$ (2^{10}) the template present in RT+ samples. At this low level, any skewing of the data from mtDNA contamination is negligible.

Our discovery of up regulation of mtDNA-encoded Mt-Co2 is relevant to mitochondrial compensatory mechanisms. The up regulation of Mt-Co2 supports the hypothesis that mitochondrial transcription is increased. As mitochondrially encoded genes are transcribed as polycistronic RNAs, up regulation of Mt-Co2 indicates a general up regulation of mtDNA encoded genes. It is possible that up regulation of mtDNA-encoded genes allows increased mitochondrial biogenesis and an increased mass of ETC complexes. The up regulation of mtDNA transcription seems to occur in diseased states and during normal aging, though often this occurs concurrently with increased total mtDNA number (Heddi et al., 1999; Masuyama et al., 2005). It is particularly interesting that only mtDNA-encoded genes were up regulated in xenomitochondrial mice. This suggests that subunits encoded by mtDNA could represent a limiting factor in assembly of ETC complexes. The concept of mtDNA encoded subunits as rate limiting in the assembly of ETC complexes is supported in the literature (Lazarou et al., 2007).

Up regulation of mtDNA transcripts without nuclear transcriptional changes to genes involved in mitochondrial biogenesis suggests independent control these factors. Treatments targeting increased mtDNA transcription might be clinically relevant in efforts aimed at alleviation of symptoms associated with mild mitochondrial dysfunction.

While evidence of altered gene expression in xenomitochondrial mice provides insight into mitochondrial biology, identification of genes with no significant alteration in expression is also informative. Interestingly, aside from Mt-Co2, no changes in genes directly associated with mitochondrial energy production were identified. Further studies involving qPCR showed that there were no mtDNA copy number alterations occurring in the xenomitochondrial mice. Clearly, when faced with polymorphic mtDNA or mild respiratory stress, cells are able to compensate well without altering nuclear gene expression patterns. The alteration of mtDNA transcription could represent a simple way to alter mitochondrial biogenesis and function.

Aside from changes in genes encoded by mtDNA, it is also possible and likely that compensatory mechanisms involve translational alterations or changes in protein or complex activation. Control of mitochondrial energy production without alterations in gene expression would allow rapid and precise adaptation to fluctuating energetic requirements and mitochondrial efficiency. Changes in expression of nuclear genes involved in mitochondrial energy production or biogenesis could occur in response to more dramatic alterations in mitochondrial efficiency or cellular energetic requirements. Compensatory mechanisms could involve altered rates of mtDNA-encoded subunit production, translation of nuclear genes involved in mitochondrial energy production, intracellular trafficking of proteins involved in mitochondrial function or activation of proteins associated with cellular respiration or mitochondrial biogenesis. Future studies will quantify mtDNA encoded protein levels in xenomitochondrial mice by western blotting of cellular lysate and BN-PAGE will allow comparisons of intact ETC complexes.

In order to investigate the possibility that xenomitochondrial mice are selectively sensitive to metabolic stress due to compensation for mtDNA polymorphisms, future experiments will challenge mice with inhibitors of mitochondrial function and MPTP (1-methyl-4-phenyl-1,2,3,6-tetrahydropyridine). Exacerbations of effects are expected in xenomitochondrial mice. Ongoing studies will examine mice aged up to 24 months, equivalent to old humans, in order to determine if divergent mtDNA sequence increases the rate of senescence in xenomitochondrial mice. (X.Y. Kong, B.V. Bui, A.J. Vingrys, C.A. Pinkert, I.A. Trounce and J. Crowston, unpublished data). It is possible that such stressors will expose phenotypes related to mitochondrial dysfunction not evident under normal conditions.

Chapter 3 – Identification of proteins involved in RNA import from total cellular lysate

Section 1 – Introduction

The following experiments identify soluble proteins associating selectively with mitochondrially imported RNAs. We hypothesize that there are specific proteins involved in the import of RNAs into mitochondria. Furthermore, we hypothesize that any proteins involved in specifying which RNAs are imported should bind imported RNAs specifically. We utilized two primary experimental approaches to identify proteins specifically binding imported RNAs. RNA affinity purification is a protocol adapted from similar protocols in the literature (Lee and Schedl, 2001; Nabel-Rosen et al., 1999). Essentially, this protocol is an immunoprecipitation with a biotinylated RNA in lieu of an antibody. This allows purification of proteins binding to a specific RNA. Numerous experiments optimized the protocol, as outlined below. The second experiment, RNA immunoprecipitation (RIP), aimed to confirm the RNA affinity purification by identifying RNAs bound to immunoprecipitated proteins (Conrad, 2008; Gilbert and Svejstrup, 2006; Peritz et al., 2006). Several pre-optimized protocols were available, so less optimization was required. This protocol involved a standard immunoprecipitation, but focuses on the preservation of RNA integrity which is of critical importance for subsequent PCR analysis.

Section 2 – Optimization of RNA affinity purification

The RNA affinity purification protocol was loosely based on protocols found in the literature and tailored to the specific requirements of these experiments (Lee and Schedl, 2001; Nabel-Rosen et al., 1999). Many aspects of the protocol had to be optimized for subsequent experiments. Concentration of NaCl in wash buffer and lysis buffers had to be adjusted. Method for removing biotinylated RNAs from avidin beads and ratio of biotin-16-rUTP : rUTP needed to

be optimized to allow recovery of biotinylated RNAs while preventing protein binding to RNA due to the presence of biotin.

RNA affinity purification wash buffer NaCl concentration optimization

NIH/3T3 cells from four ~90% confluent 10cm plates were lysed in 4ml lysis buffer (20mM Tris-HCl, 100mM NaCl, 2.5mM $MgCl_2$, 1mM sodium orthovanadate, 0.5% Nonidet P-40, pH 7.5). 20µl protease inhibitor cocktail (Calbiochem®, set III, EDTA-free) was added and lysate was mixed. A syringe was used to shear DNA. Lysate was then centrifuged for twenty minutes at 14,000 x g at 4°C. Supernatant was recovered and placed into a new tube.

Neutravidin beads were prepared for RNA affinity purification by washing with lysis buffer followed by centrifugation and one volume lysis buffer was added to beads.

PCR amplicons were used as T7 polymerase template to produce RNAs labeled with biotin (1:100 mixture of biotin-16-rUTP : rUTP). PCR amplicon was removed by DNase treatment and a G-50 sepharose column was used to purify RNA for use in RNA affinity purification.

100µl aliquot of RNase inhibitor was added to NIH/3T3 lysate (4ml) to preserve RNA integrity. General RNA binding proteins were removed from lysate by incubation with 8µg biotin-conjugated negative control 4.5S RNA for one hour at 30°C with gentle shaking. 120µl avidin bead slurry was used to bind biotinylated RNAs during a 20 minute incubation with gentle shaking followed by centrifugation. These steps were repeated once to further remove non-specifically RNA binding proteins from lysate. To remove all biotinylated RNAs and any proteins binding only to avidin beads, lysate was cleared by addition of 120µl bead slurry, 20 minute incubation and centrifugation. These steps were repeated three times. The cleared lysate was split into individual aliquots and 1µg of a biotinylated mitochondrially imported RNA was added to individual aliquots (RNase MRP). These samples were incubated at 30°C for three hours with

gentle shaking. 60µl bead slurry was added to each aliquot, incubated 20 minutes at 30°C to allow binding of biotinylated RNAs to beads. Beads were centrifuged at 2,300 x g for two minutes, supernatant was saved in a separate tube and beads were washed twice with 1ml lysis buffer. The four samples were washed with 100% lysis buffer, 50% lysis buffer, 25% lysis buffer and 12.5% lysis buffer, respectively. Biotinylated RNAs were eluted from beads by Laemmli (125mM Tris-HCl, 20% glycerol, 10% 2-mercaptoethanol, 4% SDS and 0.004% bromophenol blue, pH 6.8) buffer.

Samples isolated using RNA affinity purification and washed with varying concentrations of lysis buffer were analyzed by SDS-PAGE (Figure 2). Diluted wash buffers caused an increase in both quantity and number of proteins present in final sample indicating that higher concentration wash buffer was more stringent.

Optimization of lysis buffer for RNA affinity purification

This experiment was performed as above, with the following modifications:

Sample volume was reduced to 250µl. Three lysate samples were prepared for analysis: the first was 250µl neat lysate, the second was 250µl lysate diluted with 250µl ddH_20 and the third was 250µl lysate diluted with 500µl. Thus, the total protein per sample was the same between samples. The beads at the end were washed with lysis buffer and Laemmli buffer was added to remove RNAs and bound proteins.

Samples isolated by RNA affinity purification using varying concentration of lysis buffer were analyzed by SDS-PAGE (Figure 3). Decreased lysis buffer concentration did not affect purification of RNA binding proteins.

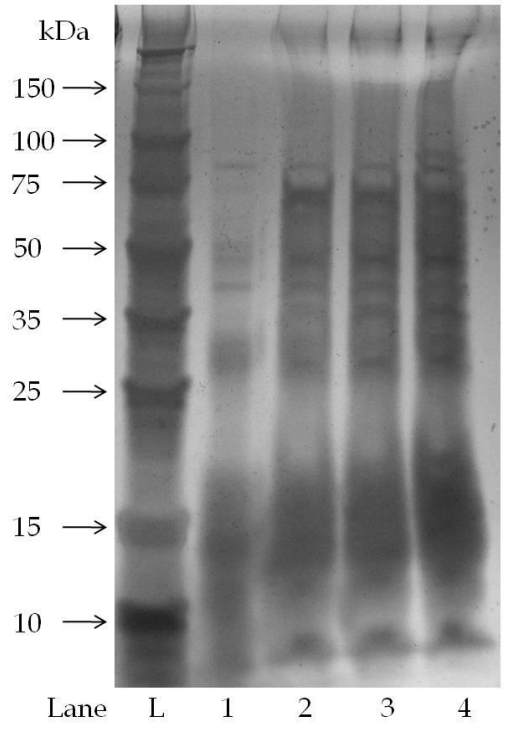

Figure 2: Silver stained SDS-PAGE analysis of proteins isolated by RNA affinity purification, testing wash buffer concentration.

Lane 1: Perfect Protein™ mass ladder, lane 2: final sample washed with standard lysis buffer, lane 3: final sample washed with 50% wash buffer, lane 4: final sample washed with 25% wash buffer, lane 5: final sample washed with 12.5% wash buffer. Note increasing intensity of bands in lanes 1-4. Increased quantity and intensity of bands in lane 4 indicates that low wash buffer concentration resulted in increased protein isolation, possibly resulting from increased non-specific binding of proteins to RNA bait. These results reveal that concentration of wash buffer affects protein isolation, with a less stringent wash buffer resulting from dilution.

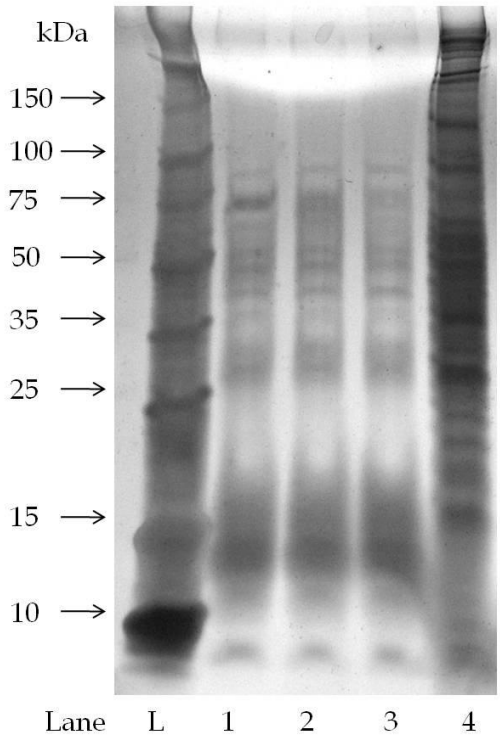

Figure 3: Silver stained SDS-PAGE analysis of proteins isolated by RNA affinity purification, testing lysis buffer concentration.

Lane 1: Perfect Protein™ mass ladder, lane 2: final sample isolated using 100% lysis buffer, lane 3: final sample isolated using 50% lysis buffer, lane 4 final sample isolated using 25% lysis buffer, lane 5: cellular lysate supernatant remaining at end of protocol, isolated using 100% lysis buffer. Note similarity of lanes 1-3 in number and intensity of bands, indicating that lysis buffer concentration did not alter final protein quantity isolated. Results demonstrate that diluted lysis buffer did not increase total protein isolated.

Optimization of biotin-16-rUTP : rUTP ratio for RNA synthesis reaction

This protocol was performed essentially as outlined above with the following exceptions: low salt lysis buffer (20mM Tris-HCl, 50mM NaCl, 2.5mM $MgCl_2$, 1mM Sodium orthovanadate, 0.5% Nonidet P-40, pH 7.5) was used and T7 production of biotinylated RNA produced RNAs with biotin-16-rUTP : rUTP ratio ranging from 1:100 to 1:5. Final bead pellet was resuspended in low salt lysis buffer and saturated NaCl was added to elute proteins from RNA.

Samples isolated by RNA affinity purification with increasing ratio of biotin-16-rUTP : rUTP were analyzed by SDS-PAGE to assess efficiency of protein isolation (Figure 4). There is a clear trend towards greater protein quantity when samples were purified with a higher ratio of biotin-16-rUTP : rUTP, with 1:5 exhibiting the most efficient purification. Note the increased number and intensity of bands in samples purified with RNAs containing more biotin molecules per RNA.

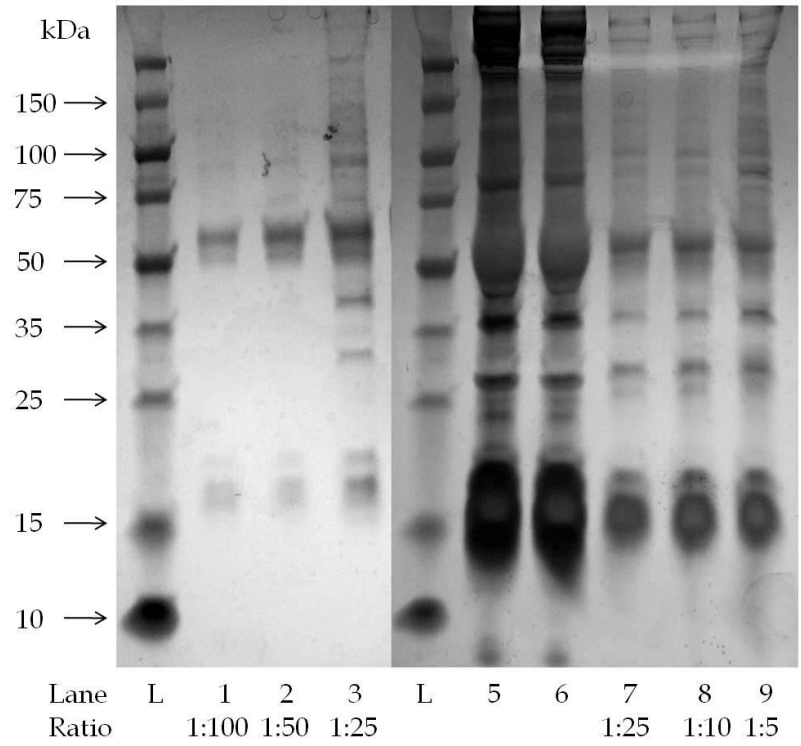

Figure 4: Silver stained SDS-PAGE analysis of proteins isolated by RNA affinity purification, testing ratio of biotin-16-rUTP : rUTP.

Lane L: Perfect Protein™ mass ladder, lane 1: final sample isolated with ratio of 1:100, lane 2: final sample isolated with ratio of 1:50, lane 3: final sample isolated with ratio of 1:25, lane L: Perfect Protein™ mass ladder, lane 5: sample isolated from blocking step, lane 6: sample isolated from blocking step, lane 7: final sample isolated with ratio of 1:25, lane 8: final sample isolated with ratio of 1:10, lane 9: final sample isolated with ratio of 1:5. Note increasing intensity and number of bands with increasing biotin-16-rUTP : rUTP ratio, which indicates that increased biotin numbers per RNA increased total protein recovered in final samples.

Optimization of elution methodology of RNAs from beads

Initial mass spectroscopy analyses of proteins isolated by RNA affinity purification revealed avidin contamination of samples due to use of Laemmli buffer elution, which prevented full analysis. Therefore, monomeric avidin beads were used in lieu of neutravidin beads. This allowed free biotin to elute bound RNAs from beads, eliminating the need for addition of Laemmli buffer. The RNA affinity purification protocol was performed essentially as outlined above, with the following modifications: Low salt lysis buffer was used to produce NIH/3T3 lysate and monomeric avidin beads were used and prepared as follows:

Monomeric avidin beads were prepared for RNA affinity purification by first centrifugation of 4ml bead slurry at 1,000 x g for three minutes to pellet beads. Beads were washed in 2ml lysis buffer and centrifuged again to pellet beads. Beads were incubated with 2ml lysis buffer containing 2mM biotin for five minutes on ice and centrifuged again to pellet beads. Beads were washed with 0.1M glycine pH 2.8 and centrifuged. Beads were washed with 2ml low salt lysis buffer, centrifuged and 2ml low salt lysis buffer was added. Beads were then incubated with lysis buffer containing 2mM biotin, incubated for 20 minutes at 30 C, then supernatants were collected after centrifugation. The beads were then incubated with lysis buffer containing 2mM biotin at 37°C.

Samples isolated by RNA affinity purification and eluted from beads under varying conditions were analyzed by SDS-PAGE to assess efficiency of protein elution (Figure 5). Initial elution left large amounts of protein bound to beads, which were eluted by incubation at 37°C.

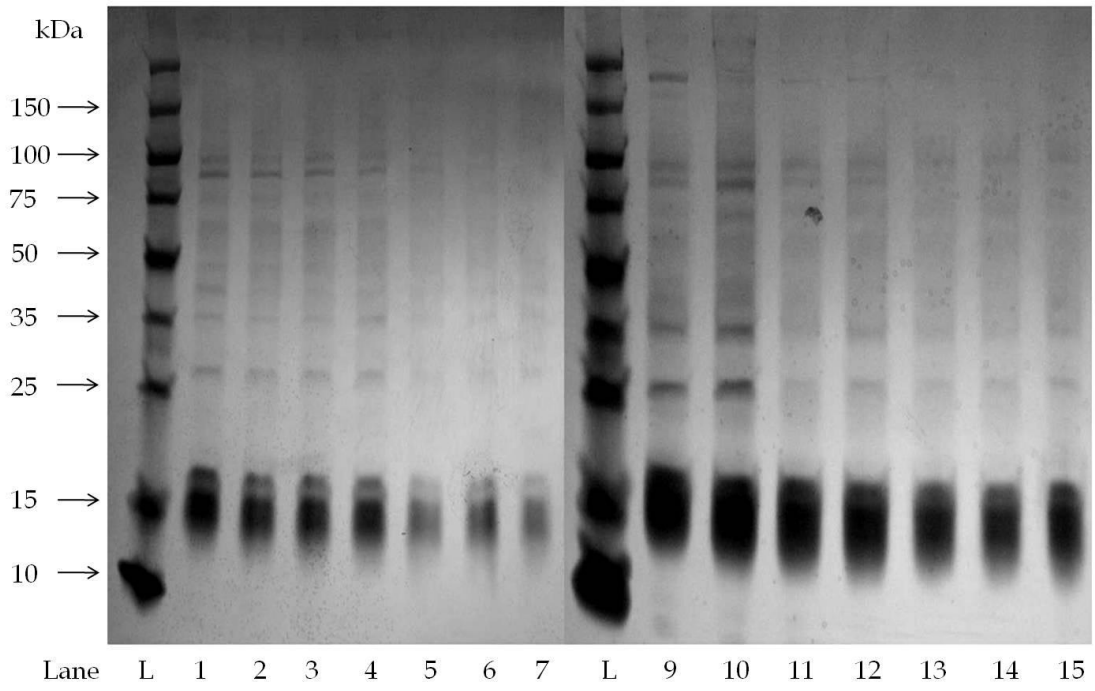

Figure 5: Silver stained SDS-PAGE analysis of experiment testing monomeric avidin bead elution conditions.

Protein gels show difference in protein eluted from avidin beads at different temperatures after RNA affinity purification. Lane L: Perfect Protein™ mass ladder, lanes 1-6, 9-14: blocking steps, lanes 7, 15: final samples, lanes 1-7: eluted by 20 minute incubation at 30°C, lanes 9-15: second elution from lane 1-7 beads, five minutes at 37°C. Note increase protein concentration in right half of figure indicating that a large quantity of protein was not eluted in the first elution step and was subsequently eluted by increased temperature.

Section 3 – Materials and methods

RNA affinity purification

RNA affinity purification experiments collected protein for liquid chromatography tandem mass spectroscopy (LC-MS/MS) analysis. Protocol was essentially as described above.

NIH/3T3 cells from four ~90% confluent 10cm plates were lysed in 8ml low salt lysis buffer (20mM Tris-HCl, 50mM NaCl, 2.5mM $MgCl_2$, 1mM Sodium orthovanadate, 0.17% Nonidet P-40, 0.17% Triton X-100, 0.17% Tween 20, pH 7.5) 120µl protease inhibitor cocktail (Calbiochem®, set III, EDTA-free) was added and lysate was mixed. Lysate was frozen in liquid nitrogen, then thawed in warm water, and placed back on ice. Lysate was shaken gently on ice for one hour and then centrifuged for twenty minutes at 14,000 x g at 4°C. Supernatant was recovered and placed into a new tube.

Monomeric avidin beads were prepared for RNA affinity purification by first centrifugation of 4ml bead slurry at 1,000 x g for three minutes to pellet beads. Beads were washed in 2ml lysis buffer and centrifuged again to pellet beads. Beads were incubated with 2ml lysis buffer containing 2mM biotin for five minutes on ice and centrifuged again to pellet beads. Beads were washed with 2ml 0.1M glycine pH 2.8 and centrifuged. Beads were washed with 2ml low salt lysis buffer, centrifuged and 2ml low salt lysis buffer was added.

PCR amplicons were used as T7 polymerase template to produce RNAs labeled with biotin (1:5 mixture of biotin-16-rUTP : rUTP). PCR amplicon was removed by DNase treatment and a G-50 sepharose column was used to purify RNA for use in RNA affinity purification.

200µl RNase inhibitor was added to NIH/3T3 lysate to preserve RNA integrity. General RNA binding proteins were removed from lysate by incubation with 8µg biotin-conjugated negative control 4.5S RNA for one hour at 30°C with gentle shaking. 480µl monomeric avidin

bead slurry was used to bind biotinylated RNAs during a 20 minute incubation with gentle shaking followed by centrifugation. These steps were repeated once to further remove non-specifically RNA binding proteins from lysate. To remove all biotinylated RNAs and any proteins binding only to avidin beads, lysate was cleared by addition of 480µl monomeric avidin bead slurry, 20 minute incubation and centrifugation. These steps were repeated three times. The cleared lysate was split into individual aliquots and 1µg of a biotinylated mitochondrially imported RNA was added to individual aliquots (5.8S rRNA, RNase MRP, RNase P and 5S rRNA). These samples were incubated at 30°C for three hours with gentle shaking. 60µl monomeric avidin bead slurry was added to each aliquot, incubated 20 minutes at 30°C to allow binding of biotinylated RNAs to beads. Beads were centrifuged at 2,300 x g for two minutes, supernatant was saved in a separate tube and beads were washed twice with 1ml lysis buffer. To elute RNA and protein, beads were incubated with lysis buffer containing 2mM biotin, incubated for 20 minutes at 30 C, then supernatant was collected after centrifugation. Protein samples were precipitated with an equal volume of 40% TCA and washed with ice-cold acetone for submission for LC-MS/MS analysis. To determine which identified proteins were of interest from mass spectroscopy results, the following selection process was utilized as visually represented in Figure 6. All identified proteins were placed into a list, with the bait RNA used noted. All proteins found to bind to negative control non-imported 4.5S RNA were removed from the list to remove any proteins not binding imported RNAs or binding to numerous RNAs in a non-specific manner. All proteins not bound to at least three imported RNAs were then removed from the list to eliminate proteins binding selectively to one or two RNAs. Alternative nomenclature was checked for remaining proteins, and any proteins that should have been removed during previous steps but included due to nomenclature were removed from the list. A BLAST search was then used to confirm that identified amino acid sequences were present only in indicated protein to prevent inclusion of proteins with uncertain identities. The short list of proteins at the end of this process was considered to be specifically interacting with imported RNAs.

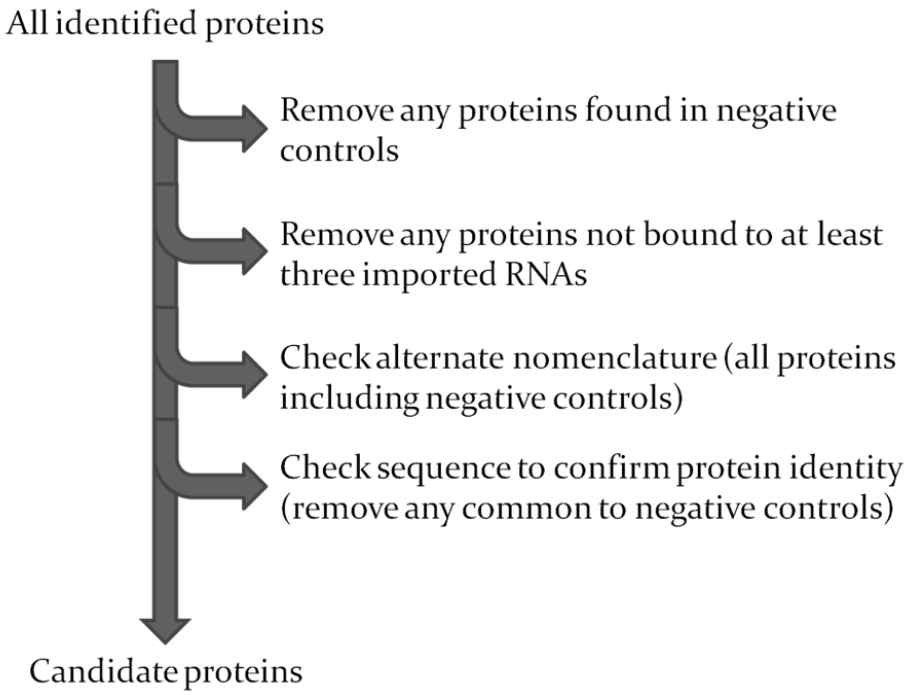

Figure 6: Selection process for identification of proteins potentially involved in RNA import from total mass spectroscopy results.

Protein hits were compiled into a single list following mass spectroscopy analysis, with RNA utilized for protein isolation noted. Proteins were removed from the list progressively utilizing the outlined procedure. Proteins not eliminated during the selection process were considered bound selectively to mitochondrially imported RNAs.

Western blotting

Antibody specificity was assessed by western blotting. Western blotting was performed according to standard protocols. Briefly, brain or heart was homogenized in RIPA buffer (150mM NaCl, 50mM Tris-HCl, 2mM EDTA, 1% NP-40, 0.5% sodium deoxycholate and 0.1% SDS, pH 7.4) with a Tissue-Tearor, then centrifuged for 20 minutes at 16,000xg. Lysate was mixed with Laemmli buffer and boiled at 100°C for ten minutes. Sample was separated by SDS-PAGE on a 10-20% gradient gel. Protein was transferred to a PVDF membrane, blocked with 5% BLOTTO for one hour at room temperature and washed three times with TBST (150mM NaCl, 20mM Tris-base and 0.1% Tween-20, pH 7.6). Membrane was placed into a Bio-Rad Mini-PROTEAN® II Multiscreen apparatus and antibody was applied to individual lanes in TBS (150mM NaCl and 20mM Tris-base, pH 7.6) with 1% BSA and incubated overnight at 4°C. In the morning, the antibody was removed and membrane was washed three times with TBST. HRP-conjugated secondary antibody in TBS was added to membrane and incubated for one hour at room temperature. Excess secondary antibody was removed by three washes with TBST. Blot was developed by incubation of membrane in 10ml 0.05% DAB in TBS (pH 6.0) with 10µl H_2O_2 for ten minutes. Once banding appeared, membrane was washed several times with TBS and imaged.

RNA immunoprecipitation

The RNA immunoprecipitation assay is designed to identify RNA: protein interactions by pulling targeted proteins out of solution by standard immunoprecipitation protocols followed by isolation and analysis of RNA from immunoprecipitated samples. The protocol used was adapted primarily from a published protocol (Conrad, 2008), with alterations inspired by Gilbert and Svejstrup (2006) and Peritz et al., (2006).

Formaldehyde crosslinking was omitted to avoid non-specific interactions. Early experiments showed that all proteins interacted with all RNAs when 0.5% formaldehyde

crosslinking was used (data not shown). In light of this, experiments were performed to determine optimal concentration of formaldehyde crosslinking for RIP analysis.

The first experiment was designed to investigate excessive crosslinking. It was noted in preliminary experiments that RNA was decreased in lysates crosslinked with formaldehyde compared to uncrosslinked controls, likely due to precipitation out of solution. In light of suspected over crosslinking, lysate RNA quantity was measured by qRT-PCR in lysates crosslinked with varying concentration of formaldehyde.

Lysates were produced from NIH/3T3 cells. Cells were washed with PBS (137mM NaCl, 2.7mM KCl, 4.3mM Na_2HPO_4 and 1.47mM KH_2PO_4, pH 7.4) once 90% confluent then incubated in 10ml PBS containing 0%, 0.025%, 0.05%, 0.1%, 0.2% or 0.4% formaldehyde and cells were crosslinked for ten minutes at room temperature. Crosslinking was terminated by 1.25ml 2M glycine pH 7.0 and incubated for five minutes at room temperature. Cells were harvested with a rubber policeman and centrifuged for three minutes at 700xg and washed twice with ice cold PBS. Cell pellet was stored at -80°C. Pellet was thawed and resuspended in 400µl RIPA-plus (0.15M NaCl, 0.05M Tris-HCl, 0.002M EDTA, 0.01M Vanadyl ribonucleoside complexes (VRC), 1% NP-40 (Nonidet® P-40 substitute, G-biosciences #DG0001), 0.5% sodium deoxycholate, 0.1% SDS and 2.5mg/ml torula yeast RNA, pH 7.4), 2µl 0.1mg/µl polyuridylic acid and 2µl 0.2M PMSF. Lysate was sonicated three times for five seconds each at setting 4. Lysate was then centrifuged at 16,000xg for ten minutes at 4°C to pellet insoluble material. Supernatant was eluted and 20µl was saved in separate tubes as the input controls. 130µl reverse buffer (0.01M Tris-HCl, 0.005M EDTA, 0.01M DTT and 1% SDS, pH 7.0) was added to lysate and samples were incubated at 70°C for 45 minutes to reverse formaldehyde crosslinks. 150µl 2X ProK (0.04M Tris-HCl, 0.005M EDTA, 0.2mg/ml proteinase K, 33.4ng/µl Glycoblue™, 0.2 mg/ml torula yeast RNA and 0.5mg/ml polyuridylic acid potassium salt, pH 7.0) and 3.75µl Promega RNase inhibitor was then added and protein was digested during a 30 minute incubation

at 37°C. RNA was isolated using TRIzol® and cDNA was created using Promega M-MLV following DNase treatment. RT± samples were analyzed by qRT-PCR using primers designed to amplify the 5S rRNA. Fold change relative to the formaldehyde negative sample was calculated to determine amount of RNA lost from lysate due to formaldehyde crosslinking.

Following this experiment, a RIP protocol was performed utilizing the two lowest concentrations of formaldehyde (0%, 0.025% and 0.05%) from the previous experiment to determine if non-specific interactions occur even when very little formaldehyde crosslinking is performed. Antibodies against 14-3-3 zeta and Tom40 were used and isolated RNA was reverse transcribed and qRT-PCR utilized 5S rRNA and 4.5 RNA specific primers. Fold change relative to the input control sample was calculated to investigate non-specific interactions due to formaldehyde crosslinking.

Final experiments were performed with no crosslinking. As reversal of crosslinking was not required, steps pertaining to reversal of crosslinking were omitted. Select proteins identified by RNA affinity purification were analyzed by RIP. Cellular role, ubiquitous expression and cellular localization were factors involved in narrowing down screened proteins. Samples were purified using either no antibody (bead only control), or antibodies (Santa Cruz) against 14-3-3 beta, 14-3-3 gamma, 14-3-3 zeta, HSP56, HSP90 alpha, Rad23B and TCP-1 gamma. Briefly, lysates were produced from NIH/3T3 cells in 10cm plates. Cells were washed with PBS once 90% confluent. Cells were harvested with a rubber policeman and centrifuged for three minutes at 700xg and washed twice with ice cold PBS. Pellet was resuspended in 400µl RIPA-plus, 2µl 0.1mg/µl polyuridylic acid and 2µl 0.2M PMSF. Lysate was sonicated six times for five seconds each at setting 4.5. Lysate was then centrifuged at 16,000xg for ten minutes at 4°C to pellet insoluble material. Supernatant was eluted and 20µl was saved in separate tubes as the input control. Protein A/G beads were prepared by washing with PBS once, incubated with 2µg antibody (no antibody or anti - 14-3-3 beta, 14-3-3 gamma, 14-3-3 zeta, HSP56, HSP90 alpha,

Rad23B or TCP-1 gamma) in 0.5ml PBS for two hours on ice, followed by two washes with RIPA-plus. 400µl supernatant was added to prepared protein A/G beads and shaken gently on ice for two hours. Beads were pelleted by centrifugation at 875xg for one minute and washed four times with ice-cold RIPA buffer through Pierce® spin columns.

RNA was isolated using TRIzol® and cDNA was created using Promega M-MLV reverse transcriptase following DNase treatment. RT± samples were analyzed by qRT-PCR using primers designed to amplify the 5S rRNA, 5.8S rRNA, RNase MRP RNA Th, RNase P RNA H1 and 4.5S RNA. Primers are listed below in Table 6.

Table 6: Primer sequences utilized in RIP qRT-PCRs

CCGGTAGTGGTGGCGCA	4.5S 1F
AGAAGAGTGCAAAGAAGAGGAGGA	4.5S R
GTCTACGGCCATACCACCC	5S 1F
AAAGCCTACAGCACCCGGTA	5S 121R C
GCGTCGATGAAGAACGCAGCGCTAGC	5.8S 31F
CAGGCGTAGCCCCGGGAGGAA	5.8S 136R
TCGCTCTGAAGGCCTGTTTCCTA	RNase MRP 4F
TCACTATGTGAGCTGACGGATGAC	RNase MRP 216R
GGGGGAGAGTAGTCTGAATTGGGTTA	RNase P 6F
GGAGGTGAGTTCCCAGAGAGCA	RNase P 6R

PCR efficiency was calculated for each primer set (Liu and Saint, 2002). Fold change of each antibody-purified sample vs. bead-only control was calculated by the following formula:

$$F=E^{(Ctc-Ctx)}$$

Where "F" is fold change, "E" is the efficiency of the PCR (2= 100% efficiency), "Ctc" is the Ct value of the control (beads) and "Ctx" is the Ct value of the experimental sample (sample purified with an antibody). RIP experiments were repeated five times to allow statistical analysis.

RIP qRT-PCR Ct results were analyzed by one-way ANOVA using SAS (N=5). A Dunnett's correction was used due to number of samples analyzed.

Section 4 – Results

RNA affinity purification

Raw mass spectroscopy results from RNA affinity purification using cellular lysate can be found in Appendix 1. From the list of all proteins identified, the proteins in Table 7 were selected as described above.

Western blots

Western blotting assays allowed evaluation of specificity of antibodies used in RIP experiments (Figure 7 and Figure 8). Antibodies assayed included 14-3-3 beta, gamma, zeta, HSP56, HSP90 alpha, TCP-1 gamma and Rad23B. Western blots using 14-3-3 beta, gamma, zeta, HSP56 and Rad23B revealed appropriate bands, though Rad23B also had one additional band. Western blots using HSP90 alpha and TCP-1 gamma antibodies had no banding, even at high primary antibody concentration (1:200).

Table 7: Proteins selected from mass spectroscopy results as likely involved in RNA import into mitochondria.

Proteins were selected utilizing procedure outlined in methods.

14-3-3 beta	Chaperones: known to be involved in protein import into mitochondria	(Morrison, 2009; Mrowiec and Schwappach, 2006; Obsilova et al., 2008)
14-3-3 gamma		
14-3-3 zeta		
Galectin-1 (β-galactoside binding protein)	Involved in apoptosis and mitogenesis	(Camby et al., 2006)
Calmodulin 1	Calcium homeostasis	(Clapham, 2007; Uhlen and Fritz, 2010)
HSP56 (FK506 binding protein 52)	Chaperone, interacts with HSP70 and HSP90	(Davies and Sanchez, 2005)
HSP90 alpha (Heat shock protein 1α or Hsp90aa1)	Mitochondrial chaperone	(Wayne and Bolon, 2007)
Keratin 6A	Intermediate filament	(Schweizer et al., 2006)
Matricin (TCP-1 gamma)	Chaperone protein	(Spiess et al., 2004)
Proteasome subunits α type-2, α type-3 and β type-2	Protease	(Jayarapu and Griffin, 2004)
RAD23B (UV excision repair protein RAD23 homolog)	Nucleotide excision DNA repair, protease	(Dantuma et al., 2009)

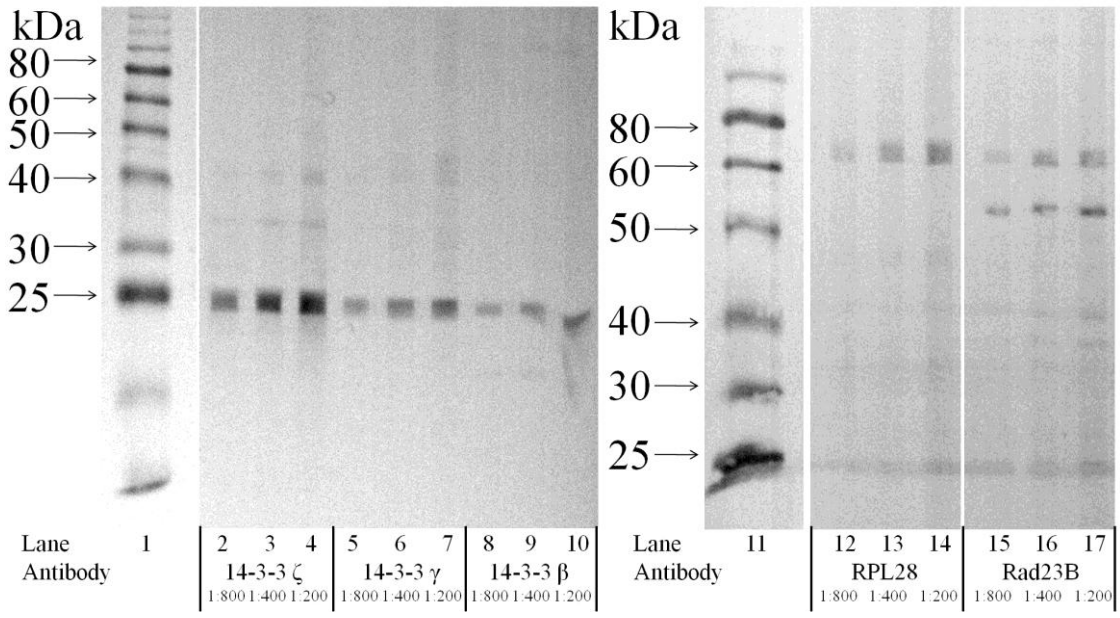

Figure 7: Western blot evaluation of antibody specificity for 14-3-3 zeta, gamma, beta, RPL28 and Rad23B.

Western blotting was used to assay specificity of antibodies used for RIP analyses. Antibody specificity was adequate for 14-3-3 zeta, gamma and beta. RPL28 had only one band, but of the wrong size (~70kDa instead of ~16kDa). Rad23B had an extra ~50kDa band. Lane1: mass ladder, lanes 2-4: 14-3-3 zeta antibody at 1:800, 1:400 and 1:200 primary antibody concentrations, lanes 5-7: 14-3-3 gamma at 1:800, 1:400 and 1:200 primary antibody concentrations, lanes 8-10: 14-3-3 beta at 1:800, 1:400 and 1:200 primary antibody concentrations, lane 11: mass ladder, lanes 12-14: RPL28 at 1:800, 1:400 and 1:200 primary antibody concentrations, lanes 15-17: Rad23B at 1:800, 1:400 and 1:200 primary antibody concentrations.

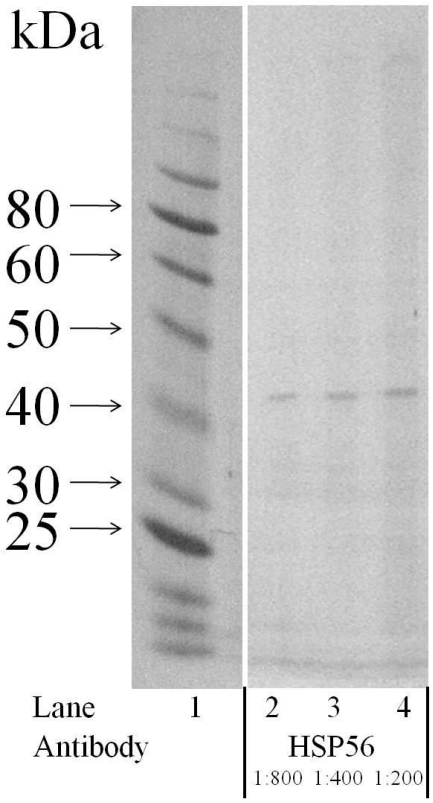

Figure 8: Western blot evaluation of antibody specificity for HSP56.

Western blotting assayed antibody specificity for HSP56. Band appeared to be ~45kDa, though due to curvature of dye front during electrophoresis, may have been closer to the proper size of 56kDa. Lane 1: mass ladder, lanes 2-4: HSP56 antibody at 1:800, 1:400 and 1:200 primary antibody concentrations

Investigation into decrease of RNA in lysate due to formaldehyde crosslinking during RNA immunoprecipitation

Experiments showed that 5S rRNA in input controls crosslinked with formaldehyde decreased dramatically with increasing formaldehyde crosslinking (Figure 9).

Assessment of non-specific protein:RNA interactions in a RIP assay using varying formaldehyde crosslinking

RNA immunoprecipitation was performed using 14-3-3 zeta and Tom40 antibodies on lysate crosslinked with varying concentrations of formaldehyde. qRT-PCR results demonstrate that 5S rRNA, which binds 14-3-3 zeta based on RNA affinity purification results, generally decreases with increasing formaldehyde concentration while 4.5S RNA, which should not bind 14-3-3 zeta increases with increasing formaldehyde concentration (Figure 10).

RIP analysis of proteins identified by RNA affinity purification

Proteins identified by RNA affinity purification were analyzed by RIP to confirm protein: RNA interactions. qRT-PCR with 5S rRNA, 5.8S rRNA, RNase MRP RNA Th, RNase P RNA H1 and 4.5S RNA primers quantified RNA samples (Figure 11). In raw PCR Ct values normalized to input lysate RNA Ct values, data were normally distributed, with no significant differences in variation between samples, nor did variation increase with mean. The only differences in RNA quantity between bead control and experimental samples was in RNase P quantity in TCP-1 samples and 5.8S rRNA quantity in RPL28 samples. No other statistically significant differences in RNA quantity were observed between bead controls and samples purified using antibodies. Statistical analysis data are presented in Appendices 6 and 7.

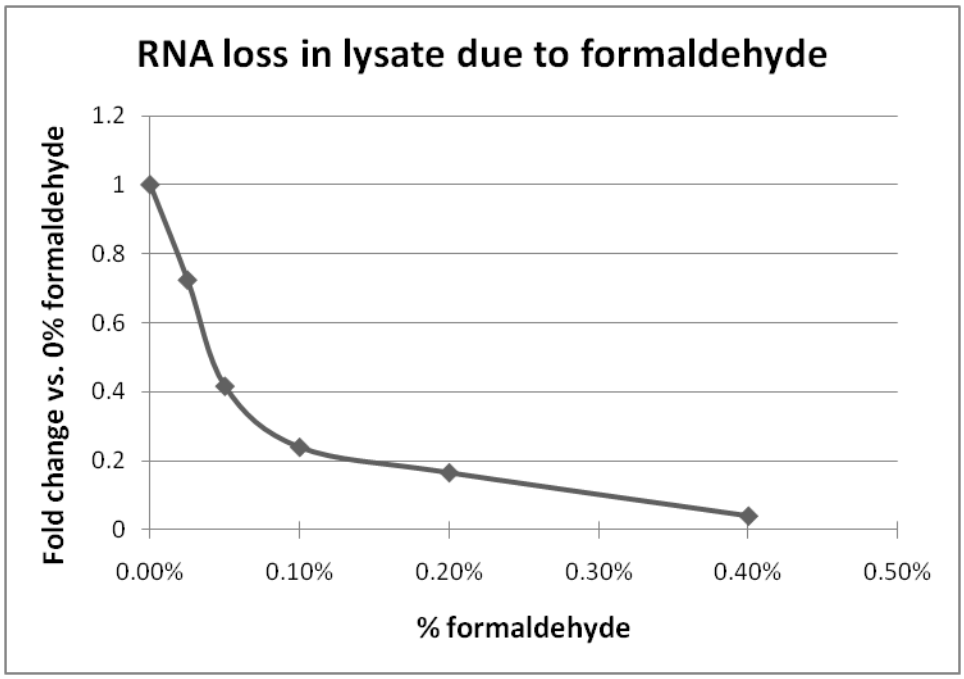

Figure 9: Formaldehyde crosslinking causes decrease of RNA in cellular lysate.

Whole cell lysate was isolated from cells crosslinked with varying amounts of formaldehyde. Following lysate isolation, formaldehyde crosslinks were reversed and RNA was isolated. 5S rRNA was quantified by qRT-PCR and was shown to decrease with increasing formaldehyde crosslinking demonstrating that increasing formaldehyde crosslinking causes a dramatic decrease in lysate RNA levels.

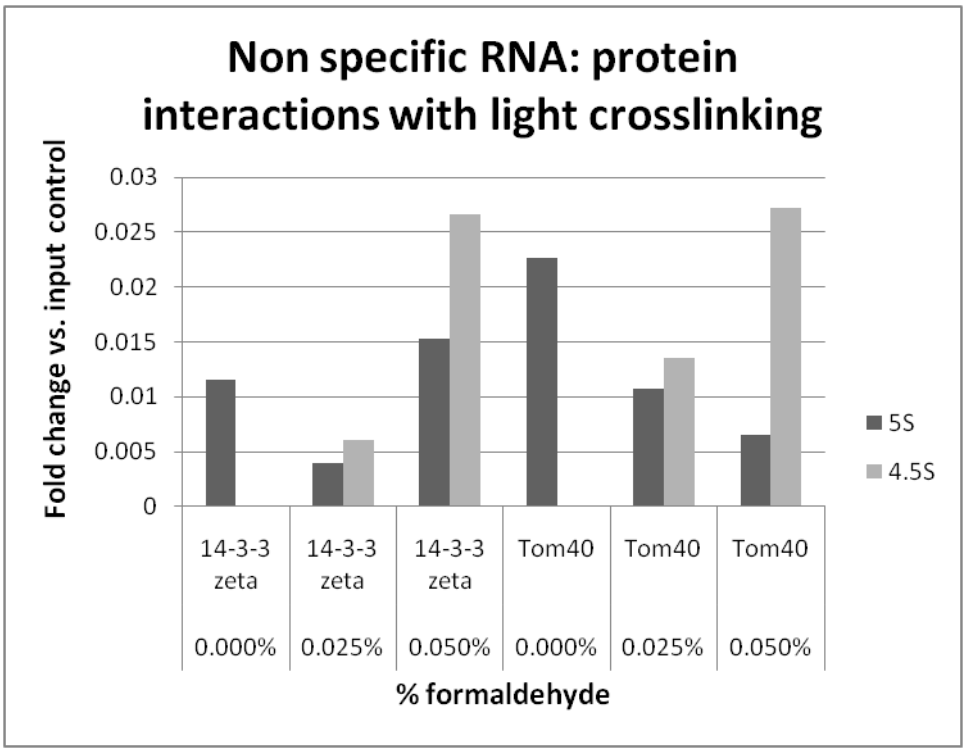

Figure 10: Non specific RNA: protein interactions with light crosslinking.

RNA immunoprecipitation was performed using 14-3-3 zeta and Tom40 with lysates either uncrosslinked or crosslinked with 0.025% or 0.05% formaldehyde. RNA was analyzed by qRT-PCR and data show that even miniscule amounts of formaldehyde are capable of inducing non-specific interactions, exhibited by increase of 4.5S RNA with increasing crosslinking.

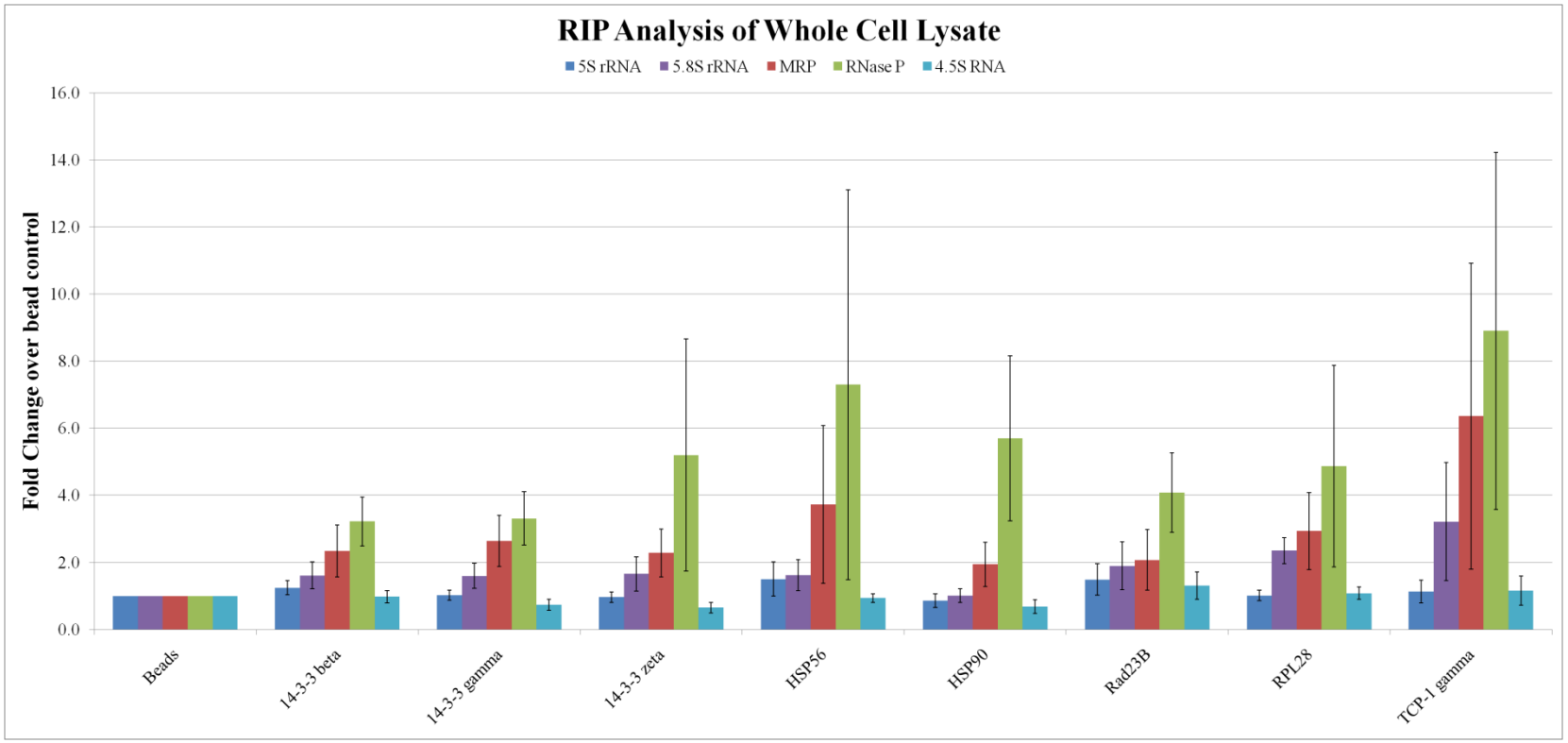

Figure 11: RNA immunoprecipitation analysis of proteins identified by RNA affinity purification of whole cell lysate.

Fold change of RNAs relative to bead control was calculated for all samples with 5S, 5.8S rRNA, RNase MRP RNA, RNase P RNA and 4.5S RNA primers (±SE). There were no differences compared to bead control ($p>0.05$), demonstrating that measured RNAs did not interact with proteins in this assay, including positive control RPL28.

Section 5 – Discussion

Data presented in the previous section demonstrate optimization of the RNA affinity purification protocol, identification of proteins specifically binding mitochondrially imported RNAs and attempts to confirm protein:RNA interactions.

Optimization steps revealed that the wash buffer concentration was important for protein: RNA interactions, with a dilute wash buffer causing a large increase in quantity of protein isolated likely representing non-specific interactions. In light of these results, wash buffer of equal concentration to the lysis buffer was used to avoid non-specific protein interactions.

The concentration of the lysis buffer seemed to be less important than the wash buffer concentration, with little difference seen in samples isolated using a more dilute lysis buffer. This is surprising in light of the wash buffer experiments, but it could represent less protein solubilized during lysis in the dilute lysis buffer leading to less protein isolated in the final steps.

The ratio of biotin-16-rUTP : rUTP was critical for efficient purification of proteins and recovery of the biotinylated RNAs. For the shortest RNA investigated, the 5S rRNA, at 121 nucleotides in length, assuming random nucleotide sequence, approximately 0.3 biotin molecules would be present on the RNA when a biotin-16-rUTP : rUTP of 1:100 is utilized ((RNA length/4) X (%rUTP biotinylated) = 121/4 X 0.01= 0.3025 biotin molecules per RNA). This increases to 0.605 biotin molecules per RNA at a 1:50 ratio, 1.21 biotin molecules per RNA at a 1:25 ratio, 3.025 biotin molecules per RNA at a 1:10 ratio and 6.05 biotin molecules per RNA at a 1:5 ratio. With roughly six biotin molecules per RNA molecule, it is very likely that the RNA will have a biotin molecule not covered by a bound

protein to allow binding of the RNA to the monomeric avidin beads and recovery out of solution. This assumption is backed up by the experiments correlating increasing ratio of biotin-16-rUTP : rUTP leading with increased protein isolated. At a higher ratio approaching 1:1 or 1:0, the inhibition of protein binding by biotin molecules would likely inhibit specific protein binding. A ratio of 1:5 was chosen for use in subsequent experiments.

Release of RNA and proteins from the beads was initially performed using neutravidin beads washed with Laemmli buffer. However, this approach led to large amounts of avidin in isolated samples, interfering with subsequent mass spectroscopy analysis. Following initial results, a protocol utilizing monomeric avidin beads eluted with free biotin proved ideal for isolation of samples. Elution time and temperature were tested and an elution of five minutes at 37°C released large amounts of protein compared to a longer incubation at 30°C. The 37°C incubation temperature was utilized in further protocols.

Affinity purification followed by LC-MS/MS revealed a long list of proteins bound to both imported and negative control non-imported RNAs. Following the outlined selection procedure, proteins bound only to imported RNAs were identified, confirming our hypothesis that proteins exist that bind specifically to imported RNAs. Several interesting proteins found bound to imported RNAs, including proteins known to act as chaperones and proteins known to associate with the mitochondria. The keratin 6A protein and the proteasome subunits likely represent proteins non-specific binding, based on their known functions.

If proteins selectively interact with imported RNAs, they are likely to play a role in the import of those RNAs into mitochondria. Thus, these experiments support the role of specific proteins in mitochondrial RNA import in mammals. Due to the solubilization conditions used, membrane complexes are unlikely to be in solution. It is therefore unlikely

that identified proteins will be part of a membrane bound complex in mitochondrial membranes. Identified proteins likely act as cytoplasmic chaperones functioning to direct imported RNAs to the mitochondrial surface for binding or transition to membrane bound proteins directing import through the mitochondrial membranes. It is therefore reasonable to suggest that the 14-3-3 beta, gamma, and zeta proteins, as well as Calmodulin 1, Galectin-1, Hsp56, Hsp90aa1, Rad23B and TCP-1 gamma are involved in the import of RNAs into mitochondria. Rhodanese, a protein recently shown to be important for mitochondrial RNA import, was not found bound to imported RNAs (Smirnov et al., 2010). Given that Rhodanese binds 5S rRNA co-translationally, binding of Rhodanese to introduced bait RNAs would not be possible during RNA affinity purification as translation stops after lysate production. It is possible that other proteins such as Rhodanese, which bind to imported RNAs co-translationally were also undetectable by the experiments performed due to the lack of translation of proteins within lysate.

Western blotting confirmed the specificity of the 14-3-3 beta, gamma and zeta antibodies for western blot analysis. HSP56 antibodies also showed a single band, though the size was slightly lower than expected. RPL28, Rad23B and TCP-1 gamma antibodies did not show single bands of the expected size, so cannot be considered specific for target proteins by western blot. However, differences between antibody recognition of denatured proteins on a membrane compared to native proteins in solution may be such that the antibody exhibits required specificity for immunoprecipitation. Determination of antibody specificity utilizing western blotting is only useful for excluding antibodies that create many bands on a western blot, indicating that they are capable of binding many different denatured targets. Therefore, western results do not indicate that any antibodies were unsuitable for RIP assays under native conditions.

RNA immunoprecipitation results show that formaldehyde crosslinking caused considerable non-specific protein-RNA interactions, even using very small amounts of formaldehyde. Experiments quantifying 5S rRNA in cellular lysates crosslinked with formaldehyde showed that formaldehyde caused a dramatic decrease in RNA in the input lysate. Interestingly, above roughly 0.1% formaldehyde, the amount of RNA lost from solution did not increase much, possibly indicating that formaldehyde crosslinking is approaching saturation. A subsequent RIP experiment demonstrated that even the lowest concentration of formaldehyde tested caused considerable increase in non-specific protein:RNA interactions, while potentially decreasing specific interactions. These results indicated that the use of formaldehyde crosslinking in RIP assays is sub-optimal.

Final RIP experiments did not confirm all protein:RNA interactions demonstrated by RNA affinity purification. Only interaction of TCP-1 with RNase P and RPL28 with 5.8S rRNA was validated. Variability in the results was higher than desired, making definitive statements regarding the other protein binding to investigated RNAs impossible.

Overall, experiments aimed at identification of proteins interacting selectively with imported RNAs revealed several proteins potentially involved in directing RNAs to the mitochondrial surface. Alternatively, proteins may bind at the outer mitochondrial membrane, recognize importable RNAs and transfer them to membrane complexes for import. These proteins function predominantly as cytoplasmic chaperones and select proteins function in the import of proteins into the mitochondria. That proteins known to play a role in mitochondrial protein import can interact with imported RNAs suggests that RNA transport across the outer mitochondrial membrane may involve the TOM complex. Hsp90aa1 binds to the TOM complex directly, while Hsp56 is capable of binding to Hsp90aa1 (Fan et al., 2006;

Silverstein et al., 1999). Thus, the identification of these proteins provides a foothold with which future research can begin to fully explore mechanisms of RNA import.

Future studies will involve focused work to demonstrate the direct binding of identified proteins to imported RNAs by RNase protection and gel mobility shift assays. These tests will not reveal, however, if a protein plays a role in RNA import not involving direct binding of the RNAs. Other approaches will be necessary to identify and characterize such proteins.

Given the apparent role of the TOM complex in RNA import across the outer mitochondrial membrane, future work will aim to characterize if and how the TOM complex is involved. A top down approach would focus on testing TOM complex ability to transport RNAs across membranes by integration of purified intact TOM complexes into liposomes, followed by RNA import assays. Integration of purified Tom40 protein alone, then in combination with TOM complex proteins, would represent a bottom up approach to evaluation of which proteins are necessary and sufficient for RNA import. Similar approaches with the TIM complexes could evaluate RNA import ability across the inner mitochondrial membrane.

Chapter 4 – Identification of proteins involved in RNA import from mitochondrial lysate

Section 1 – Introduction

Identification of proteins from the mitochondria specifically binding to imported RNAs will aid in analysis of mechanisms involved in mitochondrial RNA import. RNA affinity purification using mitochondrial lysates serve two purposes. First, enrichment of mitochondrial protein allows identification of proteins that may have been undetectable when isolated from whole cell lysates. Second, careful solubilization of mitochondria allows identification of membrane bound proteins playing a role in RNA import and provides invaluable insight into the mechanisms of RNA import. These two types of RNA affinity purification experiments also allow identification of different classes of mitochondrial proteins. RNA affinity purification using a mixture of three mild detergents facilitates purification of soluble mitochondrial proteins. Further experiments with carefully solubilized mitochondrial lysates allow isolation of membrane bound proteins. Solubilization of membrane bound proteins is a balancing act between not getting protein complexes into solution and breaking protein complexes apart and denaturing proteins. Once proper solubilization conditions are optimized, the association of RNAs with solubilized membrane proteins can be investigated by RNA affinity purification and RIP analyses to reveal membrane proteins in the mitochondria that function to import RNAs into the mitochondrial matrix. We hypothesize that proteins functioning in the recognition of RNAs for import into mitochondria should bind specifically to imported RNAs. The experiments outlined here aim to identify mitochondrial proteins selectively interacting with imported RNAs. Such proteins

are likely involved in the import of RNA into mitochondria and allow future studies will uncover the precise mechanisms of import of RNAs into the mitochondria.

Section 2 – Materials and methods

Optimization of mitochondrial solubilization

Proper mitochondrial solubilization conditions were determined by solubilization of mitochondria in various detergents at varying concentrations. Mouse liver mitochondria were isolated by standard differential centrifugation (Graham, 2001a). Mitochondrial protein concentration was measured using the Pierce® 660nM protein assay and a BSA standard. Mitochondria were resuspended in 200µl lysis buffer lacking detergent (20mM Tris-HCl, 50mM NaCl, 2.5mM $MgCl_2$, 1mM Sodium orthovanadate pH 7.5) at a total concentration of 5µg/µl (first experiment) or 10µg/µl (second experiment) and 5.25µl protease inhibitor cocktail was added. Detergent was added to each sample (from 20% dilution stock in first experiment, neat in second experiment), sample was vortexed briefly and then frozen in liquid nitrogen. Samples were then thawed in warm water and shaken on ice for 30 minutes to allow solubilization of mitochondrial protein. Samples were then centrifuged at 16,000 xg for 20 minutes at 4°C. Detergent concentrations were chosen based on published protocols. Detergents tested included digitonin, dodecyl maltoside, Triton X-100, Tween 20 and NP-40 either singly or in pairs at varying concentrations and the resultant lysate was analyzed by blue native PAGE (BN-PAGE) to assess mitochondrial solubilization (Gallagher, 2001; Krebs et al., 1979; Wittig et al., 2006).

RNA affinity purification using a mitochondrial lysate

RNA affinity purification was performed as described above, using either lysis buffer with a mixture of three detergents or carefully prepared mitochondrial lysate. Briefly, liver mitochondria were isolated by differential centrifugation and Pierce® 660nM protein assay was used to determine protein concentration. 80mg of mitochondrial protein was solubilized in 8ml lysis buffer (20mM Tris-HCl, 50mM NaCl, 2.5mM $MgCl_2$, 1mM Sodium orthovanadate pH 7.5) containing either 6mg digitonin/mg mitochondrial protein and 1.5µl Triton X-100/mg mitochondrial protein or 0.25% each NP-40, Tween 20 and Triton X-100. 210µl protease inhibitor cocktail was included to prevent protein degradation. Lysate was vortexed, frozen in liquid nitrogen, thawed in warm water and then gently shaken on ice for 30 minutes. Non-solubilized material was removed by a 20-minute centrifugation at 4°C at 16,000xg. Monomeric avidin beads were prepared by washing once with lysis buffer, then incubated with lysis buffer containing 2mM biotin for five minutes. Beads were washed with 0.1M glycine (pH 2.8), then lysis buffer and resuspended in equal volume of lysis buffer. PCR amplicons were used as template in T7 reactions to produce biotinylated RNAs with a biotin-16-rUTP : rUTP ratio of 1:5. T7 reactions were treated with DNase and RNA was purified with G-50 sepharose columns. Lysate (8ml) was first cleared twice by incubation of 8µg biotinylated 4.5S RNA in lysate for 30 minutes at 30°C with gentle shaking, followed by a five minute incubation with 480µl prepared monomeric avidin beads at 30°C with shaking. Beads were removed by centrifugation, 480µl additional beads were added, incubated for five minutes at 30°C with shaking to clear any remaining biotinylated RNAs, and beads were removed by centrifugation. This was repeated three additional times. Resulting lysates were then split into four individual aliquots and 2µg biotinylated RNA (5.8S rRNA, H1 RNA, Th RNA or 5S rRNA) were added and incubated for 30 minutes at 30°C with gentle shaking.

Prepared monomeric avidin beads (60µl) were then added and incubated for five minutes at 30°C with shaking. Supernatants were removed and beads were pelleted and washed twice through Pierce® spin columns with lysis buffer containing 1/10th volume detergents. Proteins and RNAs were eluted by incubation of beads with lysis buffer containing 2mM biotin for five minutes at 37°C. Supernatants were either precipitated with equal volume 40% TCA, stored overnight at 4°C, centrifuged for 20 minutes at 4°C and washed with ice cold acetone or analyzed by SDS-PAGE. TCA pelleted proteins were submitted for LC-MS/MS. Samples isolated with digitonin/Triton X-100 solubilized mitochondria were analyzed by SDS-PAGE for isolation of individual bands. Bands were visualized by SYPRO® Ruby and bands enriched in samples isolated using imported RNAs over non-imported 4.5S RNA lanes were excised and analyzed by LC-MS/MS. The same selection process was used to select proteins potentially involved in RNA import as was used in RNA affinity purification experiments using whole cell lysates.

Western blot

Antibody specificity was assessed by western blot. Western blots were performed according to standard protocols (Gallagher et al., 2008). Briefly, brain or heart was homogenized in RIPA buffer with a Tissue-Tearor, and then centrifuged for 20 minutes at 16,000xg. Lysate was mixed with Laemmli buffer and boiled at 100°C for ten minutes. Sample was separated by SDS-PAGE on a 10-20% gradient gel. Protein was transferred to a PVDF membrane, blocked with 5% BLOTTO for one hour at room temperature and washed three times with TBST. Membrane was placed into a Bio-Rad Mini-PROTEAN® II Multiscreen apparatus and antibody was applied to individual lanes in TBS containing 1% BSA and incubated overnight at 4°C. In the morning, the antibody was removed and

membrane was washed three times with TBST. HRP-conjugated secondary antibody in TBS was added to membrane and incubated for one hour at room temperature. Excess secondary antibody was removed by three washes with TBST. Blot was developed by incubation of membrane in 10ml 0.05% DAB in TBS (pH 6.0) with 10µl H_2O_2 for ten minutes. Once banding appeared, membrane was washed several times with TBS and imaged.

RNA immunoprecipitation

Select proteins identified by RNA affinity purification were analyzed by RIP. Additionally, Tim23, Tom40 and VDAC1 were analyzed due to potential roles in RNA import. Cellular role, ubiquitous expression and cellular localization were factors involved in narrowing down screened proteins. RNA immunoprecipitation was performed as outlined above. Briefly, lysate was produced from NIH/3T3 cells in 10cm plates. Cells were washed with PBS once 90% confluent. Cells were harvested with a rubber policeman and centrifuged for three minutes at 700xg and washed twice with ice cold PBS. Pellet was resuspended in 400µl RIPA-plus (0.15M NaCl, 0.05M Tris-HCl, 0.002M EDTA, 0.01M VRC, 1% NP-40, 0.5% sodium deoxycholate, 0.1% SDS and 2.5mg/ml torula yeast RNA pH 7.4) and 2µl 0.1mg/µl polyuridylic acid and 2µl 0.2M PMSF. Lysate was sonicated six times for five seconds each at setting 4.5, then centrifuged at 16,000xg for ten minutes at 4°C to pellet insoluble material. Supernatant was eluted and 20µl aliquots were saved in separate tubes as the input control. Protein A/G beads were prepared by washing with PBS once, incubated with 2µg antibody (anti-ATP5A, ATP5B, PCCB, Tim23, Tom40 and VDAC1) in 0.5ml PBS for two hours on ice, followed by two washes with RIPA-plus. 400µl supernatants were added to prepared protein A/G beads and shaken gently on ice for two hours. Beads were

pelleted by centrifugation at 875xg for one minute and washed four times with ice-cold RIPA buffer.

RNA was isolated using TRIzol® and cDNA was created using Promega M-MLV following DNase treatment. RT± samples were analyzed by qRT-PCR using primers designed to amplify the 5S rRNA, 5.8S rRNA, RNase MRP RNA Th, RNase P RNA H1 and 4.5S RNA.

PCR efficiency was calculated for each primer set (Liu and Saint, 2002). Primer sequences are shown in Table 8.

Fold change of each antibody-purified sample vs. bead control was calculated by the following formula:

$$F=E^{(Ctc-Ctx)}$$

Where "F" is fold change, "E" is the efficiency of the PCR (2 = 100% efficiency), "Ctc" is the Ct value of the control (beads) and "Ctx" is the Ct value of the experimental sample (sample purified with an antibody). RIP experiments were repeated five times to allow statistical analysis.

RIP qRT-PCR Ct results were analyzed by one-way ANOVA using SAS. A Dunnett's correction was used due to number of samples analyzed.

Table 8: Primer sequences utilized to quantify cDNAs for RIP analysis.

CCGGTAGTGGTGGCGCA	4.5S F
AGAAGAGTGCAAAGAAGAGGAGGA	4.5 R
GTCTACGGCCATACCACCC	5S 1F
AAAGCCTACAGCACCCGGTA	5S 121R
GCGTCGATGAAGAACGCAGCGCTAGC	5.8S 31F
CAGGCGTAGCCCCGGGAGGAA	5.8S 136R
TCGCTCTGAAGGCCTGTTTCCTA	RNase MRP 4F
TCACTATGTGAGCTGACGGATGAC	RNase MRP 216R
GGGGGAGAGTAGTCTGAATTGGGTTA	RNase P 6F
GGAGGTGAGTTCCCAGAGAGCA	RNase P 6R

Section 3 – Results

Optimization of detergent solubilization of mitochondria for mitochondrial lysates in RNA affinity purification

Experiments were undertaken to determine optimal solubilization conditions for production of lysates for RNA affinity purification. Triton X-100, Tween 20, digitonin and NP-40 were used both singly and in combination to solubilize mitochondria. Resulting lysates were separated by BN-PAGE to ascertain if high molecular weight complexes were intact in solution. Results from two separate experiments are illustrated in Figure 12 and Figure 13. A combination of digitonin and Triton X-100 solubilized high molecular weight complexes well.

RNA affinity purification

Samples prepared by RNA affinity purification were precipitated with TCA and analyzed by LC-MS/MS (samples prepared from mixture of three detergents) or analyzed by SDS-PAGE and bands found to be enriched in samples purified using imported RNAs were analyzed by LC-MS/MS to identify proteins (carefully solubilized mitochondrial lysate). Proteins identified were screened for those interacting selectively with imported RNAs. Table 9 lists proteins selected from the total list of all proteins identified (Appendices 2 and 3).

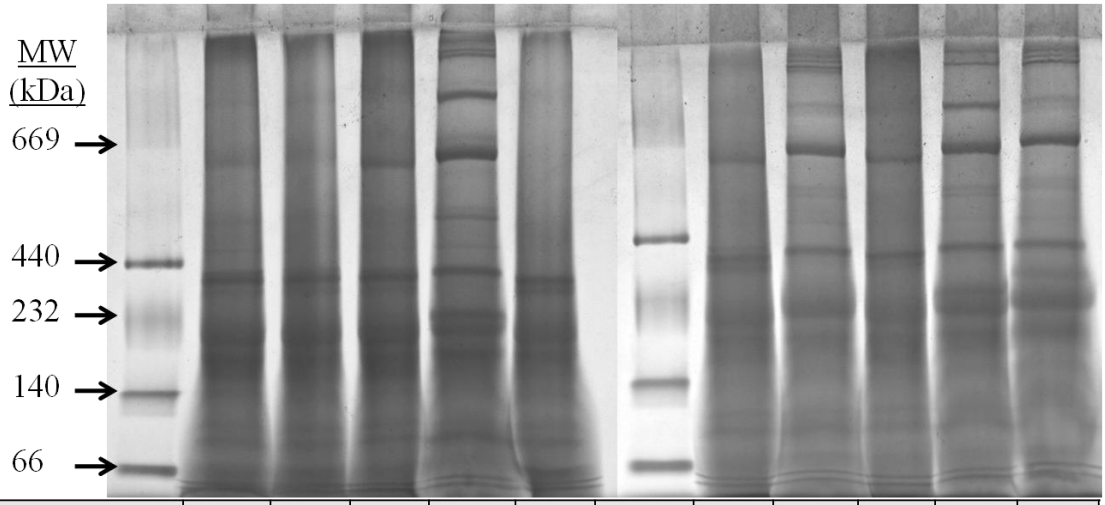

TritonX-100 (µl/mg)	3	1.5	1.5	1.5							
Tween-20 (µl/mg)		1.5			3		1.5	1.5			
D.D.M. (µl/mg)			1. 3				1. 3		2.5	1.3	
Digitonin (mg/mg)				6				6		6	12

Figure 12: BN-PAGE analysis of mitochondria solubilized with detergents to assess solubilization of high molecular weight complexes.

Triton X-100, Tween 20, dodecyl maltoside (DDM) and/or digitonin (µl or mg detergent/mg mitochondrial protein) solubilized mitochondria (5 µg/µl in 200µl) to varying degrees. Blue Native-PAGE reveals that high molecular weight complexes were solubilized in highest quantity when lysate was solubilized with digitonin. Solubilization by digitonin was enhanced by Triton X-100, evidenced by the increase in high molecular weight bands in the lane containing sample solubilized with both digitonin and Triton X-100. Increase high molecular weight bands demonstrates that mitochondrial complexes are in solution and intact.

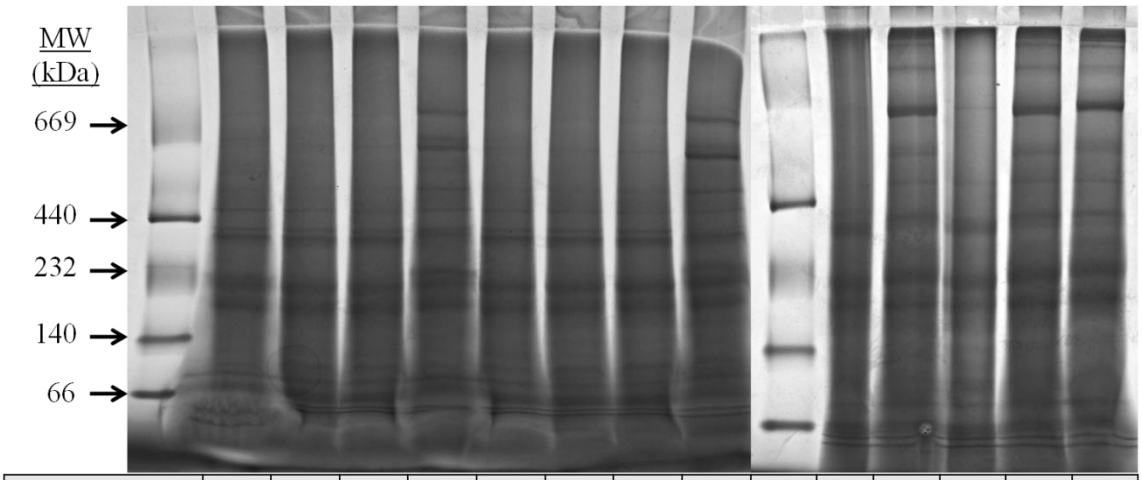

TritonX-100 (µl/mg)	3	1.5	1.5	1.5	1.5	.75	.75	.75						
NP-40 (µl/mg)		1.5	.75			1.5	.75			3	1.5	1.5	.75	
Digitonin (mg/mg)				3				3			3		3	6

Figure 13: BN-PAGE analysis of mitochondria solubilized with detergents to assess solubilization of mitochondrial complexes.

Triton X-100, NP-40 and/or digitonin (µl or mg detergent/mg mitochondrial protein) were used to solubilize mitochondria (10 µg/µl in 200ul) and resulting lysate was analyzed by BN-PAGE to determine if high molecular weight complexes were in solution. High molecular weight bands in samples purified using digitonin indicate solubilization of high molecular weight complexes in solution.

Table 9: Proteins associating specifically with imported RNAs in mitochondrial lysates identified mass spectroscopy following RNA affinity purification.

Argininosuccinate synthetase	Mitochondrial enzyme: urea cycle	(Husson et al., 2003)
ATP5A (ATP synthase, H+ transporting, mitochondrial F1 complex, alpha polypeptide)	Subunit of electron chain complex five	(Nakamoto et al., 2008)
ATP5B (ATP synthase, H+ transporting, mitochondrial F1 complex, beta polypeptide)	Subunit of electron chain complex five	(Nakamoto et al., 2008)
Mitochondrial aldehyde dehydrogenase 2	Alcohol metabolism	(Daiber et al., 2009)
PCCB (Propionyl Coenzyme A carboxylase, beta polypeptide)	Catabolism of propionyl Co-A - fatty acid metabolism	(Kim et al., 2002)
Cathepsin D	Protease	(Zaidi et al., 2008)

Protein analysis

Western blotting allowed investigation of antibody specificity for antibodies used in RIP analyses (Figure 14). ATP5B and Tom40 western blots showed that antibodies produced bands of the expected size with no additional major bands. Western blots utilizing ATP5A, PCCB, Tim23 and VDAC1 antibodies produced no bands.

RNA immunoprecipitation of proteins identified by RNA affinity purification

RNA affinity purification on did not confirm all protein:RNA interactions revealed by RNA affinity purification (Figure 15). Interaction of TOM40 with RNase P was validated by RIP analysis. Variability in the results was higher than desired, making definitive statements regarding the association of other identified proteins with imported RNAs impossible. Statistical analysis of RIP data is presented in Appendices 6 and 7.

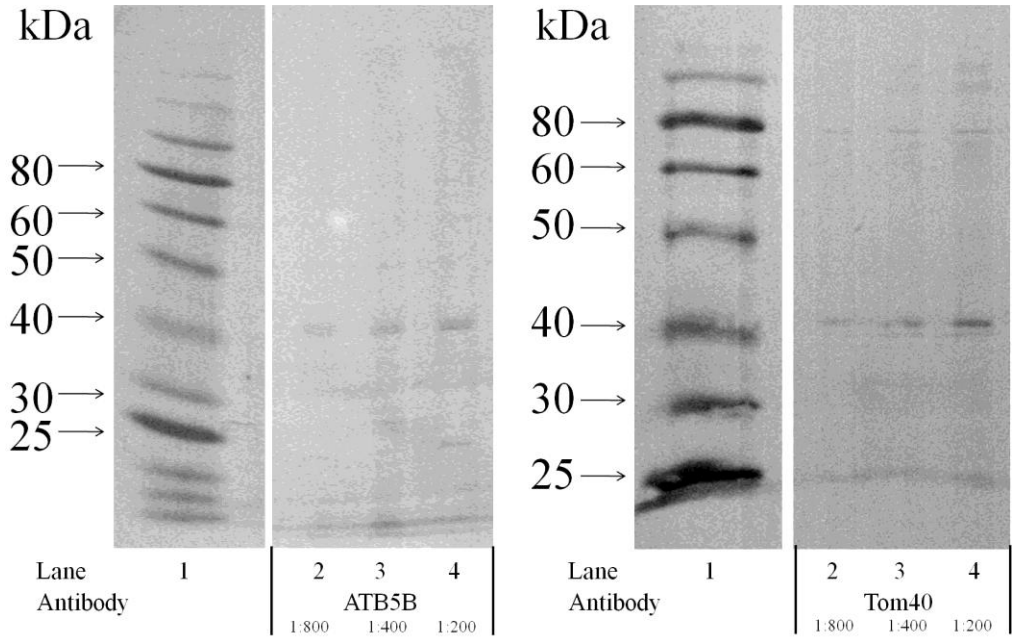

Figure 14: Western blot demonstrating specificity of ATP5B and Tom40 antibodies.

Western blots were used to assess specificity of ATP5B and Tom40 antibodies. Band from ATP5B appeared to be around 40kDa, though curvature of the dye front makes accurate determination difficult. It is possible that the band was near the appropriate size of 56kDa. Tom40 antibodies created a band of the proper size (40kDa), and a much fainter secondary band of around 80kDa. Lane 1: mass ladder, lanes 2-4: ATP5B antibodies at 1:800, 1:400 and 1:200 primary antibody concentrations, lane 5: mass ladder, lanes 6-8: Tom40 antibodies at 1:800, 1:400 and 1:200 primary antibody concentrations.

.

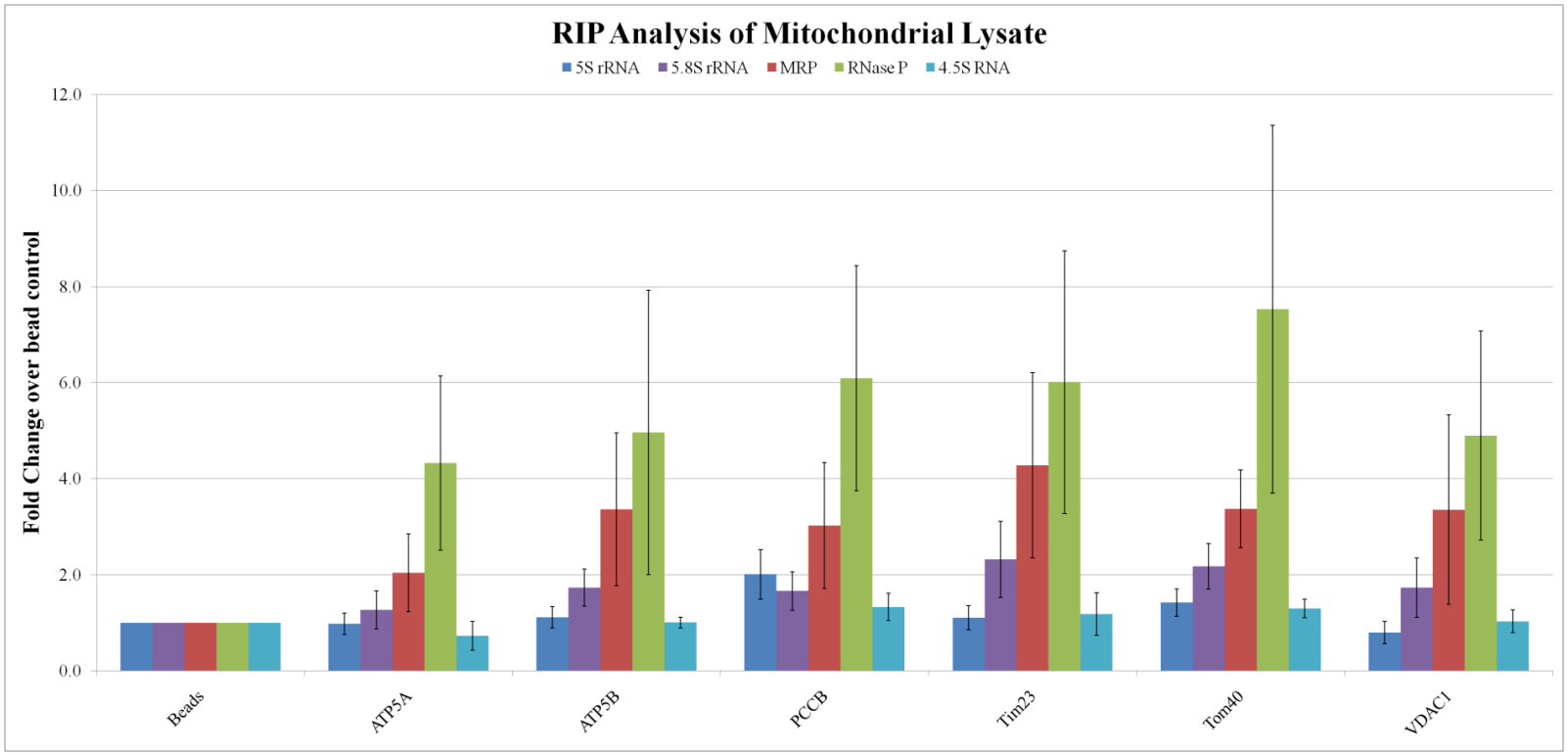

Figure 15 : RNA immunoprecipitation analysis of proteins identified by RNA affinity purification of mitochondrial lysate.

The fold change relative to bead controls was calculated for all samples for 5S, 5.8S rRNA, RNase MRP RNA, RNase P RNA and 4.5S RNA. No differences were noted in treatment groups compared to bead controls (P>0.05) demonstrating that measured RNAs did not interact with proteins in this assay.

Section 4 – Discussion

Initial experiments optimized creation of mitochondrial lysates containing solubilized membrane complexes with a role in RNA import. Complex integrity is important for subsequent experiments designed to identify membrane bound complexes binding imported RNAs. Solubilization experiments evaluated by blue native PAGE demonstrated optimal conditions to produce a lysate for RNA affinity purification.

RNA affinity purification experiments evaluating mitochondrial lysates identified several proteins associated with imported RNAs. Among the most interesting proteins identified were subunits of ATP synthase. The identification of ATP synthase subunit alpha parallels research on protists where the alpha subunit was found to be a component of a RNA import complex functioning in direct binding of imported tRNAs. The identification of ATP synthase subunit beta indicates that this protein may be involved in mammals, distinct from the protist system. The identification of argininosuccinate synthetase, mitochondrial aldehyde dehydrogenase 2 and PCCB is also interesting, as these are enzymatic proteins. Mitochondrial aldehyde dehydrogenase 2 is particularly interesting, as a recent report identified aldehyde dehydrognase as a protein potentially binding the 5S rRNA, though the authors were uncertain if the protein identified was the mitochondrial or cytoplasmic isoform (Smirnov et al., 2010). The protein PNPase was not identified during RNA affinity purification experiments, despite a recent report that this protein is important for the import of RNAs into mitochondria (Wang et al., 2010). The lack of RNA binding in the outlined experiments may be due to phosphorylation or ATP requirements of PNPase, or solubilization may have disrupted either the secondary structure or protein:protein interactions required for RNA binding.

RIP experiments were unable to confirm the interaction of identified proteins with imported RNAs due to extreme variability between replicates. The association of the TOM40 protein with RNase P was confirmed, though the association of this protein with only one imported RNA does not demonstrate a general role in mitochondrial RNA import. Additionally, neither positive nor negative controls produced satisfactory data.

Overall, experiments identified several interesting proteins potentially involved in the import of RNAs into mitochondria. While RIP experiments did not confirm protein:RNA interactions, RNA affinity purification experiments supported the interaction of identified proteins with imported RNAs and hence a role in RNA import. Proteins identified, particularly the ATP synthase subunits alpha and beta may represent subunits of a complex responsible for transporting RNAs across the inner mitochondrial membrane.

Future studies will focus on confirmation of the direct interaction of identified proteins with imported RNAs utilizing RNase protection assays and gel mobility shift assays. Further work will investigate the functional effect of inhibiting protein binding to imported RNAs. Demonstration of impaired RNA import due to altered RNA:protein interaction will strongly implicate investigated proteins in RNA import.

Chapter 5 – Search for additional RNAs imported into mammalian mitochondria

Section 1 – Introduction

Previous studies provided evidence for the presence of several nuclear encoded RNAs within the mitochondria (Li et al., 1994; Puranam and Attardi, 2001; Wong and Clayton, 1986; Yoshionari et al., 1994). Recent evidence supports the hypothesis that select tRNAs may be imported into mammalian mitochondria, where they are processed and function in translation (Rubio et al., 2008). We hypothesize that additional RNAs are imported. Import of these RNAs remains uncharacterized due to methodologies utilized in previous discoveries. In order to determine if there are any unidentifed imported RNAs within the mitochondria, experiments were undertaken to characterize all RNAs within the mitochondria. Next generation sequencing technology facilitated these experiments.

Section 2 – Materials and methods

Mitochondrial RNA isolation

Mitochondria were isolated from female ICR mouse liver using standard differential centrifugation as described elsewhere (Graham, 2001a). The mitochondria were then layered on top of a discontinuous sucrose gradient consisting of solutions of 1M and 1.7M sucrose supplemented with 10mM Tris-HCl and 20mM EDTA and centrifuged at 110,000 x g for one hour (Parsons et al., 1966). Purified mitochondria were recovered from the 1M : 1.7M sucrose interface. Mitoplasts were isolated from purified mitochondria using the swell-contract method (Magalhaes et al., 1998; Parsons et al., 1966). Mitoplasts were pelleted, washed, and resuspended in 1ml mitochondrial isolation buffer (250mM sucrose, 10mM Tris-

HCl, 20mM EDTA, pH7.5). 15µl of 0.5M CaCl2 was added and mitoplasts were treated with 100 units of micrococcal nuclease for 20 minutes at 4°C. 60µl of 0.5M EGTA was added to inactivate micrococcal nuclease. Mitoplasts were washed twice with mitochondrial isolation buffer and resuspended in a small volume of 0.5M EGTA. Trizol was then added and RNA was isolated. RNA was analyzed by gel electrophoresis to confirm integrity.

RNA sequencing

RNA was sent to the genomics facility at the Hudson Alpha Institute for Biotechnology for RNA sequencing using an Illumina Genome Analyzer IIx. For sequencing, RNA was first amplified using the Nugen Ovation RNA-seq kit to amplify the RNA and produce a cDNA library. cDNA was electrophoretically separated and gel excision allowed selection of fragments roughly 300 nucleotides in length. cDNA was then sequenced. Sequence data was then aligned to the *M.m domesticus* genome (mm9) using Bowtie, removing those sequences that align only to the *M.m domesticus* mitochondrial genome to select for nuclear coded RNAs (Langmead et al., 2009). Splice junctions were joined using Tophat (Trapnell et al., 2009). Sequenced RNAs were quantified using Cufflinks (Trapnell et al., 2010). The resulting .sam file was viewed using the Integrative Genomics Viewer (IGV-http://www.broadinstitute.org/igv), regions identified by Cufflinks were identified in IGV and the sequence was identified by megaBLAST against the mouse RefSeq library and BLASTn against all sequences. Unidentifiable sequences were checked for open reading frames using the Swiss Institute of Bioinformatics ExPASy online protein translation tool and secondary structure was modeled using mfold (Gasteiger et al., 2003; Zuker, 2003). Alignments were performed using MAFFT (Katoh et al., 2005; Katoh et al., 2002).

Tissue expression evaluation for Cuff.759, Cuff.11013, Cuff.1355 and Cuff.1357

To confirm existence of RNAs identified by RNA sequencing and determine tissue expression pattern, tissues (adipose, blood, brain, heart, kidney, liver, lung, ovary, skin, spleen, muscle) were isolated from female ICR mice and analyzed by RT-PCR. Tissues were minced with scissors in 1ml Trizol and then homogenized on ice with a glass Dounce homogenizer and RNA was isolated. 100µl of blood was added to Trizol and homogenized by repetitive pipetting prior to RNA isolation. UV absorbance determined RNA quantity and purity and RNA was diluted to 0.5µg/µl. RNA integrity of 2.25µg RNA was evaluated on a formaldehyde gel. 2.5µg RNA was DNase treated for 15 minutes followed by reverse transcriptase reaction utilizing random hexamer primers and M-MLV reverse transcriptase. RT- samples prepared without reverse transcriptase enzyme were generated for each sample to confirm elimination of contaminating DNA. RT-PCR was performed on RT+ and RT- samples utilizing primers presented in Table 10. Cuff.759 and Cuff.11013 primers were amplified with a 60°C annealing temperature for 30 cycles, while Cuff. 1355 and Cuff.1357 primers utilized a 50°C annealing temperature for 35 cycles. Due to the repetitive nature of the Cuff.1355 and Cuff.1357 RNAs, PCRs produced multiple bands when amplifying cDNA, and a smear when amplifying genomic DNA. PCR amplicons were evaluated by agarose gel electrophoresis followed by visualization with ethidium bromide.

Table 10: Primers utilized for analysis of Cuff RNAs

CCTCTTCCAGGAGAGCACAG	Cuff.759	34F
TCTGACCCTCAACCCAGAAC	Cuff.759	221R
GAGCATCCAAGGCCATCTAA	Cuff.11013	302F
GGCTTTTGCAGATTGTGGAT	Cuff.11013	403R
CGTTGGAAACGGGATTTGTA	Cuff.1355	66F
TTCCAACGAATGTGTTTTTCA	Cuff.1355	313R
GGAAAATGAGAAACATCCACTTG	Cuff.1357	134F
TTTCTCCCCATATTCCAGGTC	Cuff.1357	234R

Cytological analysis to confirm absence of *Plasmodium*

Blood was collected from ICR female utilized for tissue expression evaluation by cardiac puncture following anaesthetization with tribromoethanol (Avertin®) and cervical dislocation. 1ml blood was collected in a tube containing 2mg EDTA and mixed by gentle inversion. Blood was submitted to the Auburn University Clinical Pathology for cytological analysis including visual examination of blood smear to detect *Plasmodium* or hemozoin in phagocytic cells of the blood.

Section 3 – Results

Many nuclear coded RNAs were identified in mitochondrial RNA. Table 11 includes the ID of the RNA as well as the FKPM (Isoform-level relative abundance in Fragments Per Kilobase of exon model per Million mapped fragments), a measure of the abundance of the identified RNA, with a higher value indicating a larger abundance. Also included is the chromosome and chromosomal location of the segment of the genome aligning to identified RNAs. The methods used in preparation of sample for sequencing excluded any RNAs shorter than ~300nt; therefore, absence of short RNAs from results is expected. The majority of the identified sequences were 18S and 25S rRNA, which were omitted from Table 11 for brevity. Several partial mRNA sequences were identified as well. Several identified RNAs aligned to regions of the nuclear genome with homology to the mitochondrial genome, which likely represent nuclear mitochondrial (NUMT) sequences (Hazkani-Covo et al., 2010). Identified NUMTs were omitted from Table 11 for brevity. A surprising find was the presence of the 4.5S RNA within the mitochondrial RNA sample. RNA was also found to align to two microsatellite sequences and one large tandem repeat consisting of a 38,396nt length of genome repeating a roughly 60nt unit.

Perhaps most interesting are several identified sequences that were un-annotated in the mouse genome. There were three groups of these RNAs. The first two groups were sequences that were found to have similarity to *Plasmodium* sequence. RNAs CUFF.1473, CUFF.7729, CUFF.5889, CUFF.1359, CUFF.8541, CUFF.1357, CUFF.11127 and CUFF.2869 all aligned both to *Plasmodium* sequence for protein Pb-fam-2 and each other (see appendix 4 for alignment). RNAs CUFF.4451, CUFF.1355 and CUFF.11847 aligned to *Plasmodium* sequence for a hypothetical protein and each other (see appendix 4 for alignment). Interestingly, the RNA sequences identified in the mitochondrial RNA sample did not align to the mouse genome perfectly. However, the sequences identified were nearly identical to the *Plasmodium* sequence. The last group of RNAs were two RNAs (CUFF.759 and CUFF.11013) that were unidentifiable by BLAST and have no similarity between them. Both contain numerous stop codons in all frames, suggesting that the RNAs do not encode protein. The predicted mfold secondary structure of both RNAs shows extensive secondary structure Figure 16 and Figure 17.

Table 11: RNAs identified by RNA-sequencing.

Gene id is derived from the cufflinks program used to produce the FPKM (Isoform-level relative abundance in Fragments Per Kilobase of exon model per Million mapped fragments) quantification, with a higher FPKM indicating a more abundant RNA. Chromosomal location is also included. ID is based on blast results, *Plasmodium* sequences exhibited similarity to *Plasmodium* sequences.

Gene_id	ID	FPKM	Chr	Left	Right
CUFF.1473	*Plasmodium*	646.6	chr2	98,506,397	98,507,495
CUFF.7729	*Plasmodium*	475.0	chr12	3,109,865	3,110,127
CUFF.5889	*Plasmodium*	412.7	chr9	35,112,798	35,113,178
CUFF.10463	Mus musculus leucyl-tRNA synthetase, mitochondrial (Lars2), nuclear gene encoding mitochondrial protein, mRNA	289.1	chr17	71,312,996	71,313,236
CUFF.1359	*Plasmodium*	232.9	chr2	98,502,385	98,503,141
CUFF.10341	Hsp90ab1 partial mRNA	91.6	chr17	45,707,625	45,707,655
CUFF.8541	*Plasmodium*	50.5	chr13	77,578,168	77,578,318
CUFF.3159	Mus musculus cell division cycle 42 homolog (S. cerevisiae) (Cdc42) partial mRNA	45.8	chr4	136,884,970	136,885,029
CUFF.1357	*Plasmodium*	40.2	chr2	98,503,792	98,504,251
CUFF.8115	Calmodulin 1 partial mRNA	30.6	chr12	101,444,304	101,444,430
CUFF.6145	Giant tandem repeat of *Plasmodium* sequence	28.1	chr9	3,000,001	3,038,397
CUFF.381	Nucleolin partial mRNA	24.7	chr1	88,247,419	88,247,460
CUFF.11579	Mus musculus similar to Nucleophosmin (NPM) (Nucleolar phosphoprotein B23) (Numatrin) (Nucleolar protein NO38)	22.6	chrX	64,031,610	64,032,020
CUFF.7947	4.5S RNA	20.9	chr12	70,260,331	70,260,578
CUFF.10339	Hsp90ab1 partial mRNA	19.1	chr17	45,707,210	45,707,505

CUFF.7953	4.5S RNA	18.1	chr12	70,462,172	70,462,414
CUFF.787	Apoa2 partial mRNA	18.0	chr1	173,156,268	173,156,499
CUFF.1355	*Plasmodium*	17.6	chr2	98,505,035	98,505,378
CUFF.11127	*Plasmodium*	16.5	chr19	23,431,917	23,432,066
CUFF.3643	Mus musculus ring finger and CHY zinc finger domain containing 1 (Rchy1), partial mRNA	15.7	chr5	92,378,279	92,378,371
CUFF.2869	*Plasmodium*	15.0	chr4	70,039,156	70,039,281
CUFF.4451	*Plasmodium*	13.6	chr6	103,599,045	103,599,286
CUFF.6359	Mus musculus midline 1 (Mid1), transcript variant 1, partial mRNA	12.5	chr9	123,782,217	123,782,294
CUFF.8147	PREDICTED: Mus musculus similar to Serine (or cysteine) peptidase inhibitor, clade A, member 1a (LOC667951) partial mRNA	12.1	chr12	105,132,879	105,133,388
CUFF.3359	Dnajc2 partial mRNA	11.8	chr5	21,274,271	21,274,316
CUFF.11925	Mus musculus thymosin, beta 4, X chromosome (Tmsb4x), partial mRNA	11.6	chrX	163,645,022	163,645,452
CUFF.3623	Albumin partial mRNA	11.0	chr5	90,893,007	90,893,221
CUFF.8145	Mus musculus serine (or cysteine) peptidase inhibitor, clade A, member 1A (Serpina1a), partial mRNA	11.0	chr12	105,091,513	105,092,064
CUFF.9303	Mus musculus heat-responsive protein 12 (Hrsp12), partial mRNA	10.7	chr15	34,413,777	34,414,202
CUFF.11013	Unidentified sequence	10.6	chr19	4,063,296	4,064,352
CUFF.6993	Naca partial mRNA	10.4	chr10	127,485,298	127,485,377
CUFF.759	Unidentified sequence	10.2	chr1	171,623,877	171,624,320
CUFF.11847	*Plasmodium*	9.9	chrX	139,917,547	139,917,649
CUFF.10047	Sod1 partial	9.6	chr16	90,226,396	90,226,571
CUFF.2239	Csde1 partial mRNA	9.1	chr3	102,850,956	102,851,009
CUFF.2241	Csde1 partial mRNA	8.6	chr3	102,847,485	102,847,580
CUFF.1933	Microsatellite	8.1	chr3	35,393,345	35,393,464

CUFF.2841	Mus musculus major urinary protein partial mRNA	8.0	chr4	61,440,611	61,440,641
CUFF.909	Angel2 partial mRNA	7.8	chr1	192,769,208	192,769,245
CUFF.4245	Microsatellite	7.6	chr6	59,052,810	59,053,110
CUFF.2131	Fgb partial mRNA	7.3	chr3	82,846,170	82,846,559

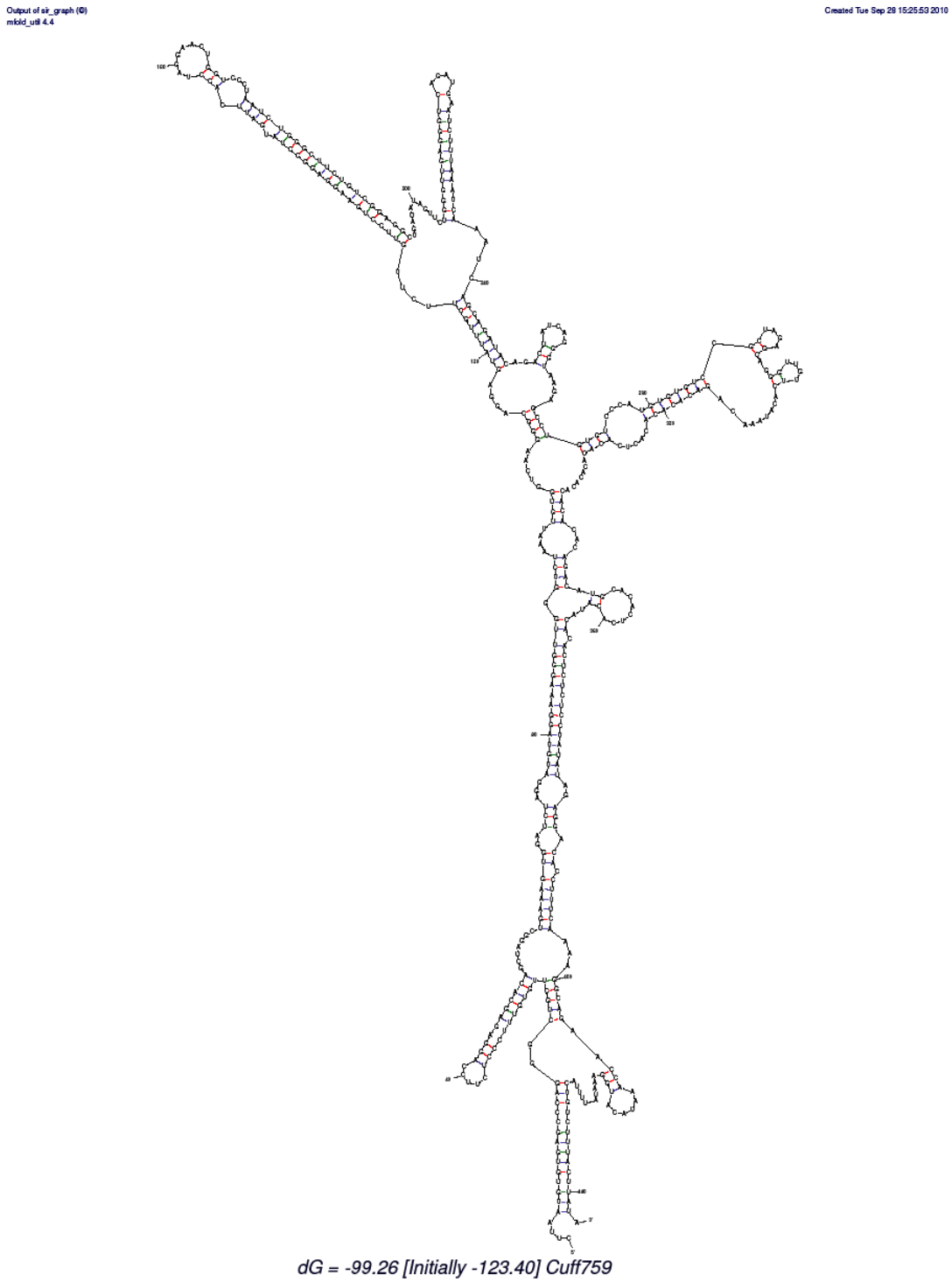

Figure 16: CUFF.759 secondary structure as calculated by mfold showing extensive secondary structure.

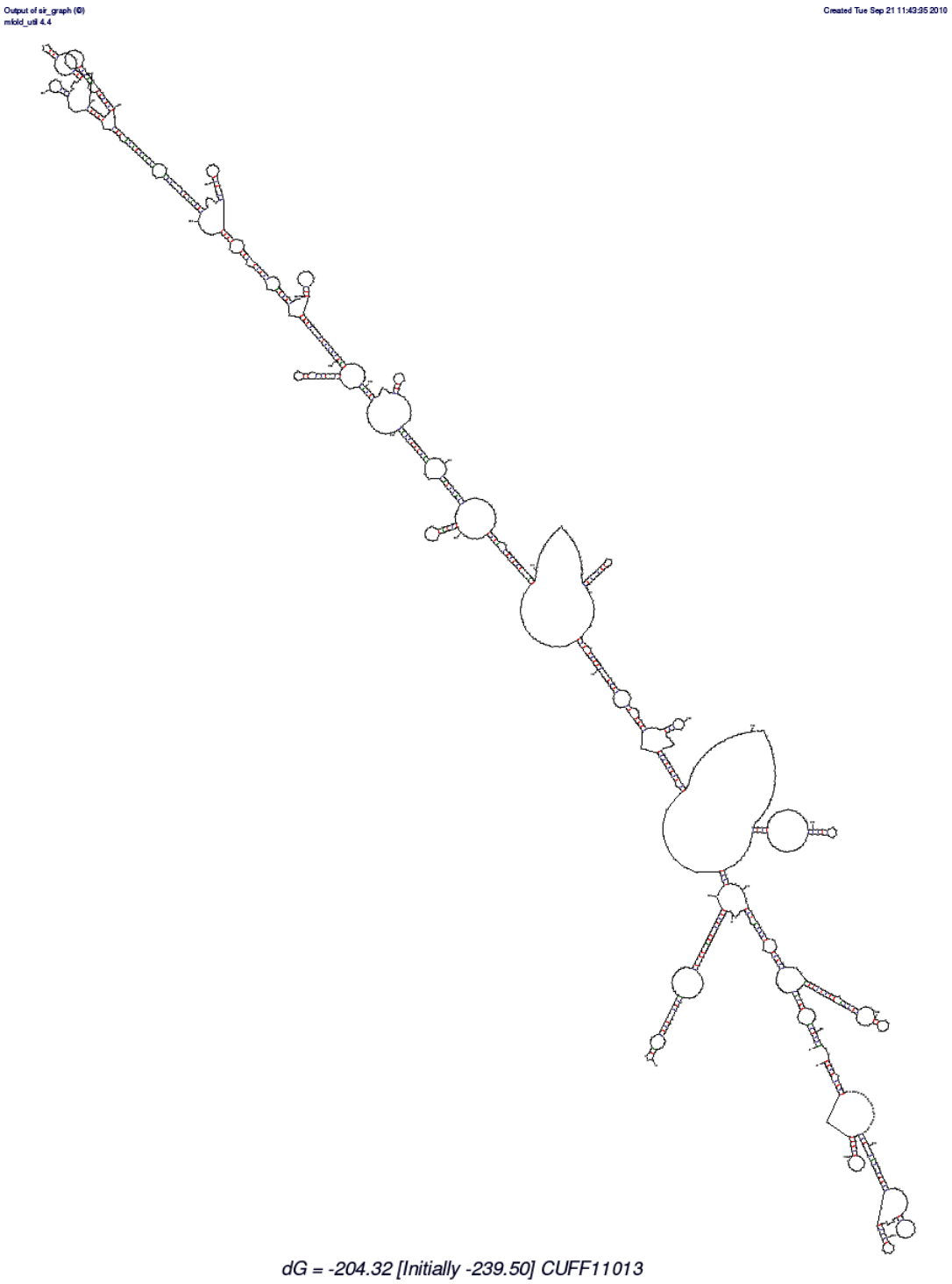

Figure 17: CUFF.11013 secondary structure as calculated by mfold showing extensive secondary structure.

Tissue expression evaluation for Cuff.759, Cuff.11013, Cuff.1355 and Cuff.1357

Denaturing agarose gel electrophoresis demonstrates integrity and equivalent quantities of isolated RNAs, with the exception of skin RNA, which was present in lower quantities than other RNAs (Figure 18).

Figure 19 summarizes tissue expression data. Cuff.759 RNA was detectible in adipose, brain, heart, kidney, liver, lung, ovary and muscle. Expression was highest per µg RNA used in reverse transcriptase reaction in adipose, heart, liver, ovaries and muscle. Cuff.11013 was expressed in adipose, brain, heart, kidney, liver, lung, ovary, spleen and muscle, with highest expression per µg RNA used in reverse transcriptase reaction in adipose, heart, liver, lung, ovary and spleen.

Cuff.1355 and Cuff.1357 PCRs produced multiple bands in addition to the expected amplicon due to the highly repetitive nature of sequences. Cuff.1355 was expressed in all tissues examined except blood. Cuff.1357 was expressed in all tissues examined except blood. Cuff.1357 muscle RT negative control had a small amount of DNA contamination. Cuff.1357 heart and kidney RT negative controls had bands slightly shorter than the expected amplicon and lacked the multiple bands seen in all positive samples and so aberrant bands likely represent primer multimers. Positive controls PCRs on genomic DNA with Cuff.1355 and Cuff.1357 primers produced extreme streaking once separated by gel electrophoresis, which likely represents multimers of amplicon or numerous priming sites within the genome.

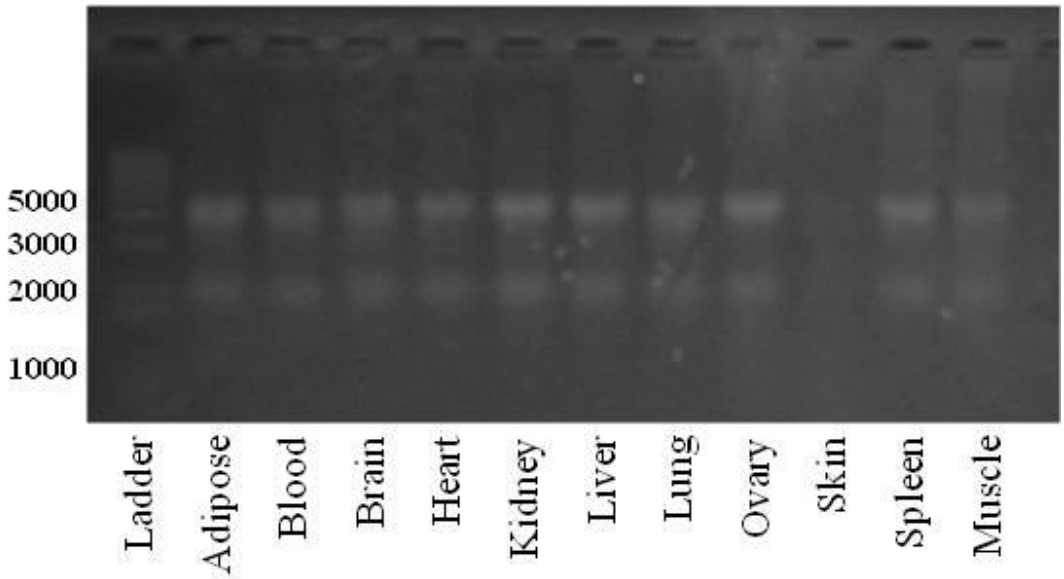

Figure 18: Denaturing gel electrophoresis of RNAs isolated from mouse tissue.

RNAs isolated from mouse tissues were analyzed by denaturing gel electrophoresis. Integrity and equivalent quantities of isolated RNAs were demonstrated, with the exception of skin RNA that was present in lower quantities than other samples. Intact major bands at ~5,000 bp and ~2,000 bp are rRNAs.

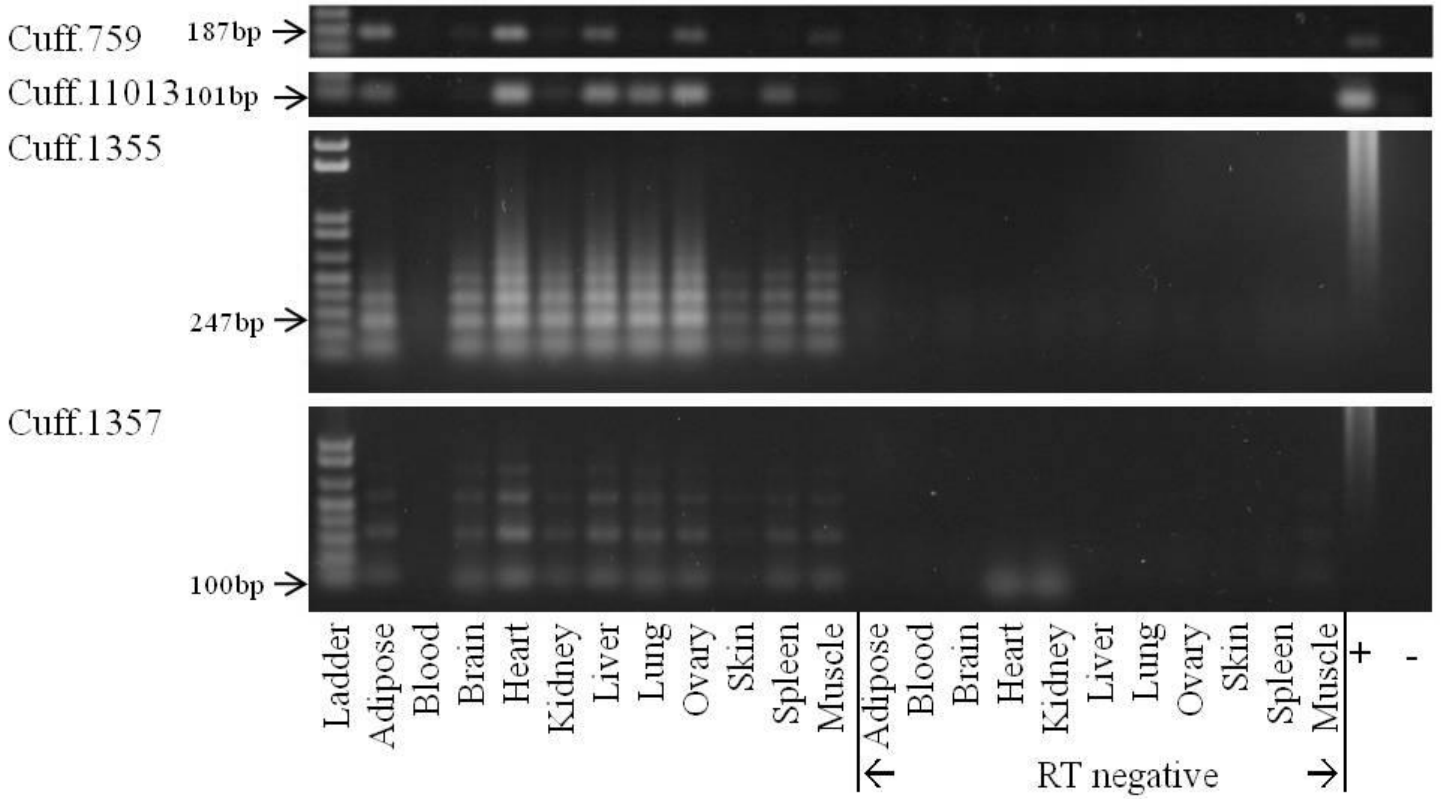

Figure 19: Cuff RNA tissue expression analysis by RT-PCR.

The tissue expression patterns of Cuff.759, Cuff.11013, Cuff.1355 and Cuff.1357 were examined. Tissues are listed below the figure. Expression confirms the existence of analyzed Cuff RNAs and reveals tissue specificity of expression. RNA targeted by primers is on the far left, with the expected amplicon size noted.

Cytological analysis to confirm absence of *Plasmodium*

Cytological analysis of ICR mouse blood revealed no *Plasmodium* in blood smears nor was hemozoin identified within phagocytic cells. Therefore, mice used to isolate tissue RNAs were free of *Plasmodium.*

Section 4 – Discussion

Numerous nuclear coded RNAs were identified within the mitochondrial RNA sample (Table 11). Considering the identification of 28S rRNA, 18S rRNAs, 4.5S RNA and select nuclear encoded mRNAs, the purity of the mitochondrial RNA sample is uncertain, thus our hypothesis cannot be definitively proven. The data suggest that these RNAs are imported into mitochondria, though the import of large cytoplasmic rRNAs and mRNAs seems highly unlikely. Proteins coded by mRNAs are also easily imported post- or co-translationally. It seems more likely that the tightly packed structure of cytoplasmic rRNAs and bound ribosomal proteins protected rRNAs from micrococcal nuclease treatment. Protection of mRNAs by ribosomes bound to the mitochondrial surface would explain partial sequence identification and explain why many of the mRNAs identified encode proteins imported into mitochondria. Overall, the presence of cytoplasmic rRNAs and select nuclear mRNAs in highly purified mitochondrial RNA suggests that ribosomes associate with the surface of the mitochondria, along with select mRNAs, which are translated at the mitochondrial surface for co-translational import of encoded proteins. Co-translational import of proteins at the mitochondrial surface has previously been described, but the results presented here suggest that the association of ribosomes with mitochondria is particularly resilient (Beddoe and Lithgow, 2002; MacKenzie and Payne, 2006). This resilience could enable future studies to identify mRNAs selectively localized at the mitochondrial surface.

Furthermore, the high levels of contamination present in mitochondrial RNA despite the extensive purification protocol used shows the unsuitability of the protocol for producing truly pure mitochondrial RNA. Previous studies have utilized this protocol to purify mitochondrial RNA, though the sensitivity of measurements made in subsequent analyses is unclear (Entelis et al., 2001a; Magalhaes et al., 1998; Puranam and Attardi, 2001; Yoshionari et al., 1994). Given these results, it is inadvisable for future studies to utilize this protocol, and alteration of the protocol is necessary to produce a pure mitochondrial RNA sample. The results from reports using this protocol have however demonstrated RNA import by complimentary methods, therefore the import status of investigated RNAs is not in question.

Despite contamination issues, RNA sequencing experiments provided substantial information. Several RNAs identified within the mitochondrial RNA sample represent previously uncharacterized RNAs. These RNAs potentially represent novel mitochondrially imported RNAs, though questionable purity of the mitochondrial RNA sample used for sequencing precludes definitive statements. There were two main types of RNAs identified.

The first type represents RNAs with similarity to *Plasmodium yoelii* and *Plasmodium berghei* sequences. Two sets of RNAs within this group aligned to two *Plasmodium* sequences, suggesting that each alignment may represent a single expressed RNA that aligned to several regions of the mouse genome during bioinformatic analysis. These sequences are highly repetitive, and their biological role is undefined. While reverse transcriptase RT- controls were negative for sequences similar to *Plasmodium* were negative, there exists the possibility that tiny amounts of DNA contamination could have caused positive signal in PCR reactions. This is highly unlikely as DNA contamination does not appear in RT- samples, which are identical to RT+ samples aside from lack of RT enzyme. Northern blot analysis

could definitively answer this question. Northern blots would additionally allow rough approximation of length of *Plasmodium*-like RNAs, and demonstrate if multiple copies of different sizes were present within murine RNA samples.

The second group of RNAs sequenced shares no homology to any sequences when queried by BLAST. These RNAs have extensive secondary structure, which future experiments will explore. These RNAs could represent RNAs imported into the mitochondria, or may have been isolated with purified mitochondrial RNA for other unknown biological reasons. Further studies will be necessary to test the presence of these RNAs within mitochondria and begin to uncover their role within the cell.

Tissue expression analysis reveals the presence of Cuff.759, Cuff.11013, Cuff.1355 and Cuff.1357 in numerous tissues. Differential expression between tissues, particularly for Cuff.759 and Cuff.11013 indicates regulation of expression of these RNAs. Regulation of expression argues against the hypothesis that these RNAs have no function. The lack of detectable quantities of Cuff.759 and Cuff.1357 in RNA isolated from blood and other tissues suggests that these RNAs may play a role that dispensable for cellular function. This argues against a critical role in mitochondrial energy production, though it is possible that the expression of Cuff.759 and Cuff.11013 is below the detectable limit of the RT-PCR assay for those samples. Specifically for the blood sample, given that nucleated cells represent a small portion of total blood, analysis of the RNAs in blood may require separation of blood cell populations.

Presence of Cuff.1355 and Cuff.1357 RNAs within all tissues except blood suggests that these RNAs may play a critical role within cells. Alternatively, the expression pattern may indicate ubiquitous, unregulated expression of "junk" RNAs that have no function. Lack

of detectable expression in blood samples could be due to the small proportion of nucleated cells within the blood and further research may reveal expression within nucleated blood cells.

Future work will focus on confirming sequence of identified novel RNAs and quantifying their expression with greater precision. Sequences with homology to *Plasmodium* and nuclear coding regions will be re-sequenced to ascertain if RNA is post-transcriptionally modified. 5' and 3' RACE and subsequent re-sequencing will allow precise determination of the length and location of ends of the RNAs. RNA affinity purification will identify proteins capable of specifically binding each uncharacterized RNA. Fluorescent in situ hybridization will reveal intracellular localization.

Subsequent work will also evaluate alternative approaches to isolation of pure mitochondrial RNA. Incubation of sucrose gradient purified mitochondria with both proteinase K and nuclease should eliminate all proteins and RNAs not protected within the mitochondrial membranes, fully eliminating all cytoplasmic contamination. Full removal of the outer mitochondrial membrane using digitonin followed by nuclease treatment is an alternative approach if proteinase K treatment is unsuccessful. Following experiments titrating proteinase K and nuclease, re-sequencing of a highly pure total mitochondrial RNA sample will evaluate both short RNAs and full length RNAs to identify previously unidentified imported RNAs and assay the mitochondrial import of RNAs identified by previous RNA sequencing experiments.

Chapter 6 – Conclusion

Xenomitochondrial compensatory mechanisms

The biological significance of xenomitochondrial studies lies in the revelation that polymorphic mtDNA can induce alterations in mitochondrial transcription to compensate for mitochondrial inefficiencies. These compensatory mechanisms function without alteration of expression of nuclear genes encoding proteins involved directly in mitochondrial energy production. Studies using xenomitochondrial mice have begun to reveal mechanisms by which compensation for mild mitochondrial inefficiencies occurs. That mitochondrial dysfunction, measured in an *in vitro* system, could be rescued *in vivo* without alteration of nuclear genes involved in mitochondrial energy production is a surprising result. Equally interesting is the noted alteration of mtDNA transcription without corresponding changes in expression of nuclear genes involved in regulation of mitochondrial transcription. This clearly indicates that it is possible to alter mtDNA transcription in response to cellular stress or energetic demands solely through activation of the involved proteins. The changes in transcription factors revealed by microarray analysis and confirmed by qRT-PCR demonstrate that diverse facets of cellular function, possibly involving oncogenesis, respond to mitochondrial alterations despite normal mitochondrial energy production. Behavioral studies demonstrated overall normal function in xenomitochondrial mice aside from select instances where xenomitochondrial mice outperformed control mice. The enhanced performance in these tests could be due to increased mtDNA transcription seen in xenomitochondrial mice. Increased transcription presumably leads to increased protein, which would then allow assembly of ETC complexes. While these complexes may work less efficiently, the greater mass of ETC complexes could allow more energy production,

potentially with the negative side effect of increased reactive oxygen species production or glucose utilization during periods of increased ATP demand.

Future work will focus on characterizing xenomitochondrial compensatory mechanisms relating to protein expression, activation and localization. Information on how changes to these parameters maintain homeostasis will expand our understanding of the biological mechanisms involved in sustaining adequate energy production in a diseased or metabolically stressed condition. Efforts will attempt to uncover mechanisms directing mtDNA transcription up regulation, with a focus on activation and localization of proteins involved in mtDNA transcription initiation and mRNA degradation.

Compensatory mechanisms enabled in xenomitochondrial mice may sensitize the organism to further insult. Compensatory mechanisms can only correct a finite amount of metabolic disruption. More severe symptoms should result from metabolic strains imposed upon xenomitochondrial mice. Exacerbated phenotypes may demonstrate how a seemingly non-deleterious mtDNA polymorphism can influence disease progression and severity.

Studies of a host of animal models and clinical samples will allow examination of a graded progression of mitochondrial dysfunction and the associated progression of various cellular compensatory mechanisms (Crimi et al., 2005). This work may encourage other scientists within the field to investigate the cellular systems compensating for mitochondrial dysfunction in their model system, or look at the effect of modulating compensatory mechanisms. By investigating compensatory mechanisms for mitochondrial dysfunction under different conditions, experiments will supplement understanding of cellular metabolic homeostasis maintenance.

Development of therapeutic interventions modulating compensatory mechanisms to treat mitochondrial diseases will follow exploration of mechanisms behind cellular and organismal metabolic homeostasis maintenance. Knowledge of mitochondrial compensatory mechanisms could uncover the role of inhibited or insufficient compensatory capacities in mitochondrial disease pathology. Identification of compensatory mechanisms may even allow diagnosis of mitochondrial dysfunction prior to the appearance of symptoms through detection of increased mtDNA transcription. Development of therapeutics to enhance the capacity of cells to deal with mitochondrial dysfunction will improve treatment regimens for diseases involving impaired mitochondrial function, thereby providing a more positive prognosis for human metabolic disorders.

Mitochondrial RNA import mechanisms

The biological significance of work relating to mitochondrial RNA import lies in the identification of selective association of proteins with imported RNAs. The selective interaction of identified proteins with imported RNAs suggests that these proteins play a role in basic mechanisms of RNA import into mitochondria. This represents the first evidence of a role in mitochondrial RNA import for these proteins.

The identification of proteins with known roles in mitochondrial biology, especially proteins involved in mitochondrial protein import is encouraging and provides additional indirect evidence for the role of the TOM complex in RNA entry into the mitochondria. Association of HSP90aa1, which interacts with the TOM complex, with imported RNAs validates a link between RNA import and protein import (Fan et al., 2006). HSP56 is known to intereact with HSP90aa1, and so may also be involved in mitochondrial import (Davies and Sanchez, 2005; Silverstein et al., 1999). That subunits of the ATP synthase can interact

with imported RNAs suggests that a complex with homology to a RNA import complex found in protists functions within mammalian mitochondria to import RNAs across the inner mitochondrial membrane. This would explain why an electrochemical gradient is not required for RNA import. If such a complex exists, however, it likely represents convergent evolution, as many of the subunits that make up the RIC have no mammalian homologues (Mukherjee et al., 2007). Information available in the literature currently and a working hypothesis based on data presented in this dissertation are presented in Figure 20.

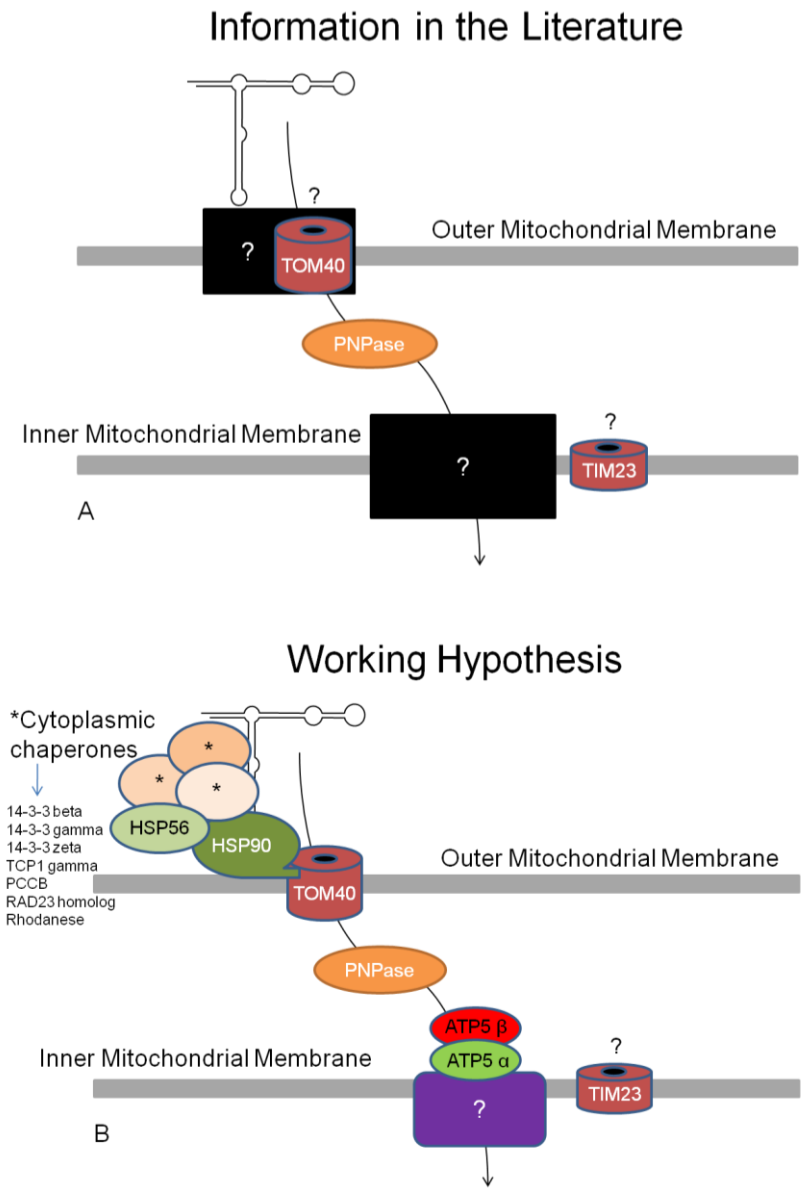

Figure 20: Information in the literature and working hypothesis based on reported research and information from the literature.

Information in the literature provides a limited view of mechanisms of mitochondrial RNA import. Information in this dissertation reveals many proteins involved in mitochondrial RNA import. Known function of identified proteins allows prediction of roles played by each in the working hypothesis.

Despite issues of cytoplasmic RNA contamination, sequencing of mitochondrial RNAs revealed previously uncharacterized RNAs that seem to have a biological connection to mitochondria. These RNAs may represent mitochondrially imported RNAs, with important roles in mitochondrial function. Alternatively, these RNAs may associate with mitochondrial RNA for other reasons and have important roles elsewhere in the cell.

RNAs identified with homology to *Plasmodium* present an interesting biological enigma. The mouse genome contains sequence homologous to *Plasmodium*. However, homology of the sequenced RNAs with the current version of the mouse genome is not perfect and sequenced RNAs had higher homology to *Plasmodium* sequence. The lack of the parasite in animals used for mitochondrial RNA isolation indicates that these RNAs represent sequences expressed from the mouse genome, though the reasons behind close homology to *Plasmodium* are unclear. The biological significance of these RNAs is unknown.

Integration into the mouse genome occurred at some point in history by an animal infected with *Plasmodium.* Given the high level of homology to *Plasmodium* sequences, either the integration event happened very recently on a biological scale, or the there is strong evolutionary pressure to maintain the sequence. If the integration event was recent, the RNA likely has no biological purpose and may mutate eventually until it is no longer recognizable. If *Plasmodium* sequence integrated into the mouse genome a long time ago, biological function forces maintenance of RNA sequence. In this case, the role played within mammalian cells likely represents a non-critical function, as the organism functioned prior to sequence integration.

The sequenced RNAs lacking identifiable homology to known sequences are even more mysterious than the *Plasmodium*-like RNAs. These RNAs do not seem to encode

protein, and exhibit extensive secondary structure, suggesting either a catalytic or a structural role. If mitochondria import these RNAs, their role in mitochondrial biology will be important to uncover.

If imported, these RNAs would represent the largest RNAs imported in any species to date. This could have implications for the development of gene therapy approaches utilizing mitochondrial RNA import. If RNAs of this length are importable, import of lengthy engineered RNAs should be possible. Lacking a length limit would open the possibility to import engineered RNAs from the nucleus encoding mtDNA-encoded proteins for translation within the mitochondria. This would represent a novel approach to allotopic expression circumventing many issues involved in import of mtDNA-encoded proteins from the nucleus. The import of engineered RNAs would also enable novel gene therapy approaches to compensate for mtDNA mutations in tRNA or rRNA genes.

Data presented here will enable future studies to continue to reveal the specifics of mitochondrial RNA import mechanisms. The identification of cytoplasmic chaperones or subunits of membrane bound RNA import complexes highlights the roles these proteins play in mitochondrial import. This expands the total scientific knowledge base relating to RNA import and other scientists within the field will be able to build upon this knowledge.

The RNA affinity purification protocol adapted and optimized in this work also provides scientists with an additional tool with which to study protein:RNA interactions.

With time and further research, the data generated in this dissertation will form a foundation for our understanding of mechanisms of mitochondrial RNA import. This foundation will allow the expansion of knowledge relating to mitochondrial RNA import and the role it plays in mitochondrial biology and dysfunction. Additionally, utilization of RNA

import mechanisms will someday allow treatment of diseases caused by mtDNA mutations, and give hope to patients afflicted with devastating metabolic disorders.

The importance of the study of mitochondrial biology lies in the critical role of mitochondrial function in numerous cellular processes and its central role in numerous pathologic states. By studying mouse models of mitochondrial disease, we gain understanding of the pathological processes and the mechanisms by which the organism attempts to maintain energetic homeostasis. This knowledge enables better predictions of human patient prognosis and can point the way towards therapeutic approaches. One such approach coming closer to reality is the import engineered RNA vectors into mitochondria to compensate for mtDNA mutations. Thus, the information presented in this dissertation represents two separate approaches to ameliorating mitochondrial deficiencies and dysfunction. Future work derived from these initial studies may one day succeed in offering a greatly enhanced quality of life for patients afflicted with mitochondrial disease.

Citations

Adhya, S. 2008. Leishmania mitochondrial tRNA importers. *Int J Biochem Cell Biol*. 40:2681-5.

Allison, L.A., M.T. North, K.J. Murdoch, P.J. Romaniuk, S. Deschamps, and M. le Maire. 1993. Structural requirements of 5S rRNA for nuclear transport, 7S ribonucleoprotein particle assembly, and 60S ribosomal subunit assembly in Xenopus oocytes. *Mol Cell Biol*. 13:6819-31.

Barrientos, A., L. Kenyon, and C.T. Moraes. 1998. Human xenomitochondrial cybrids. Cellular models of mitochondrial complex I deficiency. *J Biol Chem*. 273:14210-7.

Beddoe, T., and T. Lithgow. 2002. Delivery of nascent polypeptides to the mitochondrial surface. *Biochim Biophys Acta*. 1592:35-9.

Bermudez, O., G. Pages, and C. Gimond. 2010. The dual-specificity MAP kinase phosphatases: critical roles in development and cancer. *Am J Physiol Cell Physiol*. 299:C189-202.

Bhattacharyya, S.N., and S. Adhya. 2004a. The complexity of mitochondrial tRNA import. *RNA Biol*. 1:84-8.

Bhattacharyya, S.N., and S. Adhya. 2004b. tRNA-triggered ATP hydrolysis and generation of membrane potential by the leishmania mitochondrial tRNA import complex. *J Biol Chem*. 279:11259-63.

Bhattacharyya, S.N., S. Chatterjee, S. Goswami, G. Tripathi, S.N. Dey, and S. Adhya. 2003. "Ping-pong" interactions between mitochondrial tRNA import receptors within a multiprotein complex. *Mol Cell Biol*. 23:5217-24.

Bramham, C.R., P.F. Worley, M.J. Moore, and J.F. Guzowski. 2008. The immediate early gene arc/arg3.1: regulation, mechanisms, and function. *J Neurosci*. 28:11760-7.

Brandina, I., A. Smirnov, O. Kolesnikova, N. Entelis, I.A. Krasheninnikov, R.P. Martin, and I. Tarassov. 2007. tRNA import into yeast mitochondria is regulated by the ubiquitin-proteasome system. *FEBS Lett*. 581:4248-54.

Bunn, C.L., D.C. Wallace, and J.M. Eisenstadt. 1974. Cytoplasmic inheritance of chloramphenicol resistance in mouse tissue culture cells. *Proc Natl Acad Sci USA*. 71:1681-5.

Camby, I., M. Le Mercier, F. Lefranc, and R. Kiss. 2006. Galectin-1: a small protein with major functions. *Glycobiology*. 16:137R-157R.

Cannon, M.V., C.A. Pinkert, and I.A. Trounce. 2004. Xenomitochondrial embryonic stem cells and mice: modeling human mitochondrial biology and disease. *Gene Therapy and Regulation*. 2:283-300.

Carter, R.J., L.A. Lione, T. Humby, L. Mangiarini, A. Mahal, G.P. Bates, S.B. Dunnett, and A.J. Morton. 1999. Characterization of progressive motor deficits in mice transgenic for the human Huntington's disease mutation. *J Neurosci*. 19:3248-57.

Chang, D.D., and D.A. Clayton. 1987. A mammalian mitochondrial RNA processing activity contains nucleus-encoded RNA. *Science*. 235:1178-84.

Chatonnet, F., L.J. Wrobel, V. Mezieres, M. Pasqualetti, S. Ducret, E. Taillebourg, P. Charnay, F.M. Rijli, and J. Champagnat. 2007. Distinct roles of Hoxa2 and Krox20 in the development of rhythmic neural networks controlling inspiratory depth, respiratory frequency, and jaw opening. *Neural Dev*. 2:19.

Clapham, D.E. 2007. Calcium signaling. *Cell*. 131:1047-58.

Conrad, N.K. 2008. Chapter 15. Co-immunoprecipitation techniques for assessing RNA-protein interactions in vivo. *Methods Enzymol*. 449:317-42.

Cox, D.R. 1972. Regression models and life-tables *J Royal Stat Soc B*. 34:187-220.

Crausaz Esseiva, A., L. Marechal-Drouard, A. Cosset, and A. Schneider. 2004. The T-stem determines the cytosolic or mitochondrial localization of trypanosomal tRNAsMet. *Mol Biol Cell*. 15:2750-7.

Crawley, J.N., J.K. Belknap, A. Collins, J.C. Crabbe, W. Frankel, N. Henderson, R.J. Hitzemann, S.C. Maxson, L.L. Miner, A.J. Silva, J.M. Wehner, A. Wynshaw-Boris, and R. Paylor. 1997. Behavioral phenotypes of inbred mouse strains: implications and recommendations for molecular studies. *Psychopharmacology (Berl)*. 132:107-24.

Crimi, M., S.F. O'Hearn, D.C. Wallace, and G.P. Comi. 2005. Molecular research technologies in mitochondrial diseases: The microarray approach. *IUBMB Life*. 57:811 - 818.

Daiber, A., P. Wenzel, M. Oelze, S. Schuhmacher, T. Jansen, and T. Munzel. 2009. Mitochondrial aldehyde dehydrogenase (ALDH-2)--maker of and marker for nitrate tolerance in response to nitroglycerin treatment. *Chem Biol Interact*. 178:40-7.

Dantuma, N.P., C. Heinen, and D. Hoogstraten. 2009. The ubiquitin receptor Rad23: at the crossroads of nucleotide excision repair and proteasomal degradation. *DNA Repair (Amst)*. 8:449-60.

Davies, T.H., and E.R. Sanchez. 2005. Fkbp52. *Int J Biochem Cell Biol*. 37:42-7.

Debray, F.G., M. Lambert, and G.A. Mitchell. 2008. Disorders of mitochondrial function. *Curr Opin Pediatr*. 20:471-82.

Delage, L., A.M. Duchene, M. Zaepfel, and L. Marechal-Drouard. 2003. The anticodon and the D-domain sequences are essential determinants for plant cytosolic tRNA(Val) import into mitochondria. *Plant J*. 34:623-33.

Desmazieres, A., P. Charnay, and P. Gilardi-Hebenstreit. 2009. Krox20 controls the transcription of its various targets in the developing hindbrain according to multiple modes. *J Biol Chem*. 284:10831-40.

Devaux, F., G. Lelandais, M. Garcia, S. Goussard, and C. Jacq. 2010. Posttranscriptional control of mitochondrial biogenesis: spatio-temporal regulation of the protein import process. *FEBS Lett*. 584:4273-9.

DiMauro, S., and E.A. Schon. 2001. Mitochondrial DNA mutations in human disease. *Am J Med Genet*. 106:18-26.

Doersen, C.J., C. Guerrier-Takada, S. Altman, and G. Attardi. 1985. Characterization of an RNase P activity from HeLa cell mitochondria. Comparison with the cytosol RNase P activity. *J Biol Chem*. 260:5942-9.

Dorner, M., M. Altmann, S. Paabo, and M. Morl. 2001. Evidence for import of a lysyl-tRNA into marsupial mitochondria. *Mol Biol Cell*. 12:2688-98.

Duchene, A.M., C. Pujol, and L. Marechal-Drouard. 2009. Import of tRNAs and aminoacyl-tRNA synthetases into mitochondria. *Curr Genet*. 55:1-18.

Entelis, N.S., S. Kieffer, O.A. Kolesnikova, R.P. Martin, and I.A. Tarassov. 1998. Structural requirements of tRNALys for its import into yeast mitochondria. *Proc Natl Acad Sci U S A*. 95:2838-43.

Entelis, N.S., O.A. Kolesnikova, S. Dogan, R.P. Martin, and I.A. Tarassov. 2001a. 5 S rRNA and tRNA import into human mitochondria. Comparison of in vitro requirements. *J Biol Chem*. 276:45642-53.

Entelis, N.S., O.A. Kolesnikova, R.P. Martin, and I.A. Tarassov. 2001b. RNA delivery into mitochondria. *Adv Drug Deliv Rev*. 49:199-215.

Eyre-Walker, A., and P. Awadalla. 2001. Does human mtDNA recombine? *J Mol Evol*. 53:430-5.

Fan, A.C., M.K. Bhangoo, and J.C. Young. 2006. Hsp90 functions in the targeting and outer membrane translocation steps of Tom70-mediated mitochondrial import. *J Biol Chem*. 281:33313-24.

Fernandez-Silva, P., J.A. Enriquez, and J. Montoya. 2003. Replication and transcription of mammalian mitochondrial DNA. *Exp Physiol*. 88:41-56.

Gallagher, S., S.E. Winston, S.A. Fuller, and J.G. Hurrell. 2008. Immunoblotting and immunodetection. *Curr Protoc Mol Biol*. Chapter 10:Unit 10 8.

Gallagher, S.R. 2001. One-dimensional electrophoresis using nondenaturing conditions. *Curr Protoc Mol Biol*. Chapter 10:Unit 10 2B.

Gasteiger, E., A. Gattiker, C. Hoogland, I. Ivanyi, R.D. Appel, and A. Bairoch. 2003. ExPASy: The proteomics server for in-depth protein knowledge and analysis. *Nucleic Acids Res*. 31:3784-8.

Gilbert, C., and J.Q. Svejstrup. 2006. RNA immunoprecipitation for determining RNA-protein associations in vivo. *Curr Protoc Mol Biol*. Chapter 27:Unit 27 4.

Gogvadze, V., S. Orrenius, and B. Zhivotovsky. 2008. Mitochondria in cancer cells: what is so special about them? *Trends Cell Biol*. 18:165-73.

Goswami, S., G. Dhar, S. Mukherjee, B. Mahata, S. Chatterjee, P. Home, and S. Adhya. 2006. A bifunctional tRNA import receptor from Leishmania mitochondria. *Proc Natl Acad Sci U S A*. 103:8354-9.

Graham, J.M. 2001a. Isolation of mitochondria from tissues and cells by differential centrifugation. *Curr Protoc Cell Biol*. Chapter 3:Unit 3 3.

Graham, J.M. 2001b. Isolation of mitochondria from tissues and cells by differential centrifugation. *Curr Protoc Cell Biol*. Ch. 3:Unit 3 3.

Gray, M.W., B.F. Lang, R. Cedergren, G.B. Golding, C. Lemieux, D. Sankoff, M. Turmel, N. Brossard, E. Delage, T.G. Littlejohn, I. Plante, P. Rioux, D. Saint-Louis, Y. Zhu, and G. Burger. 1998. Genome structure and gene content in protist mitochondrial DNAs. *Nucleic Acids Res*. 26:865-78.

Hazkani-Covo, E., R.M. Zeller, and W. Martin. 2010. Molecular poltergeists: mitochondrial DNA copies (numts) in sequenced nuclear genomes. *PLoS Genet*. 6:e1000834.

He, Y.W. 2002. Orphan nuclear receptors in T lymphocyte development. *J Leukoc Biol*. 72:440-6.

Heddi, A., G. Stepien, P.J. Benke, and D.C. Wallace. 1999. Coordinate induction of energy gene expression in tissues of mitochondrial disease patients. *J Biol Chem*. 274:22968-76.

Holzmann, J., P. Frank, E. Loffler, K.L. Bennett, C. Gerner, and W. Rossmanith. 2008. RNase P without RNA: identification and functional reconstitution of the human mitochondrial tRNA processing enzyme. *Cell*. 135:462-74.

Home, P., S. Mukherjee, and S. Adhya. 2008. A mosaic of RNA binding and protein interaction motifs in a bifunctional mitochondrial tRNA import factor from Leishmania tropica. *Nucleic Acids Res*. 36:5552-61.

Howell, N. 1997. mtDNA recombination: what do in vitro data mean? *Am J Hum Genet*. 61:19-22.

Husson, A., C. Brasse-Lagnel, A. Fairand, S. Renouf, and A. Lavoinne. 2003. Argininosuccinate synthetase from the urea cycle to the citrulline-NO cycle. *Eur J Biochem*. 270:1887-99.

Jacobson, M.R., L.G. Cao, K. Taneja, R.H. Singer, Y.L. Wang, and T. Pederson. 1997. Nuclear domains of the RNA subunit of RNase P. *J Cell Sci*. 110 (Pt 7):829-37.

Jang, S.W., and J. Svaren. 2009. Induction of myelin protein zero by early growth response 2 through upstream and intragenic elements. *J Biol Chem*. 284:20111-20.

Janke, A., X. Xu, and U. Arnason. 1997. The complete mitochondrial genome of the wallaroo (Macropus robustus) and the phylogenetic relationship among Monotremata, Marsupialia, and Eutheria. *Proc Natl Acad Sci U S A*. 94:1276-81.

Jayarapu, K., and T.A. Griffin. 2004. Protein-protein interactions among human 20S proteasome subunits and proteassemblin. *Biochem Biophys Res Commun*. 314:523-8.

Kamenski, P., O. Kolesnikova, V. Jubenot, N. Entelis, I.A. Krasheninnikov, R.P. Martin, and I. Tarassov. 2007. Evidence for an adaptation mechanism of mitochondrial translation via tRNA import from the cytosol. *Mol Cell*. 26:625-37.

Katoh, K., K. Kuma, H. Toh, and T. Miyata. 2005. MAFFT version 5: improvement in accuracy of multiple sequence alignment. *Nucleic Acids Res*. 33:511-8.

Katoh, K., K. Misawa, K. Kuma, and T. Miyata. 2002. MAFFT: a novel method for rapid multiple sequence alignment based on fast Fourier transform. *Nucleic Acids Res*. 30:3059-66.

Kenyon, L., and C.T. Moraes. 1997. Expanding the functional human mitochondrial DNA database by the establishment of primate xenomitochondrial cybrids. *Proc Natl Acad Sci U S A*. 94:9131-5.

Khan, S.M., R.M. Smigrodzki, and R.H. Swerdlow. 2007. Cell and animal models of mtDNA biology: progress and prospects. *Am J Physiol Cell Physiol*. 292:C658-69.

Kim, S.N., K.H. Ryu, E.H. Lee, J.S. Kim, and S.H. Hahn. 2002. Molecular analysis of PCCB gene in Korean patients with propionic acidemia. *Mol Genet Metab*. 77:209-16.

King, M.P., and G. Attardi. 1989. Human cells lacking mtDNA: repopulation with exogenous mitochondria by complementation. *Science*. 246:500-3.

King, M.P., and G. Attardi. 1993. Post-transcriptional regulation of the steady-state levels of mitochondrial tRNAs in HeLa cells. *J Biol Chem*. 268:10228-37.

Kiss, T., and W. Filipowicz. 1992. Evidence against a mitochondrial location of the 7-2/MRP RNA in mammalian cells. *Cell*. 70:11-6.

Klapdor, K., B.G. Dulfer, A. Hammann, and F.J. Van der Staay. 1997. A low-cost method to analyse footprint patterns. *J Neurosci Methods*. 75:49-54.

Kolesnikova, O., H. Kazakova, C. Comte, S. Steinberg, P. Kamenski, R.P. Martin, I. Tarassov, and N. Entelis. 2010. Selection of RNA aptamers imported into yeast and human mitochondria. *RNA*. 16:926-41.

Kolesnikova, O.A., N.S. Entelis, C. Jacquin-Becker, F. Goltzene, Z.M. Chrzanowska-Lightowlers, R.N. Lightowlers, R.P. Martin, and I. Tarassov. 2004. Nuclear DNA-encoded tRNAs targeted into mitochondria can rescue a mitochondrial DNA mutation associated with the MERRF syndrome in cultured human cells. *Hum Mol Genet*. 13:2519-34.

Krebs, J.J., H. Hauser, and E. Carafoli. 1979. Asymmetric distribution of phospholipids in the inner membrane of beef heart mitochondria. *J Biol Chem*. 254:5308-16.

Laforest, M.J., L. Delage, and L. Marechal-Drouard. 2005. The T-domain of cytosolic tRNAVal, an essential determinant for mitochondrial import. *FEBS Lett*. 579:1072-8.

Langmead, B., C. Trapnell, M. Pop, and S.L. Salzberg. 2009. Ultrafast and memory-efficient alignment of short DNA sequences to the human genome. *Genome Biol*. 10:R25.

Lawson, V.J., K. Weston, and D. Maurice. 2010. Early growth response 2 regulates the survival of thymocytes during positive selection. *Eur J Immunol*. 40:232-41.

Lazarou, M., M. McKenzie, A. Ohtake, D.R. Thorburn, and M.T. Ryan. 2007. Analysis of the assembly profiles for mitochondrial- and nuclear-DNA-encoded subunits into complex I. *Mol Cell Biol*. 27:4228-37.

Lee, M.H., and T. Schedl. 2001. Identification of in vivo mRNA targets of GLD-1, a maxi-KH motif containing protein required for C. elegans germ cell development. *Genes Dev*. 15:2408-20.

Levy, S.E., K.G. Waymire, Y.L. Kim, G.R. MacGregor, and D.C. Wallace. 1999. Transfer of chloramphenicol-resistant mitochondrial DNA into the chimeric mouse. *Transgenic Res*. 8:137-45.

Li, K., C.S. Smagula, W.J. Parsons, J.A. Richardson, M. Gonzalez, H.K. Hagler, and R.S. Williams. 1994. Subcellular partitioning of MRP RNA assessed by ultrastructural and biochemical analysis. *J Cell Biol*. 124:871-82.

Liu, W., and D.A. Saint. 2002. A new quantitative method of real time reverse transcription polymerase chain reaction assay based on simulation of polymerase chain reaction kinetics. *Anal Biochem*. 302:52-9.

Livak, K.J., and T.D. Schmittgen. 2001. Analysis of relative gene expression data using real-time quantitative PCR and the 2(-Delta Delta C(T)) Method. *Methods*. 25:402-8.

Lu, Q., S. Wierzbicki, A.S. Krasilnikov, and M.E. Schmitt. 2010. Comparison of mitochondrial and nucleolar RNase MRP reveals identical RNA components with distinct enzymatic activities and protein components. *RNA*. 16:529-37.

MacKenzie, J.A., and R.M. Payne. 2006. Preparation of ribosomes loaded with truncated nascent proteins to study ribosome binding to mammalian mitochondria. *Mitochondrion*. 6:64-70.

Magalhaes, P.J., A.L. Andreu, and E.A. Schon. 1998. Evidence for the presence of 5S rRNA in mammalian mitochondria. *Mol Biol Cell*. 9:2375-82.

Mahata, B., S.N. Bhattacharyya, S. Mukherjee, and S. Adhya. 2005. Correction of translational defects in patient-derived mutant mitochondria by complex-mediated import of a cytoplasmic tRNA. *J Biol Chem*. 280:5141-4.

Marechal-Drouard, L., J.H. Weil, and A. Dietrich. 1993. Transfer RNAs and Transfer RNA Genes in Plants. *Annual Review of Plant Physiology and Plant Molecular Biology*. 44:13-32.

Marechal-Drouard, L., J.H. Weil, and P. Guillemaut. 1988. Import of several tRNAs from the cytoplasm into the mitochondria in bean Phaseolus vulgaris. *Nucleic Acids Res*. 16:4777-88.

Martin, R.P., J.M. Schneller, A.J. Stahl, and G. Dirheimer. 1977. Study of yeast mitochondrial tRNAs by two-dimensional polyacrylamide gel electrophoresis: characterization of isoaccepting species and search for imported cytoplasmic tRNAs. *Nucleic Acids Res*. 4:3497-510.

Martin, R.P., J.M. Schneller, A.J. Stahl, and G. Dirheimer. 1979. Import of nuclear deoxyribonucleic acid coded lysine-accepting transfer ribonucleic acid (anticodon C-U-U) into yeast mitochondria. *Biochemistry*. 18:4600-5.

Masuyama, M., R. Iida, H. Takatsuka, T. Yasuda, and T. Matsuki. 2005. Quantitative change in mitochondrial DNA content in various mouse tissues during aging. *Biochim Biophys Acta*. 1723:302-8.

McKenzie, M., M. Chiotis, C.A. Pinkert, and I.A. Trounce. 2003. Functional respiratory chain analyses in murid xenomitochondrial cybrids expose coevolutionary constraints of cytochrome b and nuclear subunits of complex III. *Mol Biol Evol*. 20:1117-24.

McKenzie, M., and I. Trounce. 2000. Expression of Rattus norvegicus mtDNA in Mus musculus cells results in multiple respiratory chain defects. *J Biol Chem*. 275:31514-9.

McKenzie, M., I.A. Trounce, C.A. Cassar, and C.A. Pinkert. 2004. Production of homoplasmic xenomitochondrial mice. *Proc Natl Acad Sci USA*. 101:1685-90.

Morrison, D.K. 2009. The 14-3-3 proteins: integrators of diverse signaling cues that impact cell fate and cancer development. *Trends Cell Biol*. 19:16-23.

Mrowiec, T., and B. Schwappach. 2006. 14-3-3 proteins in membrane protein transport. *Biol Chem*. 387:1227-36.

Mukherjee, S., S. Basu, P. Home, G. Dhar, and S. Adhya. 2007. Necessary and sufficient factors for the import of transfer RNA into the kinetoplast mitochondrion. *EMBO Rep*. 8:589-95.

Nabel-Rosen, H., N. Dorevitch, A. Reuveny, and T. Volk. 1999. The balance between two isoforms of the Drosophila RNA-binding protein how controls tendon cell differentiation. *Mol Cell*. 4:573-84.

Nakamoto, R.K., J.A. Baylis Scanlon, and M.K. Al-Shawi. 2008. The rotary mechanism of the ATP synthase. *Arch Biochem Biophys*. 476:43-50.

No, H., Y. Bang, J. Lim, S.S. Kim, H.S. Choi, and H.J. Choi. 2010. Involvement of induction and mitochondrial targeting of orphan nuclear receptor Nur77 in 6-OHDA-induced SH-SY5Y cell death. *Neurochem Int*. 56:620-6.

Obsilova, V., J. Silhan, E. Boura, J. Teisinger, and T. Obsil. 2008. 14-3-3 proteins: a family of versatile molecular regulators. *Physiol Res*. 57 Suppl 3:S11-21.

Parsons, D.F., G.R. Williams, and B. Chance. 1966. Characteristics of isolated and purified preparations of the outer and inner membranes of mitochondria. *Ann N Y Acad Sci*. 137:643-66.

Paylor, R., M. Nguyen, J.N. Crawley, J. Patrick, A. Beaudet, and A. Orr-Urtreger. 1998. Alpha7 nicotinic receptor subunits are not necessary for hippocampal-dependent learning or sensorimotor gating: a behavioral characterization of Acra7-deficient mice. *Learn Mem*. 5:302-16.

Peritz, T., F. Zeng, T.J. Kannanayakal, K. Kilk, E. Eiriksdottir, U. Langel, and J. Eberwine. 2006. Immunoprecipitation of mRNA-protein complexes. *Nat Protoc*. 1:577-80.

Pfaffl, M.W., G.W. Horgan, and L. Dempfle. 2002. Relative expression software tool (REST) for group-wise comparison and statistical analysis of relative expression results in real-time PCR. *Nucleic Acids Res*. 30:e36.

Pinkert, C.A. 2005. Xenomitochondrial mice: modeling human disease pathogenesis. H.J. Federoff and I.A. Trounce, editors, Mitochondrial Medicine 2005, St. Louis.

Pinkert, C.A., and I.A. Trounce. 2002. Production of transmitochondrial mice. *Methods*. 26:348-57.

Pinkert, C.A., and I.A. Trounce. 2007. Generation of transmitochondrial mice: development of xenomitochondrial mice to model neurodegenerative diseases. *Methods Cell Biol*. 80:549-69.

Pogozelski, W.K., L.D. Fletcher, C.A. Cassar, D.A. Dunn, I.A. Trounce, and C.A. Pinkert. 2008. The mitochondrial genome sequence of Mus terricolor: Comparison with Mus musculus domesticus and implications for xenomitochondrial mouse modeling. *Gene*. 418:27-33.

Puranam, R.S., and G. Attardi. 2001. The RNase P associated with HeLa cell mitochondria contains an essential RNA component identical in sequence to that of the nuclear RNase P. *Mol Cell Biol*. 21:548-61.

Rossmanith, W., and R.M. Karwan. 1998. Characterization of human mitochondrial RNase P: novel aspects in tRNA processing. *Biochem Biophys Res Commun*. 247:234-41.

Rossmanith, W., and T. Potuschak. 2001. Difference between mitochondrial RNase P and nuclear RNase P. *Mol Cell Biol*. 21:8236-7.

Rubio, M.A., J.J. Rinehart, B. Krett, S. Duvezin-Caubet, A.S. Reichert, D. Soll, and J.D. Alfonzo. 2008. Mammalian mitochondria have the innate ability to import tRNAs by a mechanism distinct from protein import. *Proc Natl Acad Sci U S A*. 105:9186-91.

Salinas, T., A.M. Duchene, L. Delage, S. Nilsson, E. Glaser, M. Zaepfel, and L. Marechal-Drouard. 2006. The voltage-dependent anion channel, a major component of the tRNA import machinery in plant mitochondria. *Proc Natl Acad Sci U S A*. 103:18362-7.

Salinas, T., A.M. Duchene, and L. Marechal-Drouard. 2008. Recent advances in tRNA mitochondrial import. *Trends Biochem Sci*. 33:320-9.

Salinas, T., C. Schaeffer, L. Marechal-Drouard, and A.M. Duchene. 2005. Sequence dependence of tRNA(Gly) import into tobacco mitochondria. *Biochimie*. 87:863-72.

Schmidt, O., N. Pfanner, and C. Meisinger. 2010. Mitochondrial protein import: from proteomics to functional mechanisms. *Nat Rev Mol Cell Biol*. 11:655-67.

Schneider, A., and L. Marechal-Drouard. 2000. Mitochondrial tRNA import: are there distinct mechanisms? *Trends Cell Biol*. 10:509-13.

Schweizer, J., P.E. Bowden, P.A. Coulombe, L. Langbein, E.B. Lane, T.M. Magin, L. Maltais, M.B. Omary, D.A. Parry, M.A. Rogers, and M.W. Wright. 2006. New consensus nomenclature for mammalian keratins. *J Cell Biol*. 174:169-74.

Sedelis, M., K. Hofele, G.W. Auburger, S. Morgan, J.P. Huston, and R.K. Schwarting. 2000. MPTP susceptibility in the mouse: behavioral, neurochemical, and histological analysis of gender and strain differences. *Behav Genet*. 30:171-82.

Silverstein, A.M., M.D. Galigniana, K.C. Kanelakis, C. Radanyi, J.M. Renoir, and W.B. Pratt. 1999. Different regions of the immunophilin FKBP52 determine its association with the glucocorticoid receptor, hsp90, and cytoplasmic dynein. *J Biol Chem*. 274:36980-6.

Simpson, A.M., Y. Suyama, H. Dewes, D.A. Campbell, and L. Simpson. 1989. Kinetoplastid mitochondria contain functional tRNAs which are encoded in nuclear DNA and also contain small minicircle and maxicircle transcripts of unknown function. *Nucleic Acids Res*. 17:5427-45.

Sligh, J.E., S.E. Levy, K.G. Waymire, P. Allard, D.L. Dillehay, S. Nusinowitz, J.R. Heckenlively, G.R. MacGregor, and D.C. Wallace. 2000. Maternal germ-line transmission of mutant mtDNAs from embryonic stem cell-derived chimeric mice. *Proc Natl Acad Sci USA*. 97:14461-6.

Smirnov, A., C. Comte, A.M. Mager-Heckel, V. Addis, I.A. Krasheninnikov, R.P. Martin, N. Entelis, and I. Tarassov. 2010. Mitochondrial enzyme rhodanese is essential for 5S ribosomal RNA import into human mitochondria. *J Biol Chem*. 285:30792-30803.

Smirnov, A., I. Tarassov, A.M. Mager-Heckel, M. Letzelter, R.P. Martin, I.A. Krasheninnikov, and N. Entelis. 2008. Two distinct structural elements of 5S rRNA are needed for its import into human mitochondria. *RNA*. 14:749-59.

Spiess, C., A.S. Meyer, S. Reissmann, and J. Frydman. 2004. Mechanism of the eukaryotic chaperonin: protein folding in the chamber of secrets. *Trends Cell Biol*. 14:598-604.

Suyama, Y. 1967. The origins of mitochondrial ribonucleic acids in Tetrahymena pyriformis. *Biochemistry*. 6:2829-39.

Swerdlow, R.H. 2007. Mitochondria in cybrids containing mtDNA from persons with mitochondriopathies. *J Neurosci Res*. 85:3416-28.

Taanman, J.W. 1999. The mitochondrial genome: structure, transcription, translation and replication. *Biochim Biophys Acta*. 1410:103-23.

Tapper, D.P., R.A. Van Etten, and D.A. Clayton. 1983. Isolation of mammalian mitochondrial DNA and RNA and cloning of the mitochondrial genome. *Methods Enzymol*. 97:426-34.

Tarassov, I., N. Entelis, and R.P. Martin. 1995a. An intact protein translocating machinery is required for mitochondrial import of a yeast cytoplasmic tRNA. *J Mol Biol*. 245:315-23.

Tarassov, I., N. Entelis, and R.P. Martin. 1995b. Mitochondrial import of a cytoplasmic lysine-tRNA in yeast is mediated by cooperation of cytoplasmic and mitochondrial lysyl-tRNA synthetases. *EMBO J*. 14:3461-71.

Thorburn, D.R., and H.H. Dahl. 2001. Mitochondrial disorders: genetics, counseling, prenatal diagnosis and reproductive options. *Am J Med Genet*. 106:102-14.

Tompkins, A.J., L.S. Burwell, S.B. Digerness, C. Zaragoza, W.L. Holman, and P.S. Brookes. 2006. Mitochondrial dysfunction in cardiac ischemia-reperfusion injury: ROS from complex I, without inhibition. *Biochim Biophys Acta*. 1762:223-31.

Topper, J.N., J.L. Bennett, and D.A. Clayton. 1992. A role for RNAase MRP in mitochondrial RNA processing. *Cell*. 70:16-20.

Tourtellotte, W.G., R. Nagarajan, A. Auyeung, C. Mueller, and J. Milbrandt. 1999. Infertility associated with incomplete spermatogenic arrest and oligozoospermia in Egr4-deficient mice. *Development*. 126:5061-71.

Trapnell, C., L. Pachter, and S.L. Salzberg. 2009. TopHat: discovering splice junctions with RNA-Seq. *Bioinformatics*. 25:1105-11.

Trapnell, C., B.A. Williams, G. Pertea, A. Mortazavi, G. Kwan, M.J. van Baren, S.L. Salzberg, B.J. Wold, and L. Pachter. 2010. Transcript assembly and quantification by RNA-Seq reveals unannotated transcripts and isoform switching during cell differentiation. *Nat Biotechnol*. 28:511-5.

Trounce, I.A., Y.L. Kim, A.S. Jun, and D.C. Wallace. 1996. Assessment of mitochondrial oxidative phosphorylation in patient muscle biopsies, lymphoblasts, and transmitochondrial cell lines. *Methods Enzymol*. 264:484-509.

Trounce, I.A., M. McKenzie, C.A. Cassar, C.A. Ingraham, C.A. Lerner, D.A. Dunn, C.L. Donegan, K. Takeda, W.K. Pogozelski, R.L. Howell, and C.A. Pinkert. 2004. Development and initial characterization of xenomitochondrial mice. *J Bioenerg Biomembr*. 36:421-7.

Trounce, I.A., and C.A. Pinkert. 2007. Cybrid models of mtDNA disease and transmission, from cells to mice. *Curr Top Dev Biol*. 77:157-83.

Uhlen, P., and N. Fritz. 2010. Biochemistry of calcium oscillations. *Biochem Biophys Res Commun*. 396:28-32.

Unseld, M., J.R. Marienfeld, P. Brandt, and A. Brennicke. 1997. The mitochondrial genome of Arabidopsis thaliana contains 57 genes in 366,924 nucleotides. *Nat Genet*. 15:57-61.

Uvarov, P., A. Ludwig, M. Markkanen, C. Rivera, and M.S. Airaksinen. 2006. Upregulation of the neuron-specific K+/Cl- cotransporter expression by transcription factor early growth response 4. *J Neurosci*. 26:13463-73.

Verde, P., L. Casalino, F. Talotta, M. Yaniv, and J.B. Weitzman. 2007. Deciphering AP-1 function in tumorigenesis: fra-ternizing on target promoters. *Cell Cycle*. 6:2633-9.

Wallace, D.C. 1999. Mitochondrial diseases in man and mouse. *Science*. 283:1482-8.

Wallace, D.C. 2007. Why do we still have a maternally inherited mitochondrial DNA? Insights from evolutionary medicine. *Annu Rev Biochem*. 76:781-821.

Wang, G., H.W. Chen, Y. Oktay, J. Zhang, E.L. Allen, G.M. Smith, K.C. Fan, J.S. Hong, S.W. French, J.M. McCaffery, R.N. Lightowlers, H.C. Morse, 3rd, C.M. Koehler, and M.A. Teitell. 2010. PNPASE Regulates RNA Import into Mitochondria. *Cell*. 142:456-467.

Wayne, N., and D.N. Bolon. 2007. Dimerization of Hsp90 is required for in vivo function. Design and analysis of monomers and dimers. *J Biol Chem*. 282:35386-95.

Wittig, I., H.P. Braun, and H. Schagger. 2006. Blue native PAGE. *Nat Protoc*. 1:418-28.

Wong, T.W., and D.A. Clayton. 1986. DNA primase of human mitochondria is associated with structural RNA that is essential for enzymatic activity. *Cell*. 45:817-25.

Yoshionari, S., T. Koike, T. Yokogawa, K. Nishikawa, T. Ueda, K. Miura, and K. Watanabe. 1994. Existence of nuclear-encoded 5S-rRNA in bovine mitochondria. *FEBS Lett*. 338:137-42.

Zaidi, N., A. Maurer, S. Nieke, and H. Kalbacher. 2008. Cathepsin D: a cellular roadmap. *Biochem Biophys Res Commun*. 376:5-9.

Zhao, Y., and D. Bruemmer. 2010. NR4A orphan nuclear receptors: transcriptional regulators of gene expression in metabolism and vascular biology. *Arterioscler Thromb Vasc Biol*. 30:1535-41.

Zuker, M. 2003. Mfold web server for nucleic acid folding and hybridization prediction. *Nucleic Acids Res*. 31:3406-15.

Appendix 1: Proteins identified by LC-MS/MS of RNA affinity purification samples from whole cell lysates.

Each line contains annotation of experiment ID (ie: CAPMS-10), RNA utilized for RNA affinity purification, protein identified, MOWSE score and Accession number. Identified proteins are grouped together. For example, the 14-3-3 beta protein was identified in four experiments, bound to the 5.8S, TH, H1 and 5S RNAs.

Sample ID and RNA used for affinity purification	Protein	MOWSE score	Accession Number
CAPMS-10 5S rRNA	14-3-3 eta	182	gi|1526541
CAPMS-7 5.8S rRNA	14-3-3 protein beta	184	gi|3065925
CAPMS-8 TH RNA	14-3-3 protein beta	174	gi|3065925
CAPMS-9 H1 RNA	14-3-3 protein beta	178	gi|3065925
CAPMS-10 5S rRNA	14-3-3 protein beta	242	gi|3065925
CAPMS-7 5.8S rRNA	14-3-3 protein gamma	257	gi|3065929
CAPMS-8 TH RNA	14-3-3 protein gamma	135	gi|3065929
CAPMS-10 5S rRNA	14-3-3 protein gamma	298	gi|3065929
CAPMS-9 H1 RNA	14-3-3 zeta	407	gi|1841387
CAPMS-5 5S rRNA	14-3-3 zeta	67	gi|1526539
CAPMS-7 5.8S rRNA	14-3-3 zeta	215	gi|1841387
CAPMS-8 TH RNA	14-3-3 zeta	182	gi|1841387
CAPMS-10 5S rRNA	14-3-3 zeta	464	gi|1841387
CAPMS-7 5.8S rRNA	78 kDa glucose-regulated protein	571	gi|1304157
CAPMS-8 TH RNA	78 kDa glucose-regulated protein	546	gi|1304157
CAPMS-9 H1 RNA	78 kDa glucose-regulated protein	400	gi|1304157
CAPMS-10 5S rRNA	78 kDa glucose-regulated protein	401	gi|1304157
CAPMS-20 4.5S RNA block2	78 kDa glucose-regulated protein	210	gi|1304157
CAPMS-25 4.5S RNA block1	78 kDa glucose-regulated protein	280	gi|1304157
CAPMS-26 4.5S RNA block2	78 kDa glucose-regulated protein	218	gi|1304157
CAPMS-27 5.8S rRNA	78 kDa glucose-regulated protein	162	gi|1304157
CAPMS-28 TH RNA	78 kDa glucose-regulated protein	166	gi|1304157
CAPMS-29 H1 RNA	78 kDa glucose-regulated protein	175	gi|1304157
CAPMS-30 5S rRNA	78 kDa glucose-regulated protein	183	gi|1304157

CAPMS-25 4.5S RNA block1	84 kD heat shock protein	132	gi|309317
CAPMS-25 4.5S RNA block1	acidic nuclear phosphoprotein pp32	73	gi|1763275
CAPMS-26 4.5S RNA block2	acidic nuclear phosphoprotein pp32	105	gi|1763275
CAPMS-27 5.8S rRNA	acidic nuclear phosphoprotein pp32	126	gi|1763275
CAPMS-26 4.5S RNA block2	actin, gamma 1 propeptide	190	gi|4501887
CAPMS-8 TH RNA	actin, gamma, cytoplasmic 1	207	gi|123298587
CAPMS-7 5.8S rRNA	actinin, alpha 1	69	gi|61097906
CAPMS-8 TH RNA	actinin, alpha 1	105	gi|61097906
CAPMS-20 4.5S RNA block2	actinin, alpha 1	105	gi|61097906
CAPMS-28 TH RNA	Actn1 protein	58	gi|13096866
CAPMS-30 5S rRNA	Actn1 protein	56	gi|13096866
CAPMS-26 4.5S RNA block2	aldolase A	143	gi|7548322
CAPMS-28 TH RNA	aldolase A	452	gi|7548322
CAPMS-30 5S rRNA	aldolase A	438	gi|7548322
CAPMS-5 5S rRNA	alpha actin	162	gi|74191399
CAPMS-30 5S rRNA	alpha glucosidase 2 alpha neutral subunit	73	gi|6679891
CAPMS-26 4.5S RNA block2	alpha glucosidase 2 alpha neutral subunit	68	gi|6679891
CAPMS-28 TH RNA	alpha glucosidase 2 alpha neutral subunit	130	gi|6679891
CAPMS-5 5S rRNA	alpha-A-crystallin	101	gi|387134
CAPMS-19 4.5S RNA block1	alpha-actin	131	gi|49864
CAPMS-8 TH RNA	alpha-cardiac actin	140	gi|387090
CAPMS-20 4.5S RNA block2	alpha-cardiac actin	95	gi|387090
CAPMS-28 TH RNA	alpha-cardiac actin	208	gi|387090
CAPMS-29 H1 RNA	alpha-cardiac actin	102	gi|387090
CAPMS-8 TH RNA	alpha-tubulin isotype M-alpha-2	102	gi|202210
CAPMS-25 4.5S RNA block1	alpha-tubulin isotype M-alpha-2	46	gi|202210
CAPMS-27 5.8S rRNA	alpha-tubulin isotype M-alpha-2	77	gi|202210
CAPMS-28 TH RNA	alpha-tubulin isotype M-alpha-2	96	gi|202210

CAPMS-8 TH RNA	annexin A2	65	gi|6996913
CAPMS-9 H1 RNA	annexin A2	62	gi|6996913
CAPMS-9 H1 RNA	annexin A5	48	gi|6753060
CAPMS-9 H1 RNA	ATP synthase beta-subunit	117	gi|2623222
CAPMS-10 5S rRNA	ATP synthase beta-subunit	51	gi|2623222
CAPMS-10 5S rRNA	ATP synthase, H+ transporting, mitochondrial F1 complex, alpha subunit, isoform 1	72	gi|148677499
CAPMS-20 4.5S RNA block2	ATP synthase, H+ transporting, mitochondrial F1 complex, alpha subunit, isoform 1	54	gi|148677499
CAPMS-8 TH RNA	Atp5b protein	165	gi|23272966
CAPMS-5 5S rRNA	beta-galactoside binding protein	250	gi|193442
CAPMS-28 TH RNA	beta-galactoside binding protein	111	gi|193442
CAPMS-29 H1 RNA	beta-galactoside binding protein	231	gi|193442
CAPMS-30 5S rRNA	beta-galactoside binding protein	153	gi|193442
CAPMS-7 5.8S rRNA	calmodulin	59	gi|469422
CAPMS-8 TH RNA	calmodulin	96	gi|469422
CAPMS-10 5S rRNA	calmodulin	97	gi|508526
CAPMS-26 4.5S RNA block2	calumenin isoform 1	46	gi|6680840
CAPMS-8 TH RNA	CCT (chaperonin containing TCP-1) beta subunit	105	gi|468546
CAPMS-5 5S rRNA	Chain A, Crystal Structure Of Cellular Retinoic-Acid-Binding Proteins	71	gi|999883
CAPMS-7 5.8S rRNA	chaperonin containing TCP-1 theta subunit	115	gi|5295992
CAPMS-30 5S rRNA	chaperonin containing TCP-1 theta subunit	113	gi|5295992
CAPMS-9 H1 RNA	chaperonin containing Tcp1, subunit 4 (delta)	55	gi|6753322
CAPMS-20 4.5S RNA block2	chaperonin containing Tcp1, subunit 4 (delta)	54	gi|6753322
CAPMS-9 H1 RNA	chaperonin containing Tcp1, subunit 6a	90	gi|6753324
CAPMS-26 4.5S RNA block2	chaperonin subunit 2 (beta)	88	gi|126521835
CAPMS-5 5S rRNA	cofilin 1, non-muscle	58	gi|6680924
CAPMS-19 4.5S RNA block1	collagen pro-alpha-1 type I chain	320	gi|470674

CAPMS-20 4.5S RNA block2	collagen pro-alpha-1 type I chain	84	gi|470674
CAPMS-25 4.5S RNA block1	collagen pro-alpha-1 type I chain	367	gi|470674
CAPMS-26 4.5S RNA block2	collagen pro-alpha-1 type I chain	80	gi|470674
CAPMS-9 H1 RNA	component C5 of proteasome	57	gi|1165123
CAPMS-9 H1 RNA	cytokeratin KRT2-6HF	57	gi|13272554
CAPMS-8 TH RNA	elongation factor 1-beta homolog	102	gi|5902663
CAPMS-9 H1 RNA	elongation factor 1-beta homolog	79	gi|5902663
CAPMS-7 5.8S rRNA	elongation factor Tu	219	gi|556301
CAPMS-8 TH RNA	elongation factor Tu	182	gi|556301
CAPMS-9 H1 RNA	elongation factor Tu	293	gi|556301
CAPMS-10 5S rRNA	elongation factor Tu	117	gi|556301
CAPMS-26 4.5S RNA block2	elongation factor Tu	49	gi|556301
CAPMS-28 TH RNA	elongation factor Tu	101	gi|556301
CAPMS-29 H1 RNA	elongation factor Tu	63	gi|556301
CAPMS-30 5S rRNA	elongation factor Tu	72	gi|556301
CAPMS-5 5S rRNA	epidermal keratin 10	108	gi|7638398
CAPMS-6 5S rRNA	epidermal keratin 10	135	gi|7638398
CAPMS-8 TH RNA	epidermal keratin subunit I	65	gi|387397
CAPMS-20 4.5S RNA block2	eukaryotic translation elongation factor 1 alpha 2	106	gi|6681273
CAPMS-8 TH RNA	eukaryotic translation elongation factor 2	637	gi|33859482
CAPMS-9 H1 RNA	eukaryotic translation elongation factor 2	422	gi|33859482
CAPMS-25 4.5S RNA block1	eukaryotic translation elongation factor 2	224	gi|33859482
CAPMS-26 4.5S RNA block2	eukaryotic translation elongation factor 2	197	gi|33859482
CAPMS-27 5.8S rRNA	eukaryotic translation elongation factor 2	133	gi|33859482
CAPMS-28 TH RNA	eukaryotic translation elongation factor 2	520	gi|33859482
CAPMS-29 H1 RNA	eukaryotic translation elongation factor 2	409	gi|33859482
CAPMS-30 5S rRNA	eukaryotic translation elongation factor 2	273	gi|33859482

CAPMS-19 4.5S RNA block1	Eukaryotic translation initiation factor 4B	156	gi|13938112
CAPMS-20 4.5S RNA block2	Eukaryotic translation initiation factor 4B	213	gi|13938112
CAPMS-26 4.5S RNA block2	Eukaryotic translation initiation factor 4B	61	gi|13938112
CAPMS-8 TH RNA	filamin C, gamma	113	gi|124487139
CAPMS-9 H1 RNA	filamin C, gamma	113	gi|124487139
CAPMS-10 5S rRNA	FK506 binding protein 4	134	gi|13097417
CAPMS-7 5.8S rRNA	FK506 binding protein 52	143	gi|6753882
CAPMS-8 TH RNA	FK506 binding protein 52	125	gi|6753882
CAPMS-9 H1 RNA	FK506 binding protein 52	151	gi|6753882
CAPMS-8 TH RNA	fructose-bisphosphate aldolase A	146	gi|6671539
CAPMS-9 H1 RNA	fructose-bisphosphate aldolase A	161	gi|6671539
CAPMS-10 5S rRNA	fructose-bisphosphate aldolase A	196	gi|6671539
CAPMS-20 4.5S RNA block2	fructose-bisphosphate aldolase A	49	gi|6671539
CAPMS-27 5.8S rRNA	fructose-bisphosphate aldolase A	153	gi|6671539
CAPMS-29 H1 RNA	fructose-bisphosphate aldolase A	585	gi|6671539
CAPMS-5 5S rRNA	G patch domain containing 1	63	gi|13385692
CAPMS-7 5.8S rRNA	galectin 3	159	gi|33859580
CAPMS-8 TH RNA	galectin 3	111	gi|33859580
CAPMS-9 H1 RNA	galectin 3	92	gi|33859580
CAPMS-26 4.5S RNA block2	Galectin-3	106	gi|126679
CAPMS-30 5S rRNA	Galectin-3	139	gi|126679
CAPMS-7 5.8S rRNA	gamma-actin	142	gi|809561
CAPMS-10 5S rRNA	gamma-actin	142	gi|809561
CAPMS-25 4.5S RNA block1	gamma-actin	169	gi|809561
CAPMS-30 5S rRNA	gamma-actin	197	gi|809561
CAPMS-5 5S rRNA	gelsolin, cytosolic - mouse	126	gi|90508
CAPMS-8 TH RNA	glyceraldehyde-3-phosphate dehydrogenase	166	gi|6679937
CAPMS-9 H1 RNA	glyceraldehyde-3-phosphate dehydrogenase	112	gi|6679937
CAPMS-7 5.8S rRNA	heat shock protein 1, alpha	407	gi|6754254
CAPMS-9 H1 RNA	heat shock protein 1, alpha	395	gi|6754254
CAPMS-10 5S rRNA	heat shock protein 1, alpha	649	gi|6754254
CAPMS-30 5S rRNA	heat shock protein 1, alpha	82	gi|6754254

CAPMS-7 5.8S rRNA	heat shock protein 1, beta	581	gi|40556608
CAPMS-8 TH RNA	heat shock protein 1, beta	761	gi|40556608
CAPMS-9 H1 RNA	heat shock protein 1, beta	602	gi|40556608
CAPMS-10 5S rRNA	heat shock protein 1, beta	857	gi|40556608
CAPMS-30 5S rRNA	heat shock protein 65	324	gi|51455
CAPMS-8 TH RNA	heat shock protein 65	299	gi|51455
CAPMS-9 H1 RNA	heat shock protein 65	210	gi|51455
CAPMS-10 5S rRNA	heat shock protein 65	355	gi|51455
CAPMS-19 4.5S RNA block1	heat shock protein 65	96	gi|51455
CAPMS-27 5.8S rRNA	heat shock protein 65	141	gi|51455
CAPMS-28 TH RNA	heat shock protein 65	232	gi|51455
CAPMS-5 5S rRNA	heat shock protein 70 cognate	164	gi|309319
CAPMS-6 5S rRNA	heat shock protein 70 cognate	101	gi|309319
CAPMS-7 5.8S rRNA	heat shock protein 70 cognate	707	gi|309319
CAPMS-8 TH RNA	heat shock protein 70 cognate	715	gi|309319
CAPMS-9 H1 RNA	heat shock protein 70 cognate	661	gi|309319
CAPMS-10 5S rRNA	heat shock protein 70 cognate	642	gi|309319
CAPMS-20 4.5S RNA block2	heat shock protein 70 cognate	312	gi|309319
CAPMS-25 4.5S RNA block1	heat shock protein 70 cognate	528	gi|309319
CAPMS-26 4.5S RNA block2	heat shock protein 70 cognate	559	gi|309319
CAPMS-27 5.8S rRNA	heat shock protein 70 cognate	253	gi|309319
CAPMS-28 TH RNA	heat shock protein 70 cognate	320	gi|309319
CAPMS-29 H1 RNA	heat shock protein 70 cognate	537	gi|309319
CAPMS-30 5S rRNA	heat shock protein 70 cognate	366	gi|309319
CAPMS-7 5.8S rRNA	heat shock protein 9	225	gi|162461907
CAPMS-9 H1 RNA	heat shock protein 9	199	gi|162461907
CAPMS-8 TH RNA	heat shock protein 9	126	gi|162461907
CAPMS-10 5S rRNA	heat shock protein 9	165	gi|162461907
CAPMS-26 4.5S RNA block2	Heat shock protein 90, beta (Grp94), member 1	59	gi|14714615
CAPMS-28 TH RNA	Heat shock protein 90, beta (Grp94), member 1	201	gi|14714615
CAPMS-30 5S rRNA	Heat shock protein 90, beta (Grp94), member 1	91	gi|14714615
CAPMS-26 4.5S	Heat shock protein HSP 90-beta	172	gi|123681

RNA block2			
CAPMS-28 TH RNA	Heat shock protein HSP 90-beta	158	gi|123681
CAPMS-29 H1 RNA	Heat shock protein HSP 90-beta	96	gi|123681
CAPMS-30 5S rRNA	Heat shock protein HSP 90-beta	139	gi|123681
CAPMS-20 4.5S RNA block2	heat-shock protein hsp84	59	gi|194027
CAPMS-27 5.8S rRNA	heterogeneous nuclear ribonucleoprotein	59	gi|13384620
CAPMS-26 4.5S RNA block2	heterogeneous nuclear ribonucleoprotein A1 isoform a	54	gi|4504445
CAPMS-7 5.8S rRNA	heterogeneous nuclear ribonucleoprotein K	68	gi|13384620
CAPMS-8 TH RNA	Importin subunit beta-1	70	gi|2829480
CAPMS-7 5.8S rRNA	keratin 6A	79	gi|54607171
CAPMS-8 TH RNA	keratin 6A	90	gi|54607171
CAPMS-10 5S rRNA	keratin 6A	97	gi|54607171
CAPMS-8 TH RNA	keratin 6L	54	gi|22164776
CAPMS-10 5S rRNA	keratin 6L	66	gi|22164776
CAPMS-5 5S rRNA	keratin 75	89	gi|29789317
CAPMS-10 5S rRNA	Khsrp protein	52	gi|82697008
CAPMS-7 5.8S rRNA	lectin, galactose binding, soluble 1	97	gi|6678682
CAPMS-9 H1 RNA	lectin, galactose binding, soluble 1	118	gi|6678682
CAPMS-10 5S rRNA	lectin, galactose binding, soluble 1	161	gi|6678682
CAPMS-8 TH RNA	lectin, galactose binding, soluble 1	73	gi|6678682
CAPMS-9 H1 RNA	LIM protein	57	gi|4894847
CAPMS-25 4.5S RNA block1	lipocortin I	94	gi|198845
CAPMS-27 5.8S rRNA	lysyl-tRNA synthetase isoform 2	65	gi|16716381
CAPMS-8 TH RNA	M2-type pyruvate kinase	182	gi|1405933
CAPMS-7 5.8S rRNA	matricin	78	gi|347839
CAPMS-9 H1 RNA	matricin	73	gi|347839
CAPMS-10 5S rRNA	matricin	52	gi|347839
CAPMS-9 H1 RNA	mCG140959, isoform CRA_g	174	gi|148692630
CAPMS-5 5S rRNA	mCG22560	58	gi|148706112
CAPMS-19 4.5S RNA block1	murine valosin-containing protein	94	gi|55217
CAPMS-27 5.8S rRNA	murine valosin-containing protein	109	gi|55217
CAPMS-30 5S rRNA	murine valosin-containing protein	148	gi|55217
CAPMS-8 TH RNA	myosin light chain, regulatory B-	62	gi|71037403

	like		
CAPMS-5 5S rRNA	myosin, heavy polypeptide 9	239	gi|114326446
CAPMS-7 5.8S rRNA	myosin, heavy polypeptide 9, non-muscle isoform 1	457	gi|114326446
CAPMS-8 TH RNA	myosin, heavy polypeptide 9, non-muscle isoform 1	510	gi|114326446
CAPMS-27 5.8S rRNA	myosin, heavy polypeptide 9, non-muscle isoform 1	100	gi|114326446
CAPMS-20 4.5S RNA block2	Nedd4	78	gi|1374782
CAPMS-9 H1 RNA	nonmuscle heavy chain myosin II-A	595	gi|17978023
CAPMS-10 5S rRNA	nonmuscle heavy chain myosin II-A	572	gi|17978023
CAPMS-20 4.5S RNA block2	nonmuscle heavy chain myosin II-A	95	gi|17978023
CAPMS-8 TH RNA	non-muscle myosin light chain 3	80	gi|435585
CAPMS-9 H1 RNA	Nucleolin	120	gi|13529464
CAPMS-20 4.5S RNA block2	Nucleolin	72	gi|13529464
CAPMS-30 5S rRNA	Nucleolin	67	gi|13529464
CAPMS-10 5S rRNA	Nucleolin	78	gi|13529464
CAPMS-26 4.5S RNA block2	Nucleolin	97	gi|13529464
CAPMS-28 TH RNA	Nucleolin	217	gi|13529464
CAPMS-8 TH RNA	nucleolin, isoform CRA_a	95	gi|148708273
CAPMS-27 5.8S rRNA	nucleophosmin 1	57	gi|6679108
CAPMS-30 5S rRNA	nucleophosmin 1	71	gi|6679108
CAPMS-8 TH RNA	PDGFA associated protein 1	60	gi|12018258
CAPMS-9 H1 RNA	PDGFA associated protein 1	49	gi|12018258
CAPMS-7 5.8S rRNA	peroxiredoxin 1	81	gi|6754976
CAPMS-8 TH RNA	peroxiredoxin 1	130	gi|6754976
CAPMS-9 H1 RNA	peroxiredoxin 1	267	gi|6754976
CAPMS-27 5.8S rRNA	peroxiredoxin 1	164	gi|6754976
CAPMS-28 TH RNA	peroxiredoxin 1	238	gi|123230137
CAPMS-30 5S rRNA	peroxiredoxin 1	167	gi|6754976
CAPMS-5 5S rRNA	peroxiredoxin 1	101	gi|6754976
CAPMS-10 5S rRNA	peroxiredoxin 1	149	gi|6754976
CAPMS-29 H1 RNA	peroxiredoxin 1	222	gi|6754976
CAPMS-9 H1 RNA	peroxiredoxin 2	72	gi|148747558
CAPMS-7 5.8S rRNA	peroxiredoxin 2	57	gi|148747558

CAPMS-7 5.8S rRNA	peroxiredoxin 4	82	gi|7948999
CAPMS-30 5S rRNA	phosphoglycerate dehydrogenase	44	gi|52353955
CAPMS-7 5.8S rRNA	poly(rC) binding protein 1	51	gi|6754994
CAPMS-7 5.8S rRNA	PREDICTED: similar to Heat shock protein 1 (chaperonin)	159	gi|51766670
CAPMS-26 4.5S RNA block2	PREDICTED: similar to Heat shock protein 1 (chaperonin)	180	gi|51766670
CAPMS-9 H1 RNA	PREDICTED: similar to tropomyosin 3 isoform 1	105	gi|149751320
CAPMS-9 H1 RNA	pro-alpha-1 type I collagen	63	gi|192262
CAPMS-25 4.5S RNA block1	pro-alpha-2(I) collagen	465	gi|50489
CAPMS-7 5.8S rRNA	prosaposin	115	gi|1381582
CAPMS-8 TH RNA	prosaposin	83	gi|1381582
CAPMS-9 H1 RNA	prosaposin, isoform CRA_b	96	gi|148700228
CAPMS-8 TH RNA	proteasome (prosome, macropain) subunit, alpha type 1	93	gi|33563282
CAPMS-9 H1 RNA	proteasome (prosome, macropain) subunit, alpha type 1	69	gi|33563282
CAPMS-10 5S rRNA	proteasome (prosome, macropain) subunit, alpha type 1	94	gi|33563282
CAPMS-7 5.8S rRNA	proteasome (prosome, macropain) subunit, alpha type 1, isoform CRA_d	97	gi|148685117
CAPMS-8 TH RNA	proteasome (prosome, macropain) subunit, alpha type 4	106	gi|6755196
CAPMS-10 5S rRNA	proteasome (prosome, macropain) subunit, alpha type 4	110	gi|6755196
CAPMS-20 4.5S RNA block2	proteasome (prosome, macropain) subunit, alpha type 4	53	gi|6755196
CAPMS-7 5.8S rRNA	proteasome (prosome, macropain) subunit, alpha type 4	149	gi|6755196
CAPMS-7 5.8S rRNA	proteasome (prosome, macropain) subunit, alpha type 5	107	gi|7106387
CAPMS-8 TH RNA	proteasome (prosome, macropain) subunit, alpha type 5	54	gi|7106387
CAPMS-9 H1 RNA	proteasome (prosome, macropain) subunit, alpha type 5	120	gi|7106387
CAPMS-20 4.5S RNA block2	proteasome (prosome, macropain) subunit, alpha type 5	63	gi|7106387

CAPMS-26 4.5S RNA block2	proteasome (prosome, macropain) subunit, alpha type 5	55	gi|7106387
CAPMS-7 5.8S rRNA	proteasome (prosome, macropain) subunit, alpha type 6	81	gi|6755198
CAPMS-9 H1 RNA	proteasome (prosome, macropain) subunit, alpha type 6	110	gi|6755198
CAPMS-10 5S rRNA	proteasome (prosome, macropain) subunit, alpha type 6	44	gi|6755198
CAPMS-20 4.5S RNA block2	proteasome (prosome, macropain) subunit, alpha type 6	44	gi|6755198
CAPMS-8 TH RNA	proteasome (prosome, macropain) subunit, alpha type 6	46	gi|6755198
CAPMS-10 5S rRNA	proteasome (prosome, macropain) subunit, alpha type 7	70	gi|7106389
CAPMS-20 4.5S RNA block2	proteasome (prosome, macropain) subunit, alpha type 7	49	gi|7106389
CAPMS-8 TH RNA	proteasome (prosome, macropain) subunit, beta type 1	79	gi|7242197
CAPMS-10 5S rRNA	proteasome (prosome, macropain) subunit, beta type 1	69	gi|7242197
CAPMS-7 5.8S rRNA	proteasome (prosome, macropain) subunit, beta type 5	59	gi|6755204
CAPMS-8 TH RNA	proteasome (prosome, macropain) subunit, beta type 5	156	gi|6755204
CAPMS-9 H1 RNA	proteasome (prosome, macropain) subunit, beta type 5	116	gi|6755204
CAPMS-10 5S rRNA	proteasome (prosome, macropain) subunit, beta type 5	159	gi|6755204
CAPMS-9 H1 RNA	proteasome beta 3 subunit	133	gi|6755202
CAPMS-29 H1 RNA	proteasome endopeptidase complex	101	gi|2118156
CAPMS-20 4.5S RNA block2	proteasome endopeptidase complex	69	gi|2118156
CAPMS-26 4.5S RNA block2	proteasome endopeptidase complex	80	gi|2118156
CAPMS-7 5.8S rRNA	proteasome endopeptidase complex (EC 3.4.25.1) delta chain	97	gi|2118156
CAPMS-8 TH RNA	proteasome endopeptidase complex (EC 3.4.25.1) delta chain	63	gi|2118156
CAPMS-9 H1 RNA	proteasome endopeptidase complex (EC 3.4.25.1) delta chain	101	gi|2118156

CAPMS-10 5S rRNA	proteasome endopeptidase complex (EC 3.4.25.1) delta chain	110	gi|2118156
CAPMS-7 5.8S rRNA	Proteasome subunit alpha type-2	96	gi|1709759
CAPMS-8 TH RNA	Proteasome subunit alpha type-2	133	gi|1709759
CAPMS-9 H1 RNA	Proteasome subunit alpha type-2	83	gi|1709759
CAPMS-28 TH RNA	Proteasome subunit alpha type-2	77	gi|1709759
CAPMS-10 5S rRNA	Proteasome subunit alpha type-2;	103	gi|1709759
CAPMS-7 5.8S rRNA	Proteasome subunit alpha type-3	94	gi|3914438
CAPMS-8 TH RNA	Proteasome subunit alpha type-3	104	gi|3914438
CAPMS-10 5S rRNA	Proteasome subunit alpha type-3	87	gi|3914438
CAPMS-7 5.8S rRNA	Proteasome subunit beta type-2	86	gi|9910832
CAPMS-8 TH RNA	Proteasome subunit beta type-2	68	gi|9910832
CAPMS-9 H1 RNA	Proteasome subunit beta type-2	95	gi|9910832
CAPMS-7 5.8S rRNA	Protein disulfide isomerase associated 6	343	gi|60502437
CAPMS-8 TH RNA	Protein disulfide isomerase associated 6	374	gi|60502437
CAPMS-9 H1 RNA	protein disulfide isomerase-associated 6	318	gi|58037267
CAPMS-10 5S rRNA	protein disulfide isomerase-associated 6	277	gi|58037267
CAPMS-25 4.5S RNA block1	protein disulfide isomerase-associated 6	71	gi|58037267
CAPMS-26 4.5S RNA block2	protein disulfide isomerase-associated 6	80	gi|58037267
CAPMS-30 5S rRNA	Protein disulfide-isomerase	98	gi|129729
CAPMS-9 H1 RNA	Protein disulfide-isomerase A4	65	gi|119531
CAPMS-20 4.5S RNA block2	Protein disulfide-isomerase A6	181	gi|62510933
CAPMS-27 5.8S rRNA	Protein disulfide-isomerase A6	160	gi|62510933
CAPMS-28 TH RNA	Protein disulfide-isomerase A6	253	gi|62510933
CAPMS-8 TH RNA	Protein disulfide-isomerase; Short=PDI; AltName: Full=Prolyl 4-hydroxylase subunit beta	83	gi|129729
CAPMS-9 H1 RNA	Protein disulfide-isomerase; Short=PDI; AltName: Full=Prolyl 4-hydroxylase subunit beta	126	gi|129729

CAPMS-10 5S rRNA	Protein disulfide-isomerase; Short=PDI; AltName: Full=Prolyl 4-hydroxylase subunit beta	132	gi|129729
CAPMS-28 TH RNA	protein kinase C substrate 80K-H	117	gi|6679465
CAPMS-29 H1 RNA	protein kinase C substrate 80K-H	70	gi|6679465
CAPMS-10 5S rRNA	prothymosin alpha	61	gi|7110705
CAPMS-30 5S rRNA	Psma8 protein	46	gi|18044409
CAPMS-10 5S rRNA	put. beta-actin	113	gi|49868
CAPMS-8 TH RNA	put. beta-actin (aa 27-375)	190	gi|49868
CAPMS-9 H1 RNA	put. beta-actin (aa 27-375)	208	gi|49868
CAPMS-9 H1 RNA	pyruvate kinase M	117	gi|551295
CAPMS-7 5.8S rRNA	pyruvate kinase M	75	gi|551295
CAPMS-7 5.8S rRNA	ras-related nuclear protein	152	gi|5453555
CAPMS-8 TH RNA	ras-related nuclear protein	122	gi|5453555
CAPMS-20 4.5S RNA block2	ras-related nuclear protein	100	gi|5453555
CAPMS-27 5.8S rRNA	ras-related nuclear protein	72	gi|5453555
CAPMS-28 TH RNA	ras-related nuclear protein	50	gi|5453555
CAPMS-8 TH RNA	reticulon 4 isoform B1	89	gi|34610233
CAPMS-7 5.8S rRNA	reticulon 4 isoform B2	87	gi|34610241
CAPMS-9 H1 RNA	S100 calcium binding protein A11 (calizzarin)	58	gi|21886811
CAPMS-8 TH RNA	S100 calcium binding protein A4	109	gi|33859624
CAPMS-25 4.5S RNA block1	S100 calcium binding protein A4	95	gi|33859624
CAPMS-26 4.5S RNA block2	S100 calcium binding protein A4	94	gi|33859624
CAPMS-9 H1 RNA	S100 calcium binding protein A4	87	gi|33859624
CAPMS-20 4.5S RNA block2	S100 calcium binding protein A4	82	gi|33859624
CAPMS-27 5.8S rRNA	S100 calcium binding protein A4	98	gi|33859624
CAPMS-29 H1 RNA	S100 calcium binding protein A4	92	gi|33859624
CAPMS-30 5S rRNA	S100 calcium binding protein A4	117	gi|33859624
CAPMS-5 5S rRNA	S100 calcium binding protein A6 (calcyclin)	134	gi|6755392
CAPMS-6 5S rRNA	S100 calcium binding protein A6 (calcyclin)	65	gi|6755392
CAPMS-8 TH RNA	S100 calcium binding protein A6 (calcyclin)	93	gi|6755392

CAPMS-10 5S rRNA	S100 calcium binding protein A6 (calcyclin)	51	gi|6755392
CAPMS-26 4.5S RNA block2	S100 calcium binding protein A6 (calcyclin)	74	gi|6755392
CAPMS-27 5.8S rRNA	S100 calcium binding protein A6 (calcyclin)	53	gi|6755392
CAPMS-7 5.8S rRNA	serine-tRNA ligase	77	gi|91287
CAPMS-30 5S rRNA	SET translocation	113	gi|13591862
CAPMS-8 TH RNA	similar to KIAA2019 protein	82	gi|149263538
CAPMS-7 5.8S rRNA	similar to MYL6 protein	92	gi|94363353
CAPMS-25 4.5S RNA block1	similar to Nucleophosmin 1 isoform 3	137	gi|94385641
CAPMS-10 5S rRNA	similar to Ywhaq protei	322	gi|149263879
CAPMS-25 4.5S RNA block1	Stress-70 protein, mitochondrial	132	gi|14917005
CAPMS-28 TH RNA	Stress-70 protein, mitochondrial	112	gi|14917005
CAPMS-29 H1 RNA	Stress-70 protein, mitochondrial	81	gi|14917005
CAPMS-30 5S rRNA	Stress-70 protein, mitochondrial	197	gi|14917005
CAPMS-25 4.5S RNA block1	Stress-induced phosphoprotein 1	72	gi|13277819
CAPMS-10 5S rRNA	sulfated glycoprotein	104	gi|881390
CAPMS-20 4.5S RNA block2	T-complex protein 1 subunit eta	93	gi|549060
CAPMS-9 H1 RNA	thioredoxin 1	84	gi|6755911
CAPMS-9 H1 RNA	transcription elongation factor B (SIII), polypeptide 2	58	gi|13385800
CAPMS-7 5.8S rRNA	transketolase	75	gi|6678359
CAPMS-10 5S rRNA	transketolase	88	gi|6678359
CAPMS-25 4.5S RNA block1	tropomyosin 4	54	gi|47894398
CAPMS-9 H1 RNA	Txndc5 protein	56	gi|19353593
CAPMS-27 5.8S rRNA	Txndc5 protein	53	gi|19353593
CAPMS-6 5S rRNA	type II keratin subunit protein	91	gi|4159806
CAPMS-5 5S rRNA	tyrosine 3/tryptophan 5 - monooxygenase activation protein, epsilon polypeptide	98	gi|5803225
CAPMS-7 5.8S rRNA	tyrosine 3/tryptophan 5 - monooxygenase activation protein, epsilon polypeptide	181	gi|5803225

CAPMS-8 TH RNA	tyrosine 3/tryptophan 5 - monooxygenase activation protein, epsilon polypeptide	234	gi|5803225
CAPMS-9 H1 RNA	tyrosine 3/tryptophan 5 - monooxygenase activation protein, epsilon polypeptide	215	gi|5803225
CAPMS-10 5S rRNA	tyrosine 3/tryptophan 5 - monooxygenase activation protein, epsilon polypeptide	297	gi|5803225
CAPMS-25 4.5S RNA block1	tyrosine 3/tryptophan 5 - monooxygenase activation protein, epsilon polypeptide	79	gi|5803225
CAPMS-8 TH RNA	tyrosine 3-monooxygenase/tryptophan 5-monooxygenase activation protein, theta polypeptide	225	gi|6756039
CAPMS-9 H1 RNA	tyrosine 3-monooxygenase/tryptophan 5-monooxygenase activation protein, theta polypeptide	216	gi|6756039
CAPMS-9 H1 RNA	Uap1l1 protein	121	gi|28175154
CAPMS-10 5S rRNA	Uap1l1 protein	115	gi|28175154
CAPMS-25 4.5S RNA block1	Uap1l1 protein	82	gi|28175154
CAPMS-8 TH RNA	UDP-N-acteylglucosamine pyrophosphorylase 1-like 1	143	gi|84794548
CAPMS-8 TH RNA	Ulip2 protein	53	gi|1915913
CAPMS-7 5.8S rRNA	unnamed protein product	428	gi|74140876
CAPMS-8 TH RNA	unnamed protein product	507	gi|74184925
CAPMS-9 H1 RNA	unnamed protein product	220	gi|74191399
CAPMS-10 5S rRNA	unnamed protein product	387	gi|74204678
CAPMS-10 5S rRNA	unnamed protein product	121	gi|12846283
CAPMS-10 5S rRNA	unnamed protein product	74	gi|12851618
CAPMS-8 TH RNA	UV excision repair protein RAD23 homolog B	152	gi|1709986
CAPMS-9 H1 RNA	UV excision repair protein RAD23 homolog B;	104	gi|1709986
CAPMS-10 5S rRNA	UV excision repair protein RAD23 homolog B;	128	gi|1709986
CAPMS-8 TH RNA	valosin containing protein, isoform CRA_b	96	gi|148670554

CAPMS-9 H1 RNA	valosin-containing protein	154	gi|6005942
CAPMS-8 TH RNA	Y box-binbing protein	78	gi|55451
CAPMS-19 4.5S RNA block1	YL2 protein	67	gi|743485
CAPMS-7 5.8S rRNA	Ywhaq protein	259	gi|51593617

Appendix 2: Proteins identified by LC-MS/MS of RNA affinity purification samples from mitochondrial lysates.

Each line contains annotation of experiment ID (ie: CAPMS-10), RNA utilized for RNA affinity purification, protein identified, MOWSE score and Accession number. Identified proteins are grouped together. For example, the 14-3-3 beta protein was identified in four experiments, bound to the 5.8S, TH, H1 and 5S RNAs.

Sample ID and RNA used for affinity purification	Protein	MOWSE score	Accession Number
CAPMS-11 5.8S rRNA	2,4-dienoyl CoA reductase 1, mitochondrial	89	gi|13385680
CAPMS-18 5S rRNA	2,4-dienoyl CoA reductase 1, mitochondrial	81	gi|13385680
CAPMS-21 4.5s RNA block1	2,4-dienoyl CoA reductase 1, mitochondrial	210	gi|13385680
CAPMS-22 4.5s RNA block2	2,4-dienoyl CoA reductase 1, mitochondrial	176	gi|13385680
CAPMS-14 5S rRNA	2-hydroxyacyl-CoA lyase 1	217	gi|31560355
CAPMS-16 TH RNA	2-hydroxyacyl-CoA lyase 1	142	gi|31560355
CAPMS-22 4.5s RNA block2	2-hydroxyacyl-CoA lyase 1	361	gi|31560355
CAPMS-24 4.5s RNA block2	2-hydroxyacyl-CoA lyase 1	339	gi|31560355
CAPMS-13 H1 RNA	2-hydroxyacyl-CoA lyase 1	323	gi|31560355
CAPMS-21 4.5s RNA block1	2-hydroxyacyl-CoA lyase 1	282	gi|31560355
CAPMS-11 5.8S rRNA	2-hydroxyphytanoyl-CoA lyase	484	gi|6688685
CAPMS-12 TH RNA	2-hydroxyphytanoyl-CoA lyase	406	gi|6688685
CAPMS-15 5.8S rRNA	2-hydroxyphytanoyl-CoA lyase	235	gi|6688685
CAPMS-17 H1 RNA	2-hydroxyphytanoyl-CoA lyase	255	gi|6688685
CAPMS-23 4.5s RNA block1	2-hydroxyphytanoyl-CoA lyase	298	gi|6688685
CAPMS-12 TH RNA	3-hydroxy-3-methylglutaryl-Coenzyme A lyase	77	gi|171543858

CAPMS-21 4.5s RNA block1	3-hydroxy-3-methylglutaryl-Coenzyme A synthase 1	65	gi|21618633
CAPMS-11 5.8S rRNA	3-hydroxyacyl CoA dehydrogenase	59	gi|1125026
CAPMS-15 5.8S rRNA	3-hydroxyacyl CoA dehydrogenase	83	gi|1125026
CAPMS-17 H1 RNA	3-hydroxyacyl CoA dehydrogenase	126	gi|1125026
CAPMS-21 4.5s RNA block1	3-hydroxyisobutyrate dehydrogenase precursor	107	gi|21704140
CAPMS-11 5.8S rRNA	78 kDa glucose-regulated protein	133	gi|2506545
CAPMS-14 5S rRNA	78 kDa glucose-regulated protein	119	gi|1304157
CAPMS-12 TH RNA	78 kDa glucose-regulated protein	121	gi|1304157
CAPMS-13 H1 RNA	78 kDa glucose-regulated protein	79	gi|1304157
CAPMS-16 TH RNA	78 kDa glucose-regulated protein	65	gi|1304157
CAPMS-17 H1 RNA	78 kDa glucose-regulated protein	57	gi|1304157
CAPMS-21 4.5s RNA block1	78 kDa glucose-regulated protein	395	gi|1304157
CAPMS-11 5.8S rRNA	acetyl-Coenzyme A acetyltransferase 1 precursor	157	gi|21450129
CAPMS-12 TH RNA	acetyl-Coenzyme A acetyltransferase 1 precursor	111	gi|21450129
CAPMS-13 H1 RNA	acetyl-Coenzyme A acetyltransferase 1 precursor	67	gi|21450129
CAPMS-14 5S rRNA	acetyl-Coenzyme A acetyltransferase 1 precursor	64	gi|21450129
CAPMS-15 5.8S rRNA	acetyl-Coenzyme A acetyltransferase 1 precursor	55	gi|21450129
CAPMS-16 TH RNA	acetyl-Coenzyme A acetyltransferase 1 precursor	66	gi|21450129
CAPMS-18 5S rRNA	acetyl-Coenzyme A acetyltransferase 1 precursor	64	gi|21450129
CAPMS-21 4.5s RNA block1	acetyl-Coenzyme A acetyltransferase 1 precursor	64	gi|21450129
CAPMS-22 4.5s RNA block2	acetyl-Coenzyme A acetyltransferase 1 precursor	99	gi|21450129
CAPMS-23 4.5s RNA block1	acetyl-Coenzyme A acetyltransferase 1 precursor	142	gi|21450129
CAPMS-17 H1 RNA	acetyl-Coenzyme A acyltransferase 1B	70	gi|22122797
CAPMS-21 4.5s RNA block1	acetyl-Coenzyme A acyltransferase 1B	83	gi|22122797

CAPMS-23	4.5s RNA block1	acetyl-Coenzyme A acyltransferase 1B	73	gi|22122797
CAPMS-24	4.5s RNA block2	acetyl-Coenzyme A acyltransferase 1B	110	gi|22122797
CAPMS-11	5.8S rRNA	acetyl-Coenzyme A acyltransferase 2 (mitochondrial 3-oxoacyl-Coenzyme A thiolase)	212	gi|29126205
CAPMS-17	H1 RNA	acetyl-Coenzyme A acyltransferase 2 (mitochondrial 3-oxoacyl-Coenzyme A thiolase)	155	gi|29126205
CAPMS-21	4.5s RNA block1	acetyl-Coenzyme A acyltransferase 2 (mitochondrial 3-oxoacyl-Coenzyme A thiolase),	48	gi|148677570
CAPMS-24	4.5s RNA block2	Acly protein	55	gi|18204829
CAPMS-21	4.5s RNA block1	acyl-CoA synthetase medium-chain family member 1	138	gi|16905127
CAPMS-23	4.5s RNA block1	adenylate kinase isozyme 2	101	gi|4760598
CAPMS-21	4.5s RNA block1	Agmatine ureohydrolase (agmatinase)	119	gi|109730945
CAPMS-23	4.5s RNA block1	albumin	84	gi|163310765
CAPMS-22	4.5s RNA block2	albumin	178	gi|163310765
CAPMS-24	4.5s RNA block2	Aldh4a1 protein	53	gi|18848352
CAPMS-11	5.8S rRNA	alpha glucosidase 2 alpha neutral subunit	245	gi|6679891
CAPMS-14	5S rRNA	alpha glucosidase 2 alpha neutral subunit	297	gi|6679891
CAPMS-15	5.8S rRNA	alpha glucosidase 2 alpha neutral subunit	47	gi|6679891
CAPMS-16	TH RNA	alpha glucosidase 2 alpha neutral subunit	310	gi|6679891
CAPMS-17	H1 RNA	alpha glucosidase 2 alpha neutral subunit	98	gi|6679891
CAPMS-21	4.5s RNA block1	alpha glucosidase 2 alpha neutral subunit	318	gi|6679891

CAPMS-13	H1 RNA	alpha glucosidase 2 alpha neutral subunit, isoform CRA_a	419	gi|148701451
CAPMS-18	5S rRNA	alpha glucosidase 2 alpha neutral subunit, isoform CRA_a	226	gi|148701451
CAPMS-23 block1	4.5s RNA	alpha glucosidase 2 alpha neutral subunit, isoform CRA_a	90	gi|148701451
CAPMS-18	5S rRNA	alpha-actin	116	gi|49870
CAPMS-23 block1	4.5s RNA	alpha-cardiac actin	69	gi|387090
CAPMS-15	5.8S rRNA	apolipoprotein E	107	gi|192005
CAPMS-22 block2	4.5s RNA	apolipoprotein E	120	gi|192005
CAPMS-13	H1 RNA	argininosuccinate synthetase	45	gi|192065
CAPMS-15	5.8S rRNA	argininosuccinate synthetase	51	gi|192065
CAPMS-16	TH RNA	argininosuccinate synthetase	86	gi|6996911
CAPMS-24 block2	4.5s RNA	ATP synthase, H+ transporting, mitochondrial F0 complex, subunit F	49	gi|7949005
CAPMS-11	5.8S rRNA	betaine-homocysteine methyltransferase	111	gi|7709990
CAPMS-13	H1 RNA	betaine-homocysteine methyltransferase	112	gi|7709990
CAPMS-15	5.8S rRNA	betaine-homocysteine methyltransferase	311	gi|7709990
CAPMS-16	TH RNA	betaine-homocysteine methyltransferase	100	gi|7709990
CAPMS-21 block1	4.5s RNA	betaine-homocysteine methyltransferase	263	gi|7709990
CAPMS-22 block2	4.5s RNA	betaine-homocysteine methyltransferase	273	gi|7709990
CAPMS-23 block1	4.5s RNA	betaine-homocysteine methyltransferase	304	gi|7709990
CAPMS-24 block2	4.5s RNA	betaine-homocysteine methyltransferase	313	gi|7709990
CAPMS-14	5S rRNA	betaine-homocysteine methyltransferase 2	90	gi|11907833
CAPMS-18	5S rRNA	betaine-homocysteine methyltransferase, pseudogene 1	111	gi|123229029

CAPMS-17 H1 RNA	betaine-homocysteine methyltransferase, pseudogene 1	108	gi|148668613
CAPMS-13 H1 RNA	calreticulin	72	gi|6680836
CAPMS-14 5S rRNA	calreticulin	50	gi|6680836
CAPMS-23 4.5s RNA block1	calreticulin	149	gi|6680836
CAPMS-24 4.5s RNA block2	calreticulin	178	gi|6680836
CAPMS-11 5.8S rRNA	carbamoyl-phosphate synthetase 1	339	gi|124248512
CAPMS-14 5S rRNA	carbamoyl-phosphate synthetase 1	229	gi|187466221
CAPMS-17 H1 RNA	carbamoyl-phosphate synthetase 1	517	gi|124248512
CAPMS-18 5S rRNA	carbamoyl-phosphate synthetase 1	292	gi|124248512
CAPMS-21 4.5s RNA block1	carbamoyl-phosphate synthetase 1	279	gi|124248512
CAPMS-24 4.5s RNA block2	carbamoyl-phosphate synthetase 1	101	gi|124248512
CAPMS-11 5.8S rRNA	Carnitine O-palmitoyltransferase 2, mitochondrial	79	gi|1706111
CAPMS-17 H1 RNA	Carnitine O-palmitoyltransferase 2, mitochondrial	48	gi|1706111
CAPMS-21 4.5s RNA block1	Carnitine O-palmitoyltransferase 2, mitochondrial	56	gi|1706111
CAPMS-23 4.5s RNA block1	Carnitine O-palmitoyltransferase 2, mitochondrial	62	gi|1706111
CAPMS-11 5.8S rRNA	Catalase	565	gi|115704
CAPMS-12 TH RNA	Catalase	527	gi|115704
CAPMS-13 H1 RNA	Catalase	642	gi|442441
CAPMS-14 5S rRNA	Catalase	378	gi|115704
CAPMS-15 5.8S rRNA	Catalase	647	gi|442441
CAPMS-16 TH RNA	Catalase	476	gi|115704
CAPMS-17 H1 RNA	Catalase	616	gi|115704
CAPMS-18 5S rRNA	Catalase	336	gi|115704
CAPMS-21 4.5s RNA block1	Catalase	312	gi|115704
CAPMS-22 4.5s RNA block2	Catalase	259	gi|115704
CAPMS-23 4.5s RNA block1	Catalase	173	gi|115704

CAPMS-24	4.5s RNA block2	Catalase	398	gi|115704
CAPMS-21	4.5s RNA block1	cathepsin B	74	gi|227293
CAPMS-11	5.8S rRNA	cathepsin D	45	gi|6753556
CAPMS-13	H1 RNA	cathepsin D	60	gi|6753556
CAPMS-16	TH RNA	cathepsin D	46	gi|6753556
CAPMS-15	5.8S rRNA	cathepsin D	82	gi|6753556
CAPMS-21	4.5s RNA block1	Chain A, Structure Of The Leucine-Rich Repeat Domain Of Lanp	75	gi|185177518
CAPMS-12	TH RNA	cytochrome b-5	100	gi|13385268
CAPMS-22	4.5s RNA block2	cytochrome b-5	53	gi|13385268
CAPMS-14	5S rRNA	cytochrome b-5	87	gi|13385268
CAPMS-21	4.5s RNA block1	dihydrolipoamide S-succinyltransferase (E2 component of 2-oxo-glutarate complex)	97	gi|21313536
CAPMS-13	H1 RNA	Dlst protein	59	gi|23271834
CAPMS-22	4.5s RNA block2	Electron transferring flavoprotein, alpha polypeptide	63	gi|13097375
CAPMS-21	4.5s RNA block1	electron transferring flavoprotein, beta polypeptide	70	gi|38142460
CAPMS-22	4.5s RNA block2	electron transferring flavoprotein, beta polypeptide	194	gi|38142460
CAPMS-14	5S rRNA	elongation factor Tu	60	gi|556301
CAPMS-18	5S rRNA	elongation factor Tu	54	gi|556301
CAPMS-23	4.5s RNA block1	elongation factor Tu	48	gi|556301
CAPMS-15	5.8S rRNA	Es31 protein	152	gi|29476863
CAPMS-16	TH RNA	Es31 protein	198	gi|29476863
CAPMS-17	H1 RNA	Es31 protein	151	gi|29476863
CAPMS-18	5S rRNA	Es31 protein	131	gi|29476863
CAPMS-21	4.5s RNA block1	Es31 protein	84	gi|29476863
CAPMS-23	4.5s RNA block1	Es31 protein	179	gi|29476863
CAPMS-11	5.8S rRNA	ferredoxin 1	83	gi|6679765

CAPMS-22	4.5s RNA block2	Ferritin light chain 1	50	gi|120524
CAPMS-23	4.5s RNA block1	fetuin	72	gi|2546995
CAPMS-11	5.8S rRNA	Full=Stress-70 protein, mitochondrial	119	gi|14917005
CAPMS-24	4.5s RNA block2	gamma-actin	98	gi|809561
CAPMS-18	5S rRNA	Hadh protein	146	gi|20379935
CAPMS-23	4.5s RNA block1	Hadh protein	49	gi|20379935
CAPMS-24	4.5s RNA block2	Hadh protein	108	gi|20379935
CAPMS-24	4.5s RNA block2	heat shock protein 1	181	gi|6680309
CAPMS-24	4.5s RNA block2	heat shock protein 5	102	gi|31981722
CAPMS-11	5.8S rRNA	heat shock protein 65	84	gi|51455
CAPMS-16	TH RNA	heat shock protein 65	166	gi|51455
CAPMS-18	5S rRNA	heat shock protein 65	225	gi|51455
CAPMS-21	4.5s RNA block1	heat shock protein 65	283	gi|51455
CAPMS-22	4.5s RNA block2	heat shock protein 65	645	gi|51455
CAPMS-24	4.5s RNA block2	heat shock protein 65	313	gi|51455
CAPMS-21	4.5s RNA block1	Heat shock protein 90, beta (Grp94), member 1	130	gi|14714615
CAPMS-23	4.5s RNA block1	Heat shock protein 90, beta (Grp94), member 1	53	gi|14714615
CAPMS-24	4.5s RNA block2	Hemoglobin subunit alpha	66	gi|122441
CAPMS-22	4.5s RNA block2	HIU hydrolase	64	gi|110626070
CAPMS-11	5.8S rRNA	HMG CoA synthase	56	gi|555835
CAPMS-14	5S rRNA	HMG CoA synthase	53	gi|555835
CAPMS-17	H1 RNA	HMG CoA synthase	60	gi|555835
CAPMS-18	5S rRNA	HMG CoA synthase	146	gi|555835

CAPMS-23 4.5s RNA block1	HMG CoA synthase	62	gi|555835
CAPMS-24 4.5s RNA block2	HMG CoA synthase	50	gi|555835
CAPMS-12 TH RNA	Hspd1 protein	317	gi|76779273
CAPMS-12 TH RNA	Hydroxyacid oxidase 2	117	gi|13124286
CAPMS-13 H1 RNA	Hydroxymethylglutaryl-CoA lyase, mitochondrial	90	gi|585257
CAPMS-22 4.5s RNA block2	Hydroxymethylglutaryl-CoA lyase, mitochondrial	72	gi|585257
CAPMS-11 5.8S rRNA	isovaleryl coenzyme A dehydrogenase	119	gi|9789985
CAPMS-13 H1 RNA	isovaleryl coenzyme A dehydrogenase	77	gi|9789985
CAPMS-14 5S rRNA	isovaleryl coenzyme A dehydrogenase	119	gi|9789985
CAPMS-22 4.5s RNA block2	isovaleryl coenzyme A dehydrogenase	76	gi|9789985
CAPMS-24 4.5s RNA block2	isovaleryl coenzyme A dehydrogenase	133	gi|9789985
CAPMS-11 5.8S rRNA	long chain 2-hydroxy acid oxidase	67	gi|8920285
CAPMS-13 H1 RNA	long chain 2-hydroxy acid oxidase	79	gi|8920285
CAPMS-22 4.5s RNA block2	long chain 2-hydroxy acid oxidase	69	gi|8920285
CAPMS-15 5.8S rRNA	long-chain acyl-CoA dehydrogenase	64	gi|726095
CAPMS-21 4.5s RNA block1	long-chain acyl-CoA dehydrogenase	47	gi|2570413
CAPMS-21 4.5s RNA block1	lysosomal membrane glycoprotein 2 isoform 2	167	gi|31543108
CAPMS-15 5.8S rRNA	mCG116284	144	gi|148700389
CAPMS-13 H1 RNA	mCG121563	416	gi|148667830
CAPMS-16 TH RNA	mCG121563	398	gi|148667830
CAPMS-11 5.8S rRNA	microsomal triglyceride transfer protein	66	gi|6678960
CAPMS-12 TH RNA	microsomal triglyceride transfer protein	116	gi|6678960
CAPMS-13 H1 RNA	microsomal triglyceride transfer protein	188	gi|6678960

CAPMS-14 5S rRNA	microsomal triglyceride transfer protein	100	gi|6678960
CAPMS-21 4.5s RNA block1	Microsomal triglyceride transfer protein	654	gi|15215161
CAPMS-23 4.5s RNA block1	microsomal triglyceride transfer protein	201	gi|6678960
CAPMS-24 4.5s RNA block2	microsomal triglyceride transfer protein	223	gi|6678960
CAPMS-11 5.8S rRNA	mitochondrial aldehyde dehydrogenase 2	319	gi|6753036
CAPMS-13 H1 RNA	mitochondrial aldehyde dehydrogenase 2	172	gi|6753036
CAPMS-14 5S rRNA	mitochondrial aldehyde dehydrogenase 2	99	gi|6753036
CAPMS-17 H1 RNA	mitochondrial aldehyde dehydrogenase 2	76	gi|6753036
CAPMS-22 4.5s RNA block2	mitochondrial ribosomal protein L12	68	gi|22164792
CAPMS-24 4.5s RNA block2	mitochondrial ribosomal protein L12	43	gi|22164792
CAPMS-15 5.8S rRNA	MUP	58	gi|755765
CAPMS-24 4.5s RNA block2	NADPH-dependent retinol dehydrogenase/reductase	57	gi|11559414
CAPMS-14 5S rRNA	ornithine transcarbamylase	110	gi|762985
CAPMS-22 4.5s RNA block2	ornithine transcarbamylase	113	gi|762985
CAPMS-24 4.5s RNA block2	ornithine transcarbamylase, isoform	105	gi|148703731
CAPMS-14 5S rRNA	paraoxonase 1	45	gi|7242183
CAPMS-21 4.5s RNA block1	paraoxonase 1	129	gi|7242183
CAPMS-13 H1 RNA	peptidase (mitochondrial processing) alpha	60	gi|27502349
CAPMS-11 5.8S rRNA	peroxiredoxin 1	69	gi|6754976
CAPMS-13 H1 RNA	peroxiredoxin 1	106	gi|6754976
CAPMS-15 5.8S rRNA	peroxiredoxin 1	249	gi|6754976
CAPMS-17 H1 RNA	peroxiredoxin 1	86	gi|6754976
CAPMS-21 4.5s RNA block1	peroxiredoxin 1	206	gi|6754976

CAPMS-22 4.5s RNA block2	peroxiredoxin 1	97	gi|6754976
CAPMS-23 4.5s RNA block1	peroxiredoxin 1	217	gi|6754976
CAPMS-24 4.5s RNA block2	peroxiredoxin 1	255	gi|6754976
CAPMS-18 5S rRNA	peroxiredoxin 1	94	gi|6754976
CAPMS-11 5.8S rRNA	peroxiredoxin 3	77	gi|6680690
CAPMS-17 H1 RNA	peroxiredoxin 3	60	gi|6680690
CAPMS-11 5.8S rRNA	peroxisomal acyl-CoA oxidase	324	gi|2253380
CAPMS-12 TH RNA	peroxisomal acyl-CoA oxidase	234	gi|2253380
CAPMS-13 H1 RNA	peroxisomal acyl-CoA oxidase	164	gi|2253380
CAPMS-14 5S rRNA	peroxisomal acyl-CoA oxidase	163	gi|2253380
CAPMS-15 5.8S rRNA	peroxisomal acyl-CoA oxidase	101	gi|2253380
CAPMS-16 TH RNA	peroxisomal acyl-CoA oxidase	237	gi|2253380
CAPMS-17 H1 RNA	peroxisomal acyl-CoA oxidase	114	gi|2253380
CAPMS-18 5S rRNA	peroxisomal acyl-CoA oxidase	84	gi|2253380
CAPMS-21 4.5s RNA block1	peroxisomal acyl-CoA oxidase	178	gi|2253380
CAPMS-22 4.5s RNA block2	peroxisomal acyl-CoA oxidase	151	gi|2253380
CAPMS-21 4.5s RNA block1	peroxisomal trans 2-enoyl CoA reductase	86	gi|7798702
CAPMS-23 4.5s RNA block1	peroxisomal trans 2-enoyl CoA reductase	70	gi|7798702
CAPMS-12 TH RNA	phospholipase C-alpha	46	gi|200397
CAPMS-23 4.5s RNA block1	phospholipase C-alpha	84	gi|200397
CAPMS-24 4.5s RNA block2	phospholipase C-alpha	152	gi|200397
CAPMS-24 4.5s RNA block2	phytanoyl-CoA hydroxylase	126	gi|6754564
CAPMS-22 4.5s RNA block2	Polyadenylate-binding protein 1	76	gi|129535
CAPMS-16 TH RNA	propionyl Coenzyme A carboxylase, beta polypeptide	59	gi|13385310
CAPMS-17 H1 RNA	propionyl Coenzyme A carboxylase, beta polypeptide	124	gi|13385310

CAPMS-18	5S rRNA	propionyl Coenzyme A carboxylase, beta polypeptide	78	gi|13385310
CAPMS-22	4.5s RNA block2	prosaposin	45	gi|1381582
CAPMS-21	4.5s RNA block1	protein disulfide isomerase associated 4	48	gi|86198316
CAPMS-11	5.8S rRNA	protein disulfide isomerase-associated 6	58	gi|58037267
CAPMS-11	5.8S rRNA	Protein disulfide-isomerase	300	gi|129729
CAPMS-12	TH RNA	Protein disulfide-isomerase	340	gi|129729
CAPMS-13	H1 RNA	Protein disulfide-isomerase	393	gi|129729
CAPMS-14	5S rRNA	Protein disulfide-isomerase	290	gi|129729
CAPMS-15	5.8S rRNA	Protein disulfide-isomerase	70	gi|129729
CAPMS-16	TH RNA	Protein disulfide-isomerase	159	gi|129729
CAPMS-17	H1 RNA	Protein disulfide-isomerase	49	gi|129729
CAPMS-18	5S rRNA	Protein disulfide-isomerase	81	gi|129729
CAPMS-21	4.5s RNA block1	Protein disulfide-isomerase	307	gi|129729
CAPMS-22	4.5s RNA block2	Protein disulfide-isomerase	438	gi|129729
CAPMS-23	4.5s RNA block1	Protein disulfide-isomerase	327	gi|129729
CAPMS-24	4.5s RNA block2	Protein disulfide-isomerase	105	gi|129729
CAPMS-14	5S rRNA	protein disulfide-isomerase A3	147	gi|112293264
CAPMS-12	TH RNA	Protein disulfide-isomerase A4	100	gi|119531
CAPMS-17	H1 RNA	Protein disulfide-isomerase A4	90	gi|119531
CAPMS-18	5S rRNA	Protein disulfide-isomerase A4	85	gi|119531
CAPMS-23	4.5s RNA block1	Protein disulfide-isomerase A4	166	gi|119531
CAPMS-12	TH RNA	protein kinase C substrate 80K-H	201	gi|6679465
CAPMS-14	5S rRNA	protein kinase C substrate 80K-H	138	gi|6679465
CAPMS-15	5.8S rRNA	protein kinase C substrate 80K-H	132	gi|6679465
CAPMS-16	TH RNA	protein kinase C substrate 80K-H	157	gi|6679465
CAPMS-11	5.8S rRNA	protein kinase C substrate 80K-H	205	gi|6679465
CAPMS-17	H1 RNA	protein kinase C substrate 80K-H	126	gi|6679465
CAPMS-21	4.5s RNA	protein kinase C substrate 80K-H	179	gi|6679465

block1			
CAPMS-23 4.5s RNA block1	protein kinase C substrate 80K-H	123	gi|6679465
CAPMS-21 4.5s RNA block1	putative tripeptidyl peptidase I	60	gi|3766471
CAPMS-24 4.5s RNA block2	serine (or cysteine) proteinase inhibitor, clade A, member 1a	105	gi|6678079
CAPMS-13 H1 RNA	similar to Heat shock protein 1	89	gi|51766670
CAPMS-17 H1 RNA	similar to Heat shock protein 1	213	gi|51766670
CAPMS-15 5.8S rRNA	sterol carrier protein-2	58	gi|200942
CAPMS-16 TH RNA	sterol carrier protein-2	80	gi|200942
CAPMS-18 5S rRNA	sterol carrier protein-2	76	gi|200942
CAPMS-22 4.5s RNA block2	sterol carrier protein-2	104	gi|200942
CAPMS-23 4.5s RNA block1	sterol carrier protein-2	127	gi|200942
CAPMS-24 4.5s RNA block2	sterol carrier protein-2	294	gi|200942
CAPMS-17 H1 RNA	sterol-carrier protein X	124	gi|293794
CAPMS-13 H1 RNA	Stress-70 protein, mitochondrial	82	gi|14917005
CAPMS-14 5S rRNA	Stress-70 protein, mitochondrial	141	gi|14917005
CAPMS-16 TH RNA	Stress-70 protein, mitochondrial	55	gi|14917005
CAPMS-18 5S rRNA	Stress-70 protein, mitochondrial	44	gi|14917005
CAPMS-21 4.5s RNA block1	Stress-70 protein, mitochondrial	168	gi|14917005
CAPMS-23 4.5s RNA block1	Stress-70 protein, mitochondrial	148	gi|14917005
CAPMS-23 4.5s RNA block1	thioredoxin domain containing 4	52	gi|19072792
CAPMS-11 5.8S rRNA	triacylglycerol hydrolase	225	gi|14269427
CAPMS-12 TH RNA	triacylglycerol hydrolase	168	gi|14269427
CAPMS-13 H1 RNA	triacylglycerol hydrolase	266	gi|14269427
CAPMS-14 5S rRNA	triacylglycerol hydrolase	283	gi|14269427
CAPMS-15 5.8S rRNA	triacylglycerol hydrolase	69	gi|14269427
CAPMS-17 H1 RNA	triacylglycerol hydrolase	101	gi|14269427
CAPMS-18 5S rRNA	triacylglycerol hydrolase	177	gi|14269427
CAPMS-21 4.5s RNA	triacylglycerol hydrolase	335	gi|14269427

block1				
CAPMS-23 block1	4.5s RNA	triacylglycerol hydrolase	79	gi|14269427
CAPMS-11	5.8S rRNA	vitamin D-binding protein	106	gi|193446
CAPMS-14	5S rRNA	vitamin D-binding protein	59	gi|193446
CAPMS-22 block2	4.5s RNA	vitamin D-binding protein	92	gi|193446
CAPMS-24 block2	4.5s RNA	vitamin D-binding protein	107	gi|193446

Appendix 3: Proteins identified by LC-MS/MS of bands excised from SDS-PAGE gel run of RNA affinity purification samples from mitochondrial lysates.

Mass spectroscopy results presented show proteins present within bands excised from an SDS-PAGE gel. Results on each page represent comparison of experimental (proteins bound to an imported RNA) and control samples. "Filename" above the table shows which samples were compared. Cannon 3 is the experimental sample, Cannon 2 is the control. Letters following the sample indicate band ID. For example, the first table shows that Cannon 3A and Cannon 2A were compared. 2A is the first control sample, and 3A is the first experimental sample. In the table, "A score" refers to the top sample under "filename" and "B score" is the bottom sample under "filename." Score shows quality of protein identification and emPAI (Exponentially Modified Protein Abundance Index) is a measure of protein quantity. The red/purple highlighting indicates where where a given protein is highly enriched in one sample.

	SN.Search	Filename
A	202	Cannon_3A_CAP_may12.RAW
switch A & B	B 176	Cannon_2A_CAP_may6.RAW

keratin proteins in "A" have been removed

indicates a significant protein score high in Sample A but not B (emPAI > 0.5)

A Rank	B Rank	AccNo	A Score	B Score	A emPAI	B emPAI	A Queries	B Queries	A.Mass	A.Protein name	Additional Accession
1	1	gil27532959	592	695	1.23	.93	27	30	99,502	aldehyde dehydrogenase 1 family, member L1	
2	2	gil148667830	536	420	0.48	.41	29	19	158,788	mCG121563	
3	3	gil26326751	306	313	0.50	.5	15	14	89,998	unnamed protein product	gil6005942
5		gil254540023	270		0.59		15		101,372	microsomal triglyceride transfer protein large subunit	
10		gil12859782	222		0.39		11		66,099	unnamed protein product	gil126116585
11		gil148672076	222		0.28		15		72,596	mCG17605, isoform CRA_b	gil398168
12		gil20149748	219		0.24		10		102,644	sarcosine dehydrogenase precursor	gil74201196
15	17	gil148672085	188	78	0.21	.1	5	3	38,347	mCG144996	
20		gil82950149	133		0.06		6		263,538	PREDICTED: desmoplakin isoform 2	gil148708988
24		gil52785	88		0.29		9		56,752	unnamed protein product	gil39850082
26		gil1389682	63		0.05		2		68,638	plakoglobin	gil28395018
27	18	gil16716569	57	73	0.30	.3	6	8	26,802	protease, serine, 1	
28	20	gil4105619	56	57	0.04	.04	2	2	97,792	SPAF	gil74201504
29		gil74222791	53		0.15		2		24,882	unnamed protein product	gil124249090
30		gil7513694	47		0.07		5		113,927	IgG Fc binding protein - mouse (fragment)	gil148692210
31		gil20071794	46		0.11		1		34,700	H6pd protein	gil31982147

	SN.Search	Filename
A	203	Cannon_3B_CAP_may12.RAW
switch A & B	B 193	Cannon_2B_CAP_may10.RAW

indicates a significant protein score high in Sample A but not B (emPAI > 0.5) **keratin proteins in "A" have been removed**

A Rank	B Rank	AccNo	A Score	B Score	A emPAI	B emPAI	A Queries	B Queries	A.Mass	A.Protein name	Additional Accession
5		gil34784638	220		0.42		9		61,749	Etfdh protein	gil12832501
6		gil148672075	207		0.11		7		72,240	mCG17605, isoform CRA_a	
10	9	gil124248512	150	52	0.14	.02	8	1	165,711	carbamoyl-phosphate synthetase 1 precursor	gil148667830
13		gil52785	115		0.21		14		56,752	unnamed protein product	gil39850082
14		gil2388724	112		0.34		6		62,196	very-long-chain acyl-CoA dehydrogenase	
15	7	gil26340966	111	65	0.17	.11	4	2	70,730	unnamed protein product	gil26341396
18		gil74177777	98		0.07		5		54,546	unnamed protein product	
21		gil15126777	75		0.11		2		71,101	Carnitine O-octanoyltransferase	gil17157983
22		gil6688685	68		0.06		1		64,570	2-hydroxyphytanoyl-CoA lyase	gil31560355
23		gil3851614	66		0.06		2		59,249	succinate dehydrogenase Fp subunit	gil15030102
24	10	gil16716569	63	47	0.30	.3	8	2	26,802	protease, serine, 1	
25		gil123298865	60		0.06		2		66,358	apoptosis-inducing factor, mitochondrion-associated 1	
26		gil29476863	59		0.12		2		63,790	Es31 protein	gil34980866
27		gil14917005	49		0.10		2		73,768	RecName: Full=Stress-70 protein, mitochondrial;	gil74204605

	SN.Search	Filename
A	204	Cannon_3C_CAP_may13.RAW
switch A & B	B 194	Cannon_2C_CAP_may10.RAW

indicates a significant protein score high in Sample A but not B (emPAI > 0.5)

keratin proteins in "A" have been removed

A Rank	B Rank	AccNo	A Score	B Score	A emPAI	B emPAI	A Queries	B Queries	A.Mass	A.Protein name	Additional Accession
1		gil23272966	876		3.06		37		56,632	Atp5b protein	gil31980648
6		gil6753036	254		0.66		19		57,015	aldehyde dehydrogenase 2, mitochondrial precursor	gil74181365
12		gil12859782	190		0.31		14		66,099	unnamed protein product	gil126116585
14	29	gil52785	167	93	0.29	.21	12	6	56,752	unnamed protein product	gil39850082
15		gil26324736	160		0.28		10		58,629	unnamed protein product	gil109735018
18	30	gil148672085	142	92	0.21	.21	7	4	38,347	mCG144996	
20		gil21313536	125		0.44		5		49,306	dihydrolipoyllysine-residue succinyltransferase	gil74204028
21	14	gil148672075	116	142	0.22	.16	9	9	72,240	mCG17605, isoform CRA_a	
22	15	gil148672076	115	142	0.28	.22	11	10	72,596	mCG17605, isoform CRA_b	gil398168
24		gil2253380	79		0.05		1		75,007	peroxisomal acyl-CoA oxidase	gil6429156
25		gil1352245	78		0.14		2		54,364	RecName: Full=Fatty aldehyde dehydrogenase;	gil12698456
26		gil117215	75		0.07		2		57,050	RecName: Full=Cytochrome P450 2B10; AltName:	gil1684709
28	37	gil16716569	72	84	0.30	.3	6	7	26,802	protease, serine, 1	
29		gil74213681	71		0.07		3		55,980	unnamed protein product	gil74219152
31		gil19527258	63		0.06		1		58,335	aldehyde dehydrogenase family 6, subfamily A1	gil21410418
32		gil117196	59		0.07		2		56,818	RecName: Full=Cytochrome P450 2A5; AltName:	gil28302372
33	45	gil74182195	52	57	0.12	.12	3	2	32,721	unnamed protein product	gil6680748
34		gil5921949	44		0.14		2		56,378	RecName: Full=Cytochrome P450 2C29; AltName:	gil18043757
35		gil13386414	44		0.13		5		57,198	cytochrome P450, family 2, subfamily d, polypeptide	gil81914477
36		gil7513694	41		0.03		1		113,927	IgG Fc binding protein - mouse (fragment)	gil148692210
37	44	gil51452	41	61	0.06	.2	2	4	59,004	unnamed protein product	gil51455
38		gil5921961	41		0.07		2		56,485	RecName: Full=Cytochrome P450 2C40; AltName:	gil18044474

	SN.Search	Filename
A	205	Cannon_3D_CAP_may13.RAW
switch A & B	B 196	Cannon_2D_CAP_may10.RAW

keratin proteins in "A" have been removed

indicates a significant protein score high in Sample A but not B (emPAI > 0.5)

A Rank	B Rank	AccNo	A Score	B Score	A emPAI	B emPAI	A Queries	B Queries	A.Mass	A.Protein name	Additional Accession
1	32	gi|6680748	705	44	1.19	.06	24	2	59,830	ATP synthase subunit alpha, mitochondrial precursor	gi|74139457
13	4	gi|26324736	154	388	0.36	.45	10	25	58,629	unnamed protein product	gi|109735018
14	16	gi|148672085	140	151	0.21	.32	5	8	38,347	mCG144996	
15		gi|148672075	140		0.16		7		72,240	mCG17605, isoform CRA_a	
17		gi|115704	127		0.20		5		60,013	RecName: Full=Catalase	gi|442441
21		gi|6680027	110		0.42		11		61,640	glutamate dehydrogenase 1, mitochondrial precursor	gi|26354278
22	22	gi|52785	108	117	0.29	.29	9	12	56,752	unnamed protein product	gi|39850082
23		gi|191804	81		0.14		4		55,131	aldehyde dehydrogenase II	gi|9755362
25		gi|52789	75		0.14		4		54,415	unnamed protein product	gi|309215
26		gi|6680836	73		0.08		3		48,136	calreticulin precursor	gi|74200069
27		gi|45595694	73		0.19		4		63,549	Cps1 protein	gi|26324620
28	26	gi|16716569	71	56	0.30	.3	5	2	26,802	protease, serine, 1	
29		gi|19527110	64		0.06		3		61,460	UDP glucuronosyltransferase 2 family, polypeptide	
30		gi|2501472	54		0.06		4		60,825	RecName: Full=UDP-glucuronosyltransferase 1-1;	gi|31324690
31	27	gi|7513694	51	51	0.03	.03	3	8	113,927	IgG Fc binding protein - mouse (fragment)	gi|148692210
32		gi|6753890	43		0.13		4		60,446	flavin containing monooxygenase 1	

	SN.Search	Filename
A	206	Cannon_3E_CAP_may13.RAW
switch A & B	B 200	Cannon_2E_CAP_may12.RAW

keratin proteins in "A" have been removed

indicates a significant protein score high in Sample A but not B (emPAI > 0.5)

A Rank	B Rank	AccNo	A Score	B Score	A emPAI	B emPAI	A Queries	B Queries	A.Mass	A.Protein name	Additional Accession
1		gil129729	293		1.12		18		57,507	RecName: Full=Protein disulfide-isomerase;	gil42415475
3		gil115704	195		0.43		8		60,013	RecName: Full=Catalase	gil442441
6		gil33585846	164		0.54		13		58,967	Propionyl Coenzyme A carboxylase, beta polypeptide	gil118600805
9		gil26324736	123		0.20		5		58,629	unnamed protein product	gil109735018
12		gil148692868	117		0.25		5		65,407	2-hydroxyacyl-CoA lyase 1	gil6688685
13		gil124248512	110		0.07		6		165,711	carbamoyl-phosphate synthetase 1 precursor	
14	14	gil52785	109	192	0.14	.21	6	14	56,752	unnamed protein product	gil39850082
16		gil6679421	94		0.10		2		77,394	NADPH--cytochrome P450 reductase	gil116283284
17		gil148677501	92		0.30		10		54,675	ATP synthase, H+ transporting, mitochondrial F1	gil6680748
18		gil19387947	89		0.33		3		37,891	Pm20d1 protein	gil74180844
20		gil37994713	81		0.23		5		33,925	Krt13 protein	
21		gil6680027	76		0.19		3		61,640	glutamate dehydrogenase 1, mitochondrial precursor	gil26354278
23		gil14269427	67		0.19		4		62,133	triacylglycerol hydrolase	gil14331135
24		gil148679152	61		0.12		3		63,170	mCG9581	gil162287349
25		gil21450339	58		0.12		2		61,972	liver carboxylesterase 4	gil74202015
26		gil12843046	56		0.14		1		27,074	unnamed protein product	gil71043961
27		gil729927	54		0.05		1		78,900	RecName: Full=Long-chain-fatty-acid--CoA ligase 1;	gil31560705
28		gil136725	51		0.06		3		61,386	RecName: Full=UDP-glucuronosyltransferase 2B5;	gil20381430
30		gil2444477	42		0.14		1		27,742	fibroblast growth factor-related protein FGF-13	

	SN.Search	Filename
A	207	Cannon_3F_CAP_may13.RAW
B	201	Cannon_2F_CAP_may12.RAW

indicates a significant protein score high in Sample A but not B (emPAI > 0.5)

A Rank	B Rank	AccNo	A Score	B Score	A emPAI	B emPAI	A Queries	B Queries	A.Mass	A.Protein name	Additional Accession
7		gil148672076	217		0.16		12		72,596	mCG17605, isoform CRA_b	gil398168
9	16	gil52785	159	113	0.21	.21	14	7	56,752	unnamed protein product	gil39850082
13	23	gil148672085	128	80	0.32	.1	4	3	38,347	mCG144996	
17	22	gil16716569	68	80	0.30	.3	6	7	26,802	protease, serine, 1	
19		gil2811065	50		0.09		2		40,409	RecName: Full=Galectin-9; Short=Gal-9	gil13277708

	SN.Search	Filename
A	176	Cannon_2A_CAP_may6.RAW
switch A & B	B 202	Cannon_3A_CAP_may12.RAW

indicates a significant protein score high in Sample A but not B (emPAI > 0.5) **keratin proteins in "A" have been removed**

A Rank	B Rank	AccNo	A Score	B Score	A emPAI	B emPAI	A Queries	B Queries	A.Mass	A.Protein name	Additional Accession
1	1	gil27532959	695	592	0.93	1.23	30	27	99,502	aldehyde dehydrogenase 1 family, member L1	
2	2	gil148667830	420	536	0.41	.48	19	29	158,788	mCG121563	
3	3	gil26326751	313	306	0.50	.5	14	15	89,998	unnamed protein product	gil6005942
17	15	gil148672085	78	188	0.10	.21	3	5	38,347	mCG144996	
18	27	gil16716569	73	57	0.30	.3	8	6	26,802	protease, serine, 1	
20	28	gil4105619	57	56	0.04	.04	2	2	97,792	SPAF	gil74201504
21		gil1929447	52		0.08		4		99,707	microsomal triglyceride transfer protein	gil15215161

	SN.Search	Filename
A	193	Cannon_2B_CAP_may10.RAW
switch A & B	B 203	Cannon_3B_CAP_may12.RAW

indicates a significant protein score high in Sample A but not B (emPAI > 0.5) **keratin proteins in "A" have been removed**

A Rank	B Rank	AccNo	A Score	B Score	A emPAI	B emPAI	A Queries	B Queries	A.Mass	A.Protein name	Additional Accession
3		gil148672076	106		0.10		5		72,604	mCG17605, isoform CRA_b	gil398168
7	15	gil26340966	65	111	0.11	.17	2	4	70,766	unnamed protein product	gil26341396
9	10	gil124248512	52	150	0.02	.14	1	8	165,732	carbamoyl-phosphate synthetase 1 precursor	gil148667830
10	24	gil16716569	47	63	0.30	.3	2	8	26,814	protease, serine, 1	
12		gil12832501	44		0.05		1		68,893	unnamed protein product	gil26344475
14		gil168984310	42		0.03		1		110,762	EF-hand calcium binding domain 5	gil26325728

	SN.Search	Filename
A	194	Cannon_2C_CAP_may10.RAW
switch A & B	B 204	Cannon_3C_CAP_may13.RAW

indicates a significant protein score high in Sample A but not B (emPAI > 0.5) **keratin proteins in "A" have been removed**

A Rank	B Rank	AccNo	A Score	B Score	A emPAI	B emPAI	A Queries	B Queries	A.Mass	A.Protein name	Additional Accession
1		gil148678480	652		0.35		33		231,127	mCG140437, isoform CRA_c	gil67189167
2		gil82524274	553		0.32		30		224,116	myosin, heavy polypeptide 1, skeletal muscle, adult	gil187956263
3		gil71143152	515		0.28		27		223,653	myosin, heavy polypeptide 8, skeletal muscle,	gil148678484
4		gil153792649	407		0.21		19		224,736	myosin, heavy polypeptide 3, skeletal muscle,	
5		gil4501881	349		1.54		20		42,366	actin, alpha skeletal muscle	
6		gil33585846	319		1.22		16		58,967	Propionyl Coenzyme A carboxylase, beta polypeptide	gil118600805
7		gil129729	256		0.55		17		57,507	RecName: Full=Protein disulfide-isomerase;	gil42415475
8		gil18859641	223		0.16		18		223,539	myosin, heavy polypeptide 7, cardiac muscle, beta	gil187956918
11		gil49868	160		0.31		11		39,446	put. beta-actin (aa 27-375)	
12		gil124486959	150		0.08		14		224,562	myosin, heavy polypeptide 13, skeletal muscle	gil148678485
14	21	gil148672075	142	116	0.16	.22	9	9	72,240	mCG17605, isoform CRA_a	
15	22	gil148672076	142	115	0.22	.28	10	11	72,596	mCG17605, isoform CRA_b	gil398168
18		gil115704	131		0.35		8		60,013	RecName: Full=Catalase	gil442441
21		gil6679937	117		0.35		3		36,072	glyceraldehyde-3-phosphate dehydrogenase	gil62201487
25		gil26324620	107		0.14		5		83,966	unnamed protein product	gil45595694
27		gil6688685	100		0.12		3		64,570	2-hydroxyphytanoyl-CoA lyase	gil31560355
29	14	gil52785	93	167	0.21	.29	6	12	56,752	unnamed protein product	gil39850082
30	18	gil148672085	92	142	0.21	.21	4	7	38,347	mCG144996	
31		gil2494630	90		0.08		2		48,367	RecName: Full=Glyceraldehyde-3-phosphate	gil6679939
32		gil149751320	89		0.44		7		29,231	PREDICTED: similar to tropomyosin 3 isoform 1	gil40254525
34		gil149272161	86		0.22		2		36,442	PREDICTED: similar to glyceraldehyde-3-phosphate-	
35		gil21307732	86		0.19		8		104,438	actinin alpha 2	gil157951643
36		gil52789	85		0.14		4		54,415	unnamed protein product	gil309215
37	28	gil16716569	84	72	0.30	.3	7	6	26,802	protease, serine, 1	
38		gil109081395	78		0.24		4		32,736	PREDICTED: similar to Tropomyosin 1 alpha chain	gil148694194
40		gil7949078	70		0.20		1		19,057	myosin light chain, phosphorylatable, fast skeletal	
41		gil19387947	69		0.21		2		37,891	Pm20d1 protein	gil74180844
42		gil6671539	66		0.09		2		39,787	fructose-bisphosphate aldolase A isoform 2	gil7548322
43		gil29789016	63		0.19		1		20,695	myosin light chain 1/3, skeletal muscle isoform	gil37589525
44	37	gil51452	61	41	0.20	.06	4	2	59,004	unnamed protein product	gil51455
45	33	gil74182195	57	52	0.12	.12	2	3	32,721	unnamed protein product	gil6680748
46		gil200397	53		0.07		1		57,042	phospholipase C-alpha	gil1083311
48		gil6679421	51		0.05		1		77,394	NADPH--cytochrome P450 reductase	gil116283284
49		gil14269427	50		0.06		2		62,133	triacylglycerol hydrolase	gil14331135
50		gil2501472	50		0.13		4		60,825	RecName: Full=UDP-glucuronosyltransferase 1-1;	gil31324690
51		gil6755863	48		0.04		2		92,703	endoplasmin	gil14714615
52		gil10946936	47		0.16		2		23,330	adenylate kinase 1	gil13959400

	SN.Search	Filename
A	194	Cannon_2C_CAP_may10.RAW
switch A & B	B 204	Cannon_3C_CAP_may13.RAW

indicates a significant protein score high in Sample A but not B (emPAI > 0.5) **keratin proteins in "A" have been removed**

A Rank	B Rank	AccNo	A Score	B Score	A emPAI	B emPAI	A Queries	B Queries	A.Mass	A.Protein name	Additional Accession
53		gil7670405	47		0.07		1		52,664	unnamed protein product	gil126521835
54		gil136725	47		0.06		1		61,386	RecName: Full=UDP-glucuronosyltransferase 2B5;	gil19527110
55		gil15489037	45		0.04		1		97,825	Liver glycogen phosphorylase	gil20178036

	SN.Search	Filename
A	196	Cannon_2D_CAP_may10.RAW
switch A & B	B 205	Cannon_3D_CAP_may13.RAW

indicates a significant protein score high in Sample A but not B (emPAI > 0.5) **keratin proteins in "A" have been removed**

A Rank	B Rank	AccNo	A Score	B Score	A emPAI	B emPAI	A Queries	B Queries	A.Mass	A.Protein name	Additional Accession
4	13	gil26324736	388	154	0.45	.36	25	10	58,629	unnamed protein product	gil109735018
7		gil148672076	273		0.57		20		72,596	mCG17605, isoform CRA_b	gil398168
11		gil12859782	248		0.31		13		66,099	unnamed protein product	gil126116585
16	14	gil148672085	151	140	0.32	.21	8	5	38,347	mCG144996	
18		gil28395018	147		0.25		11		82,490	junction plakoglobin	
21		gil148708988	125		0.09		15		322,522	mCG20427	gil149264086
22	22	gil52785	117	108	0.29	.29	12	9	56,752	unnamed protein product	gil39850082
23		gil76252651	78		0.36		1		11,119	immunoglobulin lambda light chain variable region	
24		gil74222791	68		0.15		4		24,882	unnamed protein product	gil124249090
25		gil9790161	57		0.05		2		82,270	plakophilin 1	
26	28	gil16716569	56	71	0.30	.3	2	5	26,802	protease, serine, 1	
27	31	gil7513694	51	51	0.03	.03	8	3	113,927	IgG Fc binding protein - mouse (fragment)	gil148692210
28		gil4928654	51		0.07		3		50,652	m6a methyltransferase	gil33301387
29		gil3212348	49		0.16		1		23,785	Chain H, Diels Alder Catalytic Antibody Germline	gil4389277
30		gil32129201	46		0.10		4		115,408	desmoglein 1 beta precursor	gil32379079
31		gil551295	46		0.06		2		58,394	pyruvate kinase M	gil1405933
32	1	gil6680748	44	705	0.06	1.19	2	24	59,830	ATP synthase subunit alpha, mitochondrial precursor	gil74139457
33		gil118595720	43		0.01		1		289,241	RecName: Full=Centrosomal protein of 290 kDa;	gil148689712
34		gil26352888	40		0.11		2		35,118	unnamed protein product	

	SN.Search	Filename
A	200	Cannon_2E_CAP_may12.RAW
switch A & B	B 206	Cannon_3E_CAP_may13.RAW

keratin proteins in "A" have been removed

indicates a significant protein score high in Sample A but not B (emPAI > 0.5)

A Rank	B Rank	AccNo	A Score	B Score	A emPAI	B emPAI	A Queries	B Queries	A.Mass	A.Protein name	Additional Accession
1		gi|23272966	538		0.89		19		56,632	Atp5b protein	gi|31980648
14	14	gi|52785	192	109	0.21	.14	14	6	56,752	unnamed protein product	gi|39850082
16		gi|148672085	173		0.21		7		38,347	mCG144996	
19		gi|21313536	139		0.34		5		49,306	dihydrolipoyllysine-residue succinyltransferase	gi|74204028
23		gi|6753036	62		0.07		2		57,015	aldehyde dehydrogenase 2, mitochondrial precursor	gi|74139792
24		gi|6680836	61		0.08		1		48,136	calreticulin precursor	gi|74200069
26		gi|16716569	49		0.30		6		26,802	protease, serine, 1	
27		gi|6755893	48		0.14		2		26,941	trypsin 4	gi|51010909
28		gi|51452	47		0.06		3		59,004	unnamed protein product	gi|51455
29		gi|6016097	42		0.09		1		41,048	RecName: Full=Galanin receptor type 3;	gi|226530468

	SN.Search	Filename
A	201	Cannon_2F_CAP_may12.RAW
switch A & B	B 207	Cannon_3F_CAP_may13.RAW

indicates a significant protein score high in Sample A but not B (emPAI > 0.5)

A Rank	B Rank	AccNo	A Score	B Score	A emPAI	B emPAI	A Queries	B Queries	A.Mass	A.Protein name	Additional Accession
15		gil52789	121		0.22		6		54,415	unnamed protein product	gil309215
16	9	gil52785	113	159	0.21	.21	7	14	56,752	unnamed protein product	gil39850082
18		gil31982273	98		0.15		4		79,945	peroxisomal multifunctional enzyme type 2	gil74179905
20		gil7798702	93		0.25		2		32,535	peroxisomal trans 2-enoyl CoA reductase	gil12845570
21		gil585257	85		0.11		1		34,595	RecName: Full=Hydroxymethylglutaryl-CoA lyase,	gil1292952
22	17	gil16716569	80	68	0.30	.3	7	6	26,802	protease, serine, 1	
23	13	gil148672085	80	128	0.10	.32	3	4	38,347	mCG144996	
24		gil21450129	80		0.08		1		45,129	acetyl-Coenzyme A acetyltransferase 1 precursor	gil74194628
25		gil6678145	78		0.20		3		19,153	translocon-associated protein subunit delta isoform 2	gil262050625
27		gil17066601	60		0.10		2		36,206	peroxisomal acyl-CoA thioesterase 2	gil254587964
28		gil555835	58		0.08		2		48,384	HMG CoA synthase	gil12836439
29		gil148688082	55		0.55		3		15,767	peroxisomal membrane protein 2, isoform CRA_b	
30		gil18482377	51		0.06		1		62,350	acyl-CoA thioesterase 12	gil19484128
31		gil14548301	48		0.07		1		53,420	RecName: Full=Cytochrome b-c1 complex subunit 1,	gil17390954

Appendix 4: Alignment of two groups of RNAs identified by mitochondrial RNA sequencing.

Both groups align to *Plasmodium* sequence (*P. yoelii* or *P. berghei*) but not each other. Similar RNAs were grouped and aligned to show high similarity between RNAs.

```
CLUSTAL format alignment by MAFFT (v6.821b)

CUFF.1473   ------------------------------------------------------------
CUFF.5889   ------------------------------------------------------------
CUFF.8541   ------------------------------------------------------------
CUFF.1357   ------------------------------------------------------------
CUFF.7729   ------------------------------------------------------------
CUFF.2869   ------------------------------------------------------------
CUFF.11127  ------------------------------------------------------------
CUFF.1359   GCTGCATGTCCTTCAGTGTGCATTTCTCATTTTTCACGTTTTTTAGTGATTTCGTCATTT


CUFF.1473   ------------------------------------------------------------
CUFF.5889   ------------------------------------------------------------
CUFF.8541   ------------------------------------------------------------
CUFF.1357   ------------------------------------------------------------
CUFF.7729   ------------------------------------------------------------
CUFF.2869   ------------------------------------------------------------
CUFF.11127  ------------------------------------------------------------
CUFF.1359   TTCAAGTCGTCAAGTAGATGTTTCTCATTTTCCATGATTTTCAGTTTTCTTGCCATATTC


CUFF.1473   ------------------------------------------------------------
CUFF.5889   ------------------------------------------------------------
CUFF.8541   ------------------------------------------------------------
CUFF.1357   ------------------------------------------------------------
CUFF.7729   ------------------------------------------------------------
CUFF.2869   ------------------------------------------------------------
CUFF.11127  ------------------------------------------------------------
CUFF.1359   CACGTCCTGCACTGGACATTTCTAAATTTTCCACCTTTTTCAGTTTTCCTTGCCATATTT


CUFF.1473   ------------------------------------------------------------
CUFF.5889   ------------------------------------------------------------
CUFF.8541   ------------------------------------------------------------
CUFF.1357   ------------------------------------------------------------
CUFF.7729   ------------------------------------------------------------
CUFF.2869   ------------------------------------------------------------
CUFF.11127  ------------------------------------------------------------
CUFF.1359   CACGTCCTAAAGTGTGTATTTCTCATTTTCCGTGATTTTCAGTTTTCTCGCCATATTCCA
```

```
CUFF.1473   ------------------------------------------------------------
CUFF.5889   ------------------------------------------------------------
CUFF.8541   ------------------------------------------------------------
CUFF.1357   ------------------------------------------------------------
CUFF.7729   ------------------------------------------------------------
CUFF.2869   ------------------------------------------------------------
CUFF.11127  ------------------------------------------------------------
CUFF.1359   GGTTCTTCAGTGTGCATTTCACATTTTTCACGTATCATTTTCCATGTTTTTCATTGTAAC

CUFF.1473   -----GATATACACTGTTCTACAATGCCGGTTTCCAACGAATGTGTTTTTCAGTGTAACT
CUFF.5889   ------------------------------------------------------------
CUFF.8541   ------------------------------------------------------------
CUFF.1357   ------------------------------------------------------------
CUFF.7729   ------------------------------------------------------------
CUFF.2869   ------------------------------------------------------------
CUFF.11127  ------------------------------------------------------------
CUFF.1359   TCATTGATATACACTGTTCTACAAATCCCGTTTCCAACGAATGTGTTTTTCAGTGTAACT

CUFF.1473   CACACATCTAATATGTTCTACAGTGTGGTTTTTATCATTTTCCATGTTTCTCATTGTAAC
CUFF.5889   ------------------------------------------------------------
CUFF.8541   ------------------------------------------------------------
CUFF.1357   ------------------------------------------------------------
CUFF.7729   ------------------------------------------------------------
CUFF.2869   ------------------------------------------------------------
CUFF.11127  ------------------------------------------------------------
CUFF.1359   CACTCATCTAATACGTTCTGCAGTGTGGTTTTTATCATTTTCGATGTTTTTCATTGTAAC

CUFF.1473   TCATTGATATACACTGTTCTAAAAAATCCCGTTTCCAACGAATGTGTTTTTCAGTGTAAC
CUFF.5889   ------------------------------------------------------------
CUFF.8541   ------------------------------------------------------------
CUFF.1357   ------------------------------------------------------------
CUFF.7729   ------------------------------------------------------------
CUFF.2869   ------------------------------------------------------------
CUFF.11127  ------------------------------------------------------------
CUFF.1359   TCATTGATATACACTGTTCT-ACAAATCCCGTTTCCAACGAATGTGTTTTTCATTGTAAC

CUFF.1473   TCACTCATCTAATATGTTCTACAGTGTTGTTTTTATCATTTTCCATGTTTCTCATTGTAA
CUFF.5889   ------------------------------------------------------------
CUFF.8541   ------------------------------------------------------------
CUFF.1357   ------------------------------------------------------------
CUFF.7729   ------------------------------------------------------------
CUFF.2869   ------------------------------------------------------------
CUFF.11127  ------------------------------------------------------------
CUFF.1359   TCACTCATCTAATATGTTCTACAGTGTGGTTTTTATCATTTTCCATGTTT-TCATTGTAA

CUFF.1473   CTCATTGATATACACTGTTCTACAATGCCGGTTTCCAACGTATGTGTTTTTTTTGTGTGT
CUFF.5889   ------------------------------------------------------------
CUFF.8541   ------------------------------------------------------------
CUFF.1357   ------------------------------------------------------------
CUFF.7729   ------------------------------------------------------------
CUFF.2869   ------------------------------------------------------------
CUFF.11127  ------------------------------------------------------------
CUFF.1359   GTCATTGATATACACTATTCTACAATGCCGGTTTCCAACGTATGTGTTTTT---------
```

```
CUFF.1473   GTACCTACTTTGGAAAGAAAACTGAAAATCATGGAAAATGAGAAACATCCACTTGACGAC
CUFF.5889   ------------------------------------------------------------
CUFF.8541   ------------------------------------------------------------
CUFF.1357   ---AGGAATATGGTAAGAAAACTGAAAATCATGGAAAATGAGAAATATCCACTTGACGAC
CUFF.7729   ------------------------------------------------------------
CUFF.2869   ------------------------------------------------------------
CUFF.11127  ------------------------------------------------------------
CUFF.1359   ------------------------------------------------------------

CUFF.1473   TTGAAAAATGACGAAATCACTAAAATACGTGAAAAATGAGAAATGCACACTGAAGGACCT
CUFF.5889   ----------------------------------------AGGTGCACACTGAAGGACCT
CUFF.8541   ------------------------------------------------------------
CUFF.1357   TAGAAAAATGATGAAATCAATGAAAAACCTGAAAAATGATAAATGCACACTGTAAGACCT
CUFF.7729   ------------------------------------------------------------
CUFF.2869   ------------------------------------------------------------
CUFF.11127  ------------------------------------------------------------
CUFF.1359   ------------------------------------------------------------

CUFF.1473   GGAATATGGAGAGAAAACTGAAAATCACGGAAAATGAGAAATACACACTTTAGGACGTGA
CUFF.5889   GGAATTATGCGAGAAAACTGAAAATCACGGAAAATGAGAAATACACACTTTAGGACGTGA
CUFF.8541   ----------------------------------------------------------CGTGA
CUFF.1357   GGAATATGGCGAGAAAACTGAAAATCACGGAAAATGAGAAATACACACTTTAGGAAGTGA
CUFF.7729   ---------TAAAATCACTGAAAATCACGGAAAATGAGAAATACACACTTTAGGACGTGA
CUFF.2869   ------------------------------------------------------------
CUFF.11127  ------------------------------------------------------------
CUFF.1359   ------------------------------------------------------------

CUFF.1473   AATATGGCGAGGAAAACTGAAAAAGGTGGAATATTTAGAAATGTCCACTGTAGGACGTGG
CUFF.5889   AAAATGGCGAGGAAAACTGAAAAAGGTGGAAAATTTAGAAATGTCCTCTGTAGGACATGG
CUFF.8541   AATATGGCGAAGAAAACTGAAAAAGGTGGATAATTTAGTAATGTCCACTGTAGGACATGG
CUFF.1357   AATATGACGAGGAAAACTGAAAAAGGTGGGAAATTTAGAAATGTCCACTGTAGGACATGG
CUFF.7729   AATATGGCGAGGAAAACTGAAAAAGGTGGAAAATTTAGAAATGTCCACTGTAGGACATGG
CUFF.2869   ---------GAAATTACTGAAAAACGTGAAAAA-TGAGAAATGCACACTGCAGGACCTGG
CUFF.11127  ----------------------------------TGAGAAATGCACACTGTAGGACCAGG
CUFF.1359   ----------------CAGTGTAACTCGGAAAATTTAGAAATGTCCACTGTAGGACGTGG
                                              * ** ****  * *** *****  **

CUFF.1473   AATATTGCAAGAAAACTGAAAATCATGGAAAATGAGAAACATCTACTTGACGACTTGAAA
CUFF.5889   AATATGGCAAGAAAACTGAAAATCATGGAAAATGAGAAACATCCACTTGATGACTTGAAA
CUFF.8541   AATATGGCAAGAAAACTGAAAATCATGGAAAATGAGAAACATCCACTTGACGACTTGAAA
CUFF.1357   AATATGTCAAGAAAACTGAAAATCATGGAAAATGAGAAACATCCACTTGAC--TTGAAAA
CUFF.7729   AATATGGCAAGAAAACTGAAAATCATGGAAAATGAGAAACATCCACTTGACGACTTGAAA
CUFF.2869   AATATGGCGAGAAAACTGAACATCACGGAAAATGAGAATAACACTCTTTAGGTAGTGAAA
CUFF.11127  AGTATGGCGAGAAAACTGAAAATCATGGAAAATGAGAAACACACAATGT-----------
CUFF.1359   AATATGGCAAGAAAATTGAAAATCATGGAAAATGAGAAACATCGACTTGACGACTTGAAA
            * ***  * ****** **** **** ************  *     *

CUFF.1473   AATGACGAAATCACTAAAAAACGTGAAAAATGTGAAATGCACACTGAAGGACCTGGAATA
CUFF.5889   AATGACGAAATCATTAAAAAACGTGAAAAATGAGAAATGCCCACTGAAGGACCTGGAATA
CUFF.8541   AATGACGAAATCACTGAAAAACTTG-----------------------------------
CUFF.1357   AATGATGAAATCACTCAAAAACGTGAAAAAT-AGAAGTGCACACTGTAAGACCTGGAATA
CUFF.7729   AATGACAAAATCACTGAAAAAGGTGAAAAATGAGAAATGCACACTGTAGGACTTGGAATA
CUFF.2869   TATGACGAGAAATA------------------------------------------------
CUFF.11127  ------------------------------------------------------------
CUFF.1359   AATGACGAAATCACTAAAATACGTGAAAAATGAGAAATGCACACTGAAGGACCTGTAATT
```

```
CUFF.1473   TGGCGAGAAACCTGAAAATCACGGAAAATGAGAAATACACACTTTAGGACGTGAAATATG
CUFF.5889   TGGGGAGAAAACTGAAAATCACGGAAAATGAGAAATACACACTTTAGGACGTGAAATATG
CUFF.8541   ------------------------------------------------------------
CUFF.1357   TGGGGAGAAAACTGAAAATCACGGAAAATGAGAAATACACACTTTAGGAAATCAAATGTG
CUFF.7729   TGGCGAGAAAACTGAAAATCACGGAAGTGAG-----------------------------
CUFF.2869   ------------------------------------------------------------
CUFF.11127  ------------------------------------------------------------
CUFF.1359   TAA---------------------------------------------------------


CUFF.1473   GCGAGGAAAACTGAAAAAGGTGGAAAATTTAGAAATGTCCACTGTAGGACGTGGAGTATG
CUFF.5889   GCGAGGAAAACTGAAAAAGGTGGAATATTTAGAAATGTCCACTGTAGGACGTGGAATATA
CUFF.8541   ------------------------------------------------------------
CUFF.1357   CCGAGGAAAACTGAAAAAGGTGGAAAATTTAGAAATGGCACTCT----------------
CUFF.7729   ------------------------------------------------------------
CUFF.2869   ------------------------------------------------------------
CUFF.11127  ------------------------------------------------------------
CUFF.1359   ------------------------------------------------------------


CUFF.1473   GCAAGAAAACTGAAAATCAAAGAAAACTGAAAATCATGGAAAATGAGAAACATCCACTTG
CUFF.5889   ------------------------------------------------------------
CUFF.8541   ------------------------------------------------------------
CUFF.1357   ------------------------------------------------------------
CUFF.7729   ------------------------------------------------------------
CUFF.2869   ------------------------------------------------------------
CUFF.11127  ------------------------------------------------------------
CUFF.1359   ------------------------------------------------------------


CUFF.1473   ACTACTTGAAAAATGACGAAATCACTAAAAAACGTGAAAAATGAGAAATGCACACTGAAG
CUFF.5889   ------------------------------------------------------------
CUFF.8541   ------------------------------------------------------------
CUFF.1357   ------------------------------------------------------------
CUFF.7729   ------------------------------------------------------------
CUFF.2869   ------------------------------------------------------------
CUFF.11127  ------------------------------------------------------------
CUFF.1359   ------------------------------------------------------------


CUFF.1473   GACCTGGAATATGGCGAGAAAACTGAAAATCACGGAAAATGAGAAATACACACTTTAGGA
CUFF.5889   ------------------------------------------------------------
CUFF.8541   ------------------------------------------------------------
CUFF.1357   ------------------------------------------------------------
CUFF.7729   ------------------------------------------------------------
CUFF.2869   ------------------------------------------------------------
CUFF.11127  ------------------------------------------------------------
CUFF.1359   ------------------------------------------------------------


CUFF.1473   CGTGAAATATGGCGAGGAAAACTGAAAAAGGTGGAATATTTAGAAATGTCCACTGTAGGA
CUFF.5889   ------------------------------------------------------------
CUFF.8541   ------------------------------------------------------------
CUFF.1357   ------------------------------------------------------------
CUFF.7729   ------------------------------------------------------------
CUFF.2869   ------------------------------------------------------------
CUFF.11127  ------------------------------------------------------------
CUFF.1359   ------------------------------------------------------------
```

```
CUFF.1473   CGTGAAATATGGCAAGAAAACTGAAAATCATGGAAAATGAGAAACATCCACTTGACGACT
CUFF.5889   ------------------------------------------------------------
CUFF.8541   ------------------------------------------------------------
CUFF.1357   ------------------------------------------------------------
CUFF.7729   ------------------------------------------------------------
CUFF.2869   ------------------------------------------------------------
CUFF.11127  ------------------------------------------------------------
CUFF.1359   ------------------------------------------------------------


CUFF.1473   TGAAAAATGACGAAATCATCTG
CUFF.5889   ----------------------
CUFF.8541   ----------------------
CUFF.1357   ----------------------
CUFF.7729   ----------------------
CUFF.2869   ----------------------
CUFF.11127  ----------------------
CUFF.1359   ----------------------



CLUSTAL format alignment by MAFFT (v6.821b)

CUFF.4451   ---------------------------------CAACGGATGTGTTTTTCAGTGTAACTC
CUFF.1355   CATTGATATACACTGTTCTACAAATCCCGTTTCCAACGAATGTGTTTTTCAGTGTAACTC
CUFF.11847  ------------------------------------------------------------


CUFF.4451   ACTCATCTAATATGTTCTACAGTGTGGTTTTTTATCATTTTCCATGTTCCTCATTGTAAC
CUFF.1355   ACTCATCTAATCTGTTCTCCAGTGTGG-TTTTTATCATTTTCCATGTTTCTCATTGTAAC
CUFF.11847  ----------------------------------------------GTTTCTCATTGTAAC
                                                           *** ***********

CUFF.4451   TCATTGATATACACTGTTCTACAATTCCCGTTTCCAACGAATGTGTTTTTCAGTGTAACT
CUFF.1355   TCATTGATATACACTGTTCTACAAATCCCGTTTCCAACGAATGTGTTTTTCAGTGTATCT
CUFF.11847  TCATTGATATACACTGTTCTACAATGCCCGTTTCCAACGTATGTGTTTTTCAGTGTAACT
            ************************  ************* ***************** **

CUFF.4451   CACTCATCTAATATGTTCTACAGTGTGGTTTTTATCATTTTCCATGTTTCTCATTGTAAC
CUFF.1355   CACTCATCTAATACGTTCTGCAGTGTGGTTTTTATCATTTTCGATGTTTTTCATTGTAAG
CUFF.11847  CACTCATCTAATATGTTCTACAGTGTG---------------------------------
            ************* ***** *******

CUFF.4451   TCATTGATATACACTGTTCTACAAATCCCGTTT----------------------------
CUFF.1355   TCATTGATATACACTCTTCTACAAATCCCGTTTCCAACGAATTTGTTTTTCAGGTTAACT
CUFF.11847  ------------------------------------------------------------


CUFF.4451   -------------------------------------------
CUFF.1355   CACTCATCTAATATGTTCTACAGTGTAGTTTTTATCATTTTCCT
CUFF.11847  -------------------------------------------
```

Appendix 5: Sequences of RNAs identified by mitochondrial RNA sequencing, grouped by similarity.

RNAs are grouped by their similarity as found by BLAST searches. RNAs labeled *Plasmodium* are RNAs expressed from the mouse genome that have high similarity to *Plasmodium* sequences.

Plasmodium	CUFF.1473	GATATACACTGTTCTACAATGCCGGTTTCCAACGAA TGTGTTTTTCAGTGTAACTCACACATCTAATATGTTC TACAGTGTGGTTTTTATCATTTTCCATGTTTCTCATT GTAACTCATTGATATACACTGTTCTAAAAAATCCCG TTTCCAACGAATGTGTTTTTCAGTGTAACTCACTCAT CTAATATGTTCTACAGTGTTGTTTTTATCATTTTCCA TGTTTCTCATTGTAACTCATTGATATACACTGTTCTA CAATGCCGGTTTCCAACGTATGTGTTTTTTTTGTGTG TGTACCTACTTTGGAAAGAAAACTGAAAATCATGGA AAATGAGAAACATCCACTTGACGACTTGAAAAATG ACGAAATCACTAAAATACGTGAAAAATGAGAAATG CACACTGAAGGACCTGGAATATGGAGAGAAAACTG AAAATCACGGAAAATGAGAAATACACACTTTAGGA CGTGAAATATGGCGAGGAAAACTGAAAAAGGTGGA ATATTTAGAAATGTCCACTGTAGGACGTGGAATATT GCAAGAAAACTGAAAATCATGGAAAATGAGAAACA TCTACTTGACGACTTGAAAAATGACGAAATCACTAA AAAACGTGAAAAATGTGAAATGCACACTGAAGGAC CTGGAATATGGCGAGAAACCTGAAAATCACGGAAA ATGAGAAATACACACTTTAGGACGTGAAATATGGC GAGGAAAACTGAAAAAGGTGGAAAATTTAGAAATG TCCACTGTAGGACGTGGAGTATGGCAAGAAAACTG AAAATCAAAGAAAACTGAAAATCATGGAAAATGAG AAACATCCACTTGACTACTTGAAAAATGACGAAATC ACTAAAAAACGTGAAAAATGAGAAATGCACACTGA AGGACCTGGAATATGGCGAGAAAACTGAAAATCAC GGAAAATGAGAAATACACACTTTAGGACGTGAAAT ATGGCGAGGAAAACTGAAAAAGGTGGAATATTTAG AAATGTCCACTGTAGGACGTGAAATATGGCAAGAA AACTGAAAATCATGGAAAATGAGAAACATCCACTT GACGACTTGAAAAATGACGAAATCATCTG
Plasmodium	CUFF.7729	TAAAATCACTGAAAATCACGGAAAATGAGAAATAC ACACTTTAGGACGTGAAATATGGCGAGGAAAACTG AAAAAGGTGGAAAATTTAGAAATGTCCACTGTAGG ACATGGAATATGGCAAGAAAACTGAAAATCATGGA AAATGAGAAACATCCACTTGACGACTTGAAAAATG ACAAAATCACTGAAAAAGGTGAAAAATGAGAAATG

		CACACTGTAGGACTTGGAATATGGCGAGAAAACTG AAAATCACGGAAGTGAG
Plasmodium	CUFF.5889	AGGTGCACACTGAAGGACCTGGAATTATGCGAGAA AACTGAAAATCACGGAAAATGAGAAATACACACTT TAGGACGTGAAAAATGGCGAGGAAAACTGAAAAAG GTGGAAAATTTAGAAATGTCCTCTGTAGGACATGGA ATATGGCAAGAAAACTGAAAATCATGGAAAATGAG AAACATCCACTTGATGACTTGAAAAATGACGAAATC ATTAAAAAACGTGAAAAATGAGAAATGCCCACTGA AGGACCTGGAATATGGGGAGAAAACTGAAAATCAC GGAAAATGAGAAATACACACTTTAGGACGTGAAAT ATGGCGAGGAAAACTGAAAAAGGTGGAATATTTAG AAATGTCCACTGTAGGACGTGGAATATA
Plasmodium	CUFF.1359	GCTGCATGTCCTTCAGTGTGCATTTCTCATTTTTCAC GTTTTTTAGTGATTTCGTCATTTTTCAAGTCGTCAAG TAGATGTTTCTCATTTTCCATGATTTTCAGTTTTCTTG CCATATTCCACGTCCTGCACTGGACATTTCTAAATTT TCCACCTTTTTCAGTTTTCCTTGCCATATTTCACGTC CTAAAGTGTGTATTTCTCATTTTCCGTGATTTTCAGT TTTCTCGCCATATTCCAGGTTCTTCAGTGTGCATTTC ACATTTTTCACGTATCATTTTCCATGTTTTTCATTGT AACTCATTGATATACACTGTTCTACAAATCCCGTTTC CAACGAATGTGTTTTTCAGTGTAACTCACTCATCTA ATACGTTCTGCAGTGTGGTTTTTATCATTTTCGATGT TTTTCATTGTAACTCATTGATATACACTGTTCTACAA ATCCCGTTTCCAACGAATGTGTTTTTCATTGTAACTC ACTCATCTAATATGTTCTACAGTGTGGTTTTTATCAT TTTCCATGTTTTCATTGTAAGTCATTGATATACACTA TTCTACAATGCCGGTTTCCAACGTATGTGTTTTTCAG TGTAACTCGGAAAATTTAGAAATGTCCACTGTAGGA CGTGGAATATGGCAAGAAAATTGAAAATCATGGAA AATGAGAAACATCGACTTGACGACTTGAAAAATGA CGAAATCACTAAAATACGTGAAAAATGAGAAATGC ACACTGAAGGACCTGTAATTTAA
Plasmodium	CUFF.8541	CAAGTTTTTCAGTGATTTCGTCATTTTTCAAGTCGTC AAGTGGATGTTTCTCATTTTCCATGATTTTCAGTTTT CTTGCCATATTCCATGTCCTACAGTGGACATTACTA AATTATCCACCTTTTTCAGTTTTCTTCGCCATATTTC ACG
Plasmodium	CUFF.1357	AGAGTGCCATTTCTAAATTTTCCACCTTTTTCAGTTT TCCTCGGCACATTTGATTTCCTAAAGTGTGTATTTCT CATTTTCCGTGATTTTCAGTTTTCTCCCCATATTCCA GGTCTTACAGTGTGCACTTCTATTTTTCACGTTTTTG AGTGATTTCATCATTTTTTCAAGTCAAGTGGATGTTT CTCATTTTCCATGATTTTCAGTTTTCTTGACATATTC CATGTCCTACAGTGGACATTTCTAAATTTCCCACCTT

		TTTCAGTTTTCCTCGTCATATTTCACTTCCTAAAGTG TGTATTTCTCATTTTCCGTGATTTTCAGTTTTCTCGCC ATATTCCAGGTCTTACAGTGTGCATTTATCATTTTTC AGGTTTTTCATTGATTTCATCATTTTTCTAGTCGTCA AGTGGATATTTCTCATTTTCCATGATTTTCAGTTTTC TTACCATATTCCT
Plasmodium	CUFF.11127	TGAGAAATGCACACTGTAGGACCAGGAGTATGGCG AGAAAACTGAAAATCATGGAAAATGAGAAACACAC AATGT
Plasmodium	CUFF.2869	GAAATTACTGAAAAACGTGAAAAATGAGAAATGCA CACTGCAGGACCTGGAATATGGCGAGAAAACTGAA CATCACGGAAAATGAGAATAACACTCTTTAGGTAGT GAAATATGACGAGAAATA

Plasmodium	CUFF.4451	CAACGGATGTGTTTTTCAGTGTAACTCACTCATCTA ATATGTTCTACAGTGTGGTTTTTTATCATTTTCCATG TTCCTCATTGTAACTCATTGATATACACTGTTCTACA ATTCCCGTTTCCAACGAATGTGTTTTTCAGTGTAACT CACTCATCTAATATGTTCTACAGTGTGGTTTTTATCA TTTTCCATGTTTCTCATTGTAACTCATTGATATACAC TGTTCTACAAATCCCGTTT
Plasmodium	CUFF.1355	AGGAAAATGATAAAAACTACACTGTAGAACATATT AGATGAGTGAGTTAACCTGAAAAACAAATTCGTTGG AAACGGGATTTGTAGAAGAGTGTATATCAATGACTT ACAATGAAAAACATCGAAAATGATAAAAACCACAC TGCAGAACGTATTAGATGAGTGAGATACACTGAAA AACACATTCGTTGGAAACGGGATTTGTAGAACAGTG TATATCAATGAGTTACAATGAGAAACATGGAAAAT GATAAAAACCACACTGGAGAACAGATTAGATGAGT GAGTTACACTGAAAAACACATTCGTTGGAAACGGG ATTTGTAGAACAGTGTATATCAATG
Plasmodium	CUFF.11847	GTTTCTCATTGTAACTCATTGATATACACTGTTCTAC AATGCCCGTTTCCAACGTATGTGTTTTTCAGTGTAAC TCACTCATCTAATATGTTCTACAGTGTG

Micro-satellite	CUFF.1933	ACAGAGGCCAGGGCAAGGAATTTCAGTGGCAGGAC ACACATACACACACAGCATAACACACAAAGATACA CATCATGTACATACAACATAAACATCACACACCACT ACACACACACACA

Micro-satellite	CUFF.4245	TAGGAACATAGAAAGACAGATCTGATAAGAGCAAG GGAAAGAGGGAGAGAGAGAGACAGAGACAGAGAA AGCGACAAAGAGAGACAGAGACACAGAGATACACA GAGAGAGACAGAGAGAGAGAGACAGAGACATAAA GAAAGATAGACTGACACATATACACACATATGCAC ACACACACACACAGACAGAGACCTAAAGAAAGATA GACTGACACATACACACACACACACACACACAC

		ACACACACACACACACACATACACACACACAGA GAGAGACCTTAAGAAAGATAGA

Unknown	CUFF.11013	GAACAGTTGGATAATGTTTTCAAGAGCGTTAGTCAG CCATCGGTCATGGGGGCTGAACCACACTTTCTAGGA CATGTGCCAAGTTTTGTCTCAGAGTCAATTTATCTGC GTCCTTGACCAGAAGCCACTATGTGCAGACAAGCAG GCCATCTTACAGCCACCAGGTCTAATTTTTTACAAG TATGTCACAGGTCTTTTTCCAGGGTCCCAATCTCTGA GTAAGAACTTTTTTTGGCAATACCTTTGTTCTCAGTC ACATCTAGGAGTCCCATAGCTGGGGATAACATTAGG GCAGTCTCAAGAGCATCCAAGGCCATCTAAGATTGT TCTTTTTTTTTTCTATACGAAGGGCTGTTTATCTCTTT AACTCAGCAAAACCTGGAATCCACAATCTGCAAAA GCCCGCAGTGCCCAGGAACTTTTTAGCTTGTTTTGC ACTGGTCGGTGGAGGAGTATGAAACACAGTCTCTTT TTTTAGCTGCTTTAACAGGTAGGCCACCGGACTCTTT TAAGGACTCAGCTTCTGTATTAGCACCCCTTTTGTTA TCTCTTAAACACATTGATCTTTAGCCAAAAGCTTTTT TTTGTTGCCAGGTACTATCTAGGTTTTTTTAATTTTC CTGACTTTTGTGACCAGCATTTTATTTCTCTTATCTC TTTGTCTCACAGCACAGCTCTGATTCTGACTCTGGTC TCTGTCTTTGTCAGCCTCATGTTTCTTTAACTCTTCTT CTTGTCTGACTCTTATTTACTGTTTTTTTTTTTTAAAT ATTTTTCATTCAGAGTATCTTTCTCATTTTAGACCTC TCTAATCTCTTTTATCTCTATTTTTACTTCTCTTCACT GTTAACCTATCTCTTCTGGGTCTGCTGAAGATTTGCT TTTAGCTTACTTCTTTGCAGACCTCTGTCCTTCCTTT GTTTCTCCTCCTCTGCACTTTCTTATCTACTTACACT AACTTTTTTACCAACTTATCCTGTCCTTCTCTTAACT TTTGTAACTTTCTGTTACCTTGGTCAGATTGTTGGGA CACTTTCTAGTCCCACAGAGAGG

Unknown	CUFF.759	CTTAATGTGTGAGCCCAGGGCTGCTTGTGTTTCCCTC TTCCAGGAGAGCACAGCTAGGCTGAAAGTGGATCT AGGATGTAGGAAAGGGTTGGGTCTAAATTGTGGTCA AGGGCAGGAGTATTTGCTTCTTGTTCCTGAAGGAGG CCTATGATTCACCTAGGAACTGGTCCCTAATCTGGG CTTCTGTCGGAGGCTGATATAGTTCTGGGTTGAGGG TCAGATGAATCTTTAAATCAAATCAGCAGATACAGA CTATCAGGGTAAGAGCCTGTGTCCCATGTGTGTCCG CTAGAGCAGGGTTGTTCACATAAACAGACACACAC ACTCACACACACACACACACACAGACATGCACACTC ACATACACACTCTCTCCTATATAGAGGACACCTTTC AAAAGGCAGAACCAAATACATGGAAATATTTTACT

		GTCTTTACTTATA

Giant tandem repeat (sample - 1000nt out of 38,396nt)	CUFF.6145	GATCCTACAGTGTGCATTTCTCATTTTTCACGTTTTT CAGTGATTTCGTCATTTTTCAAGTCATCAAGTGGCTG TTTCTCATTTTCCATGATTTTCAGTTTTCTTGCCATAT TCCTTGTCCTACAGTGGACATTTCTAAATTTTCCACC TTTTTCAGTTTTCCTTGTCATATTTCAGGTCCTACAG TGTGTATTTCTCATTTTTCACGTTTTTCATTGATTTCG TCATTTTTCAAGTTGTCAAGTGCATGTTTCTCATTTT CCATGATTTTCAGTTTTCTTGCCATATTCCATGTCCT ACAATGGACATTTCTAAATTTTCCAACTTTTTCAGTT TTCCTCGCCATATTTCACGTCCTAAAGTGTGTATTTC TCATTTTCCGTGATTTTCAGTTTTCTCGACATATTCC AGGTCCTACAGTGTGCATTTCTCATTTTTCACGTTTT TCAGTGATTTCGTCATTTTTCACGTCGTCAAGTGGAT GTTTCTCATTTTCCATGATTTTCAGTTTTCTTGCCATA TTCCATGTCCTACAGTGGACATTTCTAAATTTTCCAC CTTTTTCAGTTTTCCTCGCCATATTTCACGTCCTAAA GTGTGTATTTCTCATTTTCCGTGATTTTCAGTTTTCTC GACATATTCCAGGTCTTACAGGGTGCATTTCTCATTT TTCACGTTTTTCAGTGATTTCATCATTTTTCAAGTCG TCAACTGTATGTTTCTCATTTTCAATGATTTTCATTTT TCTTGCCATATTCCACGTCCTATAGTGGACATTTCTA AATTTTCCACCTTTTTCAGTTTTCCTTGCCATATTTCA GGTCCTACAGTGTGCATTTCTCATTTTTCACGTTTTT CAGTGATTTCGTCATTTTTCAAGTGGTCAAATGCAT GTTTCTCATTTTCCATGATTTTCAGTTTTCTTGCCATA TTCCATGTCCTACAGTGGACATTTCTAAATTTTCCAC CTTTTTCAGTTTTCCTCGCCATATTTCACGTC

Appendix 6: Statistical analysis of fold change RNA immunoprecipitation data.

ANOVA analysis with a dunnett's correction was performed on fold change transformed RIP data. ANOVA identified no differences among RNA quantities precipitated with different antibodies. Dunnett's analysis revealed no differences in RNA quantity between bead control and antibody purified sample, evidenced by overlapping confidence intervals.

Fold Change over Beads

---------- exp=**5S rRNA** ----------

The GLM Procedure

Class Level Information

Class	Levels	Values
TRT	15	ATP5A ATP5B HSP56 HSP90 PCCB RPL28 Rad23B TCP-1 Tim23 Tom40 VDAC1 beads beta gamma zeta

Number of Observations Read 75
Number of Observations Used 75

Fold Change over Beads

---------- exp=**5S rRNA** ----------

The GLM Procedure

Dependent Variable: RNA1

Source	DF	Sum of Squares	Mean Square	F Value	Pr > F
Model	14	6.86539200	0.49038514	1.11	0.3666
Error	60	26.46132000	0.44102200		
Corrected Total	74	33.32671200			

R-Square	Coeff Var	Root MSE	RNA1 Mean
0.206003	56.41309	0.664095	1.177200

Source	DF	Type I SS	Mean Square	F Value	Pr > F
TRT	14	6.86539200	0.49038514	1.11	0.3666

Source	DF	Type III SS	Mean Square	F Value	Pr > F
TRT	14	6.86539200	0.49038514	1.11	0.3666

Fold Change over Beads

---------- exp=**5S rRNA** ----------

The GLM Procedure

Dunnett's t Tests for RNA1

NOTE: This test controls the Type I experimentwise error for comparisons of all treatments against a control.

Alpha	0.05
Error Degrees of Freedom	60
Error Mean Square	0.441022
Critical Value of Dunnett's t	2.90141
Minimum Significant Difference	1.2186

Comparisons significant at the 0.05 level are indicated by ***.

TRT Comparison	Difference Between Means	Simultaneous 95% Confidence Limits	
PCCB - beads	1.0060	-0.2126	2.2246
HSP56 - beads	0.5020	-0.7166	1.7206
Rad23B - beads	0.4880	-0.7306	1.7066
Tom40 - beads	0.4180	-0.8006	1.6366
beta - beads	0.2460	-0.9726	1.4646
TCP-1 - beads	0.1340	-1.0846	1.3526
ATP5B - beads	0.1180	-1.1006	1.3366
Tim23 - beads	0.1040	-1.1146	1.3226
gamma - beads	0.0300	-1.1886	1.2486
RPL28 - beads	0.0120	-1.2066	1.2306
ATP5A - beads	-0.0200	-1.2386	1.1986
zeta - beads	-0.0360	-1.2546	1.1826
HSP90 - beads	-0.1400	-1.3586	1.0786
VDAC1 - beads	-0.2040	-1.4226	1.0146

Fold Change over Beads

---------- exp=**MRP** ----------

The GLM Procedure

Class Level Information

Class	Levels	Values
TRT	15	ATP5A ATP5B HSP56 HSP90 PCCB RPL28 Rad23B TCP-1 Tim23 Tom40 VDAC1 beads beta gamma zeta

Number of Observations Read	75
Number of Observations Used	75

Fold Change over Beads

---------- exp=**MRP** ----------

The GLM Procedure

Dependent Variable: RNA1

Source	DF	Sum of Squares	Mean Square	F Value	Pr > F
Model	14	109.1889387	7.7992099	0.53	0.9027
Error	60	875.5990000	14.5933167		
Corrected Total	74	984.7879387			

R-Square	Coeff Var	Root MSE	RNA1 Mean
0.110876	128.1117	3.820120	2.981867

Source	DF	Type I SS	Mean Square	F Value	Pr > F
TRT	14	109.1889387	7.7992099	0.53	0.9027

Source	DF	Type III SS	Mean Square	F Value	Pr > F
TRT	14	109.1889387	7.7992099	0.53	0.9027

Fold Change over Beads

---------- exp=**MRP** ----------

The GLM Procedure

Dunnett's t Tests for RNA1

NOTE: This test controls the Type I experimentwise error for comparisons of all treatments against a control.

Alpha	0.05
Error Degrees of Freedom	60
Error Mean Square	14.59332
Critical Value of Dunnett's t	2.90141
Minimum Significant Difference	7.01

Comparisons significant at the 0.05 level are indicated by ***.

TRT Comparison	Difference Between Means	Simultaneous 95% Confidence Limits	
TCP-1 - beads	5.362	-1.648	12.372
Tim23 - beads	3.276	-3.734	10.286
HSP56 - beads	2.730	-4.280	9.740
Tom40 - beads	2.370	-4.640	9.380
ATP5B - beads	2.362	-4.648	9.372
VDAC1 - beads	2.356	-4.654	9.366
PCCB - beads	2.020	-4.990	9.030

RPL28 - beads	1.934	-5.076	8.944
gamma - beads	1.640	-5.370	8.650
beta - beads	1.340	-5.670	8.350
zeta - beads	1.282	-5.728	8.292
Rad23B - beads	1.074	-5.936	8.084
ATP5A - beads	1.040	-5.970	8.050
HSP90 - beads	0.942	-6.068	7.952

Fold Change over Beads

---------- exp=**RNase P** ----------

The GLM Procedure

Class Level Information

Class	Levels	Values
TRT	15	ATP5A ATP5B HSP56 HSP90 PCCB RPL28 Rad23B TCP-1 Tim23 Tom40 VDAC1 beads beta gamma zeta

Number of Observations Read	75
Number of Observations Used	75

Fold Change over Beads

---------- exp=**RNase P** ----------

The GLM Procedure

Dependent Variable: RNA1

Source	DF	Sum of Squares	Mean Square	F Value	Pr > F
Model	14	263.391739	18.813696	0.41	0.9645
Error	60	2724.211760	45.403529		
Corrected Total	74	2987.603499			

R-Square	Coeff Var	Root MSE	RNA1 Mean
0.088162	130.5889	6.738214	5.159867

Source	DF	Type I SS	Mean Square	F Value	Pr > F
TRT	14	263.3917387	18.8136956	0.41	0.9645

Source	DF	Type III SS	Mean Square	F Value	Pr > F
TRT	14	263.3917387	18.8136956	0.41	0.9645

Fold Change over Beads

---------- exp=**RNase P** ----------

The GLM Procedure

Dunnett's t Tests for RNA1

NOTE: This test controls the Type I experimentwise error for comparisons of all treatments against a control.

Alpha	0.05
Error Degrees of Freedom	60
Error Mean Square	45.40353
Critical Value of Dunnett's t	2.90141
Minimum Significant Difference	12.365

Comparisons significant at the 0.05 level are indicated by ***.

TRT Comparison	Difference Between Means	Simultaneous 95% Confidence Limits	
TCP-1 - beads	7.902	-4.463	20.267
Tom40 - beads	6.532	-5.833	18.897
HSP56 - beads	6.300	-6.065	18.665
PCCB - beads	5.094	-7.271	17.459
Tim23 - beads	5.014	-7.351	17.379
HSP90 - beads	4.704	-7.661	17.069
zeta - beads	4.200	-8.165	16.565
ATP5B - beads	3.960	-8.405	16.325
VDAC1 - beads	3.898	-8.467	16.263
RPL28 - beads	3.866	-8.499	16.231
ATP5A - beads	3.322	-9.043	15.687
Rad23B - beads	3.080	-9.285	15.445
gamma - beads	2.308	-10.057	14.673
beta - beads	2.218	-10.147	14.583

Fold Change over Beads

---------- exp=**5.8S rRNA** ----------

The GLM Procedure

Class Level Information

Class	Levels	Values
TRT	15	ATP5A ATP5B HSP56 HSP90 PCCB RPL28 Rad23B TCP-1 Tim23 Tom40 VDAC1 beads beta gamma zeta

Number of Observations Read	75
Number of Observations Used	75

Fold Change over Beads

---------- exp=**5.8S rRNA** ----------

The GLM Procedure

Dependent Variable: RNA1

Source	DF	Sum of Squares	Mean Square	F Value	Pr > F
Model	14	22.2502747	1.5893053	0.76	0.7060
Error	60	125.4397200	2.0906620		
Corrected Total	74	147.6899947			

R-Square	Coeff Var	Root MSE	RNA1 Mean
0.150655	80.78925	1.445912	1.789733

Source	DF	Type I SS	Mean Square	F Value	Pr > F
TRT	14	22.25027467	1.58930533	0.76	0.7060

Source	DF	Type III SS	Mean Square	F Value	Pr > F
TRT	14	22.25027467	1.58930533	0.76	0.7060

Fold Change over Beads

---------- exp=**5.8S rRNA** ----------

The GLM Procedure

Dunnett's t Tests for RNA1

NOTE: This test controls the Type I experimentwise error for comparisons of all treatments against a control.

Alpha	0.05
Error Degrees of Freedom	60
Error Mean Square	2.090662
Critical Value of Dunnett's t	2.90141
Minimum Significant Difference	2.6533

Comparisons significant at the 0.05 level are indicated by ***.

TRT Comparison	Difference Between Means	Simultaneous 95% Confidence Limits	
TCP-1 - beads	2.2180	-0.4353	4.8713
RPL28 - beads	1.3560	-1.2973	4.0093
Tim23 - beads	1.3200	-1.3333	3.9733
Tom40 - beads	1.1740	-1.4793	3.8273
Rad23B - beads	0.8980	-1.7553	3.5513
VDAC1 - beads	0.7320	-1.9213	3.3853
ATP5B - beads	0.7280	-1.9253	3.3813
PCCB - beads	0.6560	-1.9973	3.3093
zeta - beads	0.6560	-1.9973	3.3093
HSP56 - beads	0.6220	-2.0313	3.2753
beta - beads	0.6160	-2.0373	3.2693
gamma - beads	0.5960	-2.0573	3.2493
ATP5A - beads	0.2680	-2.3853	2.9213
HSP90 - beads	0.0060	-2.6473	2.6593

Fold Change over Beads

---------- exp=**4.5S RNA** ----------

The GLM Procedure

Class Level Information

Class	Levels	Values
TRT	15	ATP5A ATP5B HSP56 HSP90 PCCB RPL28 Rad23B TCP-1 Tim23 Tom40 VDAC1 beads beta gamma zeta

Number of Observations Read	75
Number of Observations Used	75

Fold Change over Beads

---------- exp=**4.5S RNA** ----------

The GLM Procedure

Dependent Variable: RNA1

Source	DF	Sum of Squares	Mean Square	F Value	Pr > F
Model	14	3.66576800	0.26184057	0.78	0.6818
Error	60	20.03656000	0.33394267		
Corrected Total	74	23.70232800			

R-Square	Coeff Var	Root MSE	RNA1 Mean
0.154659	57.42028	0.577878	1.006400

Source	DF	Type I SS	Mean Square	F Value	Pr > F
TRT	14	3.66576800	0.26184057	0.78	0.6818

Source	DF	Type III SS	Mean Square	F Value	Pr > F
TRT	14	3.66576800	0.26184057	0.78	0.6818

Fold Change over Beads

---------- exp=**4.5S RNA** ----------

The GLM Procedure

Dunnett's t Tests for RNA1

NOTE: This test controls the Type I experimentwise error for comparisons of all treatments against a control.

Alpha	0.05
Error Degrees of Freedom	60
Error Mean Square	0.333943
Critical Value of Dunnett's t	2.90141
Minimum Significant Difference	1.0604

Comparisons significant at the 0.05 level are indicated by ***.

TRT Comparison	Difference Between Means	Simultaneous 95% Confidence Limits	
PCCB - beads	0.3320	-0.7284	1.3924
Rad23B - beads	0.3120	-0.7484	1.3724
Tom40 - beads	0.2980	-0.7624	1.3584
Tim23 - beads	0.1800	-0.8804	1.2404
TCP-1 - beads	0.1520	-0.9084	1.2124
RPL28 - beads	0.0860	-0.9744	1.1464

VDAC1	- beads	0.0260	-1.0344	1.0864
ATP5B	- beads	0.0060	-1.0544	1.0664
beta	- beads	-0.0240	-1.0844	1.0364
HSP56	- beads	-0.0660	-1.1264	0.9944
gamma	- beads	-0.2640	-1.3244	0.7964
ATP5A	- beads	-0.2720	-1.3324	0.7884
HSP90	- beads	-0.3160	-1.3764	0.7444
zeta	- beads	-0.3540	-1.4144	0.7064

Appendix 7: Statistical measure of RNA affinity purification data by ANOVA with dunnett's correction and evaluation of normality of data and residual analysis.

Experimental Ct values were divided by input lysate quantities for each RNA to normalize data to input lysate RNA quantities.

ANOVA results identify differences in amounts of 5.8S rRNA and 4.5S RNA between samples isolated with antibodies.

Dunnett's analysis identified differenced in RNase P RNA amounts relative to bead control for samples isolated with TCP-1 and TOM40 antibodies.

Data were shown to fit a normal distribution model. There were no significant differences in the variances and the variances did not tend to increase with the response, as seen in residual plots below.

Summary of the ANOVA for Each Experiment

Experiment	R-square	p-value
5S rRNA	0.955	0.180
MRP	0.899	0.464
RNase P	0.852	0.308
5.8S rRNA	0.873	**0.046**
4.5S RNA	0.824	**0.041**

Test for Normality for Each Experiment

	p-values for each test*			
Experiment	**SW**	**KW**	**CVM**	**AD**
5S rRNA	0.2054	0.0567	0.1038	0.1750
MRP	0.6962	0.1500	0.2500	0.2500
RNase P	0.4478	0.1500	0.1258	0.2163
5.8S rRNA	0.6794	0.1500	0.2500	0.2500
4.5S RNA	0.0064	0.0253	0.0769	0.0899

*SW=Sharpio Wilk, KW=Kolmogorov Smirnov, CVM=Cramer von Mises, AD=Anderson Darling

Results of Dunnett Test for 5S rRNA

Experiment	Comparison	Difference	LowerCL	UpperCL
5S rRNA	VDAC1 - beads	0.04115	-0.02160	0.10389
	HSP90 - beads	0.02619	-0.03655	0.08893
	ATP5A - beads	0.01365	-0.04909	0.07640
	zeta - beads	0.00983	-0.05291	0.07258
	RPL28 - beads	0.00420	-0.05855	0.06694
	gamma - beads	0.00290	-0.05984	0.06565
	TCP-1 - beads	0.00224	-0.06051	0.06498
	Tim23 - beads	0.00162	-0.06113	0.06436
	ATP5B - beads	0.00144	-0.06130	0.06419
	HSP56 - beads	-0.00951	-0.07225	0.05324
	beta - beads	-0.01017	-0.07292	0.05257
	Tom40 - beads	-0.01413	-0.07687	0.04862
	Rad23B - beads	-0.01421	-0.07696	0.04853
	PCCB - beads	-0.03631	-0.09905	0.02644

Results of the Dunnett Test for MRP

Experiment	Comparison	Difference	LowerCL	UpperCL
MRP	HSP90 - beads	-0.01941	-0.10933	0.07050
	ATP5A - beads	-0.02180	-0.11171	0.06812
	VDAC1 - beads	-0.02979	-0.11970	0.06013
	Rad23B - beads	-0.03289	-0.12281	0.05702
	zeta - beads	-0.03612	-0.12603	0.05379
	HSP56 - beads	-0.04316	-0.13307	0.04675
	beta - beads	-0.04459	-0.13450	0.04532
	PCCB - beads	-0.04472	-0.13463	0.04519
	ATP5B - beads	-0.04940	-0.13932	0.04051
	gamma - beads	-0.05543	-0.14534	0.03449
	RPL28 - beads	-0.05750	-0.14741	0.03242
	Tim23 - beads	-0.07081	-0.16073	0.01910
	TCP-1 - beads	-0.07288	-0.16279	0.01703
	Tom40 - beads	-0.08127	-0.17118	0.00864

Results of Dunnetts Test for RNase P

Experiment	Comparison	Difference	LowerCL	UpperCL
RNase P	ATP5B - beads	-0.04075	-0.11674	0.03525
	zeta - beads	-0.04777	-0.12377	0.02822
	HSP56 - beads	-0.05002	-0.12601	0.02598
	RPL28 - beads	-0.05071	-0.12671	0.02528
	ATP5A - beads	-0.05131	-0.12731	0.02468
	beta - beads	-0.05312	-0.12912	0.02287
	gamma - beads	-0.05692	-0.13291	0.01908
	VDAC1 - beads	-0.06126	-0.13726	0.01473
	PCCB - beads	-0.06513	-0.14113	0.01086
	Rad23B - beads	-0.06676	-0.14276	0.00923
	HSP90 - beads	-0.06691	-0.14291	0.00908
	Tim23 - beads	-0.06958	-0.14557	0.00642
	TCP-1 - beads	**-0.08066**	**-0.15665**	**-0.00466**
	Tom40 - beads	**-0.08803**	**-0.16403**	**-0.01204**

Results of Dunnetts Test for 5.8S rRNA

Experiment	Comparison	Difference	LowerCL	UpperCL
5.8S rRNA	HSP90 - beads	0.00878	-0.07379	0.09134
	ATP5A - beads	-0.01004	-0.09261	0.07252
	HSP56 - beads	-0.03380	-0.11636	0.04876
	VDAC1 - beads	-0.03468	-0.11724	0.04788
	zeta - beads	-0.03727	-0.11983	0.04529
	beta - beads	-0.03912	-0.12169	0.04344
	gamma - beads	-0.04039	-0.12296	0.04217
	Rad23B - beads	-0.04070	-0.12326	0.04187
	PCCB - beads	-0.04106	-0.12362	0.04151
	ATP5B - beads	-0.04694	-0.12950	0.03562
	Tim23 - beads	-0.06709	-0.14965	0.01547
	Tom40 - beads	-0.07440	-0.15696	0.00816
	TCP-1 - beads	-0.07976	-0.16232	0.00280
	RPL28 - beads	**-0.08754**	**-0.17010**	**-0.00497**

Results of the Dunnetts test for 4.5S RNA

Experiment	Comparison	Difference	LowerCL	UpperCL
4.5S RNA	ATP5A - beads	0.04050	-0.01182	0.09282
	zeta - beads	0.03553	-0.01679	0.08785
	HSP90 - beads	0.03522	-0.01710	0.08754
	gamma - beads	0.02763	-0.02469	0.07995
	TCP-1 - beads	0.01306	-0.03926	0.06537
	HSP56 - beads	0.00766	-0.04465	0.05998
	beta - beads	0.00565	-0.04667	0.05797
	VDAC1 - beads	0.00512	-0.04720	0.05744
	ATP5B - beads	0.00155	-0.05077	0.05387
	Tim23 - beads	0.00096	-0.05136	0.05328
	RPL28 - beads	-0.00095	-0.05327	0.05137
	Rad23B - beads	-0.00756	-0.05988	0.04476
	PCCB - beads	-0.01315	-0.06546	0.03917
	Tom40 - beads	-0.01475	-0.06707	0.03757

Histogram and QQ Plots for 5S rRNA

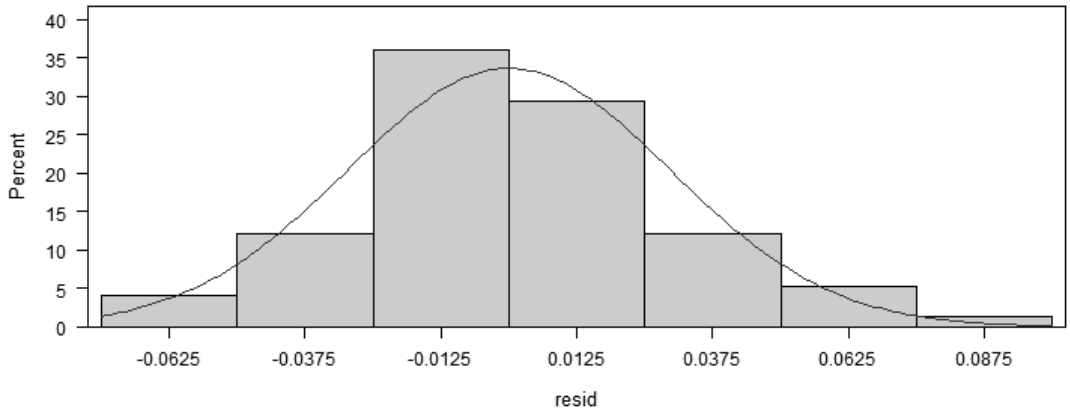

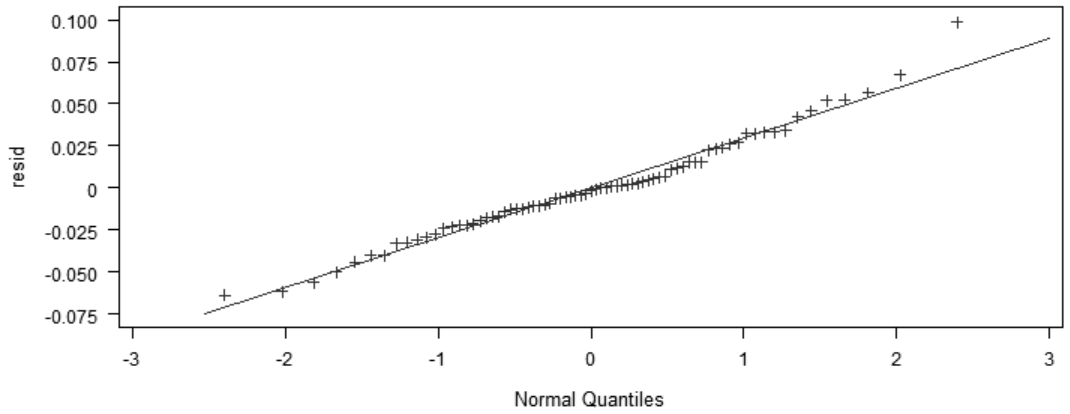

Histogram and QQ Plots for MRP

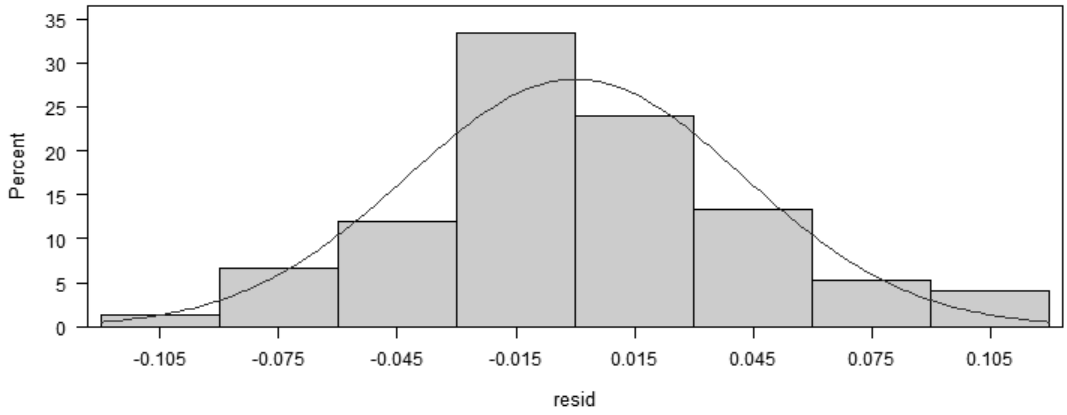

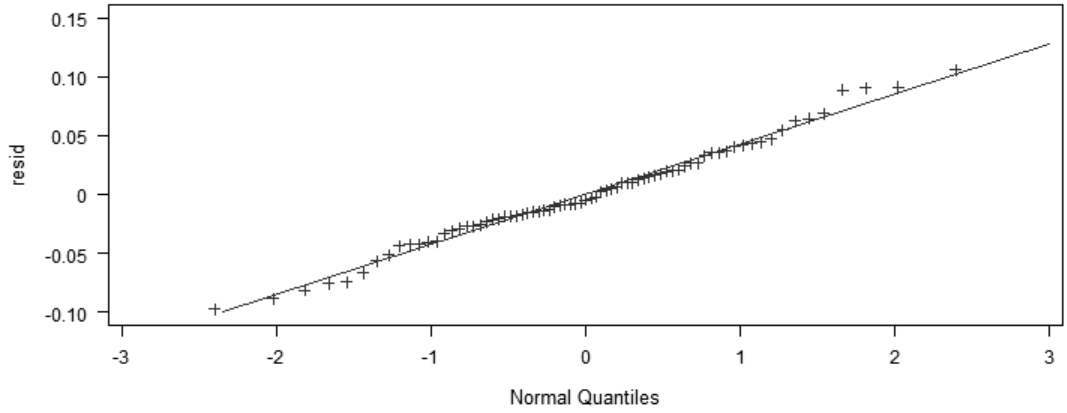

Histogram and QQ Plots for RNase P

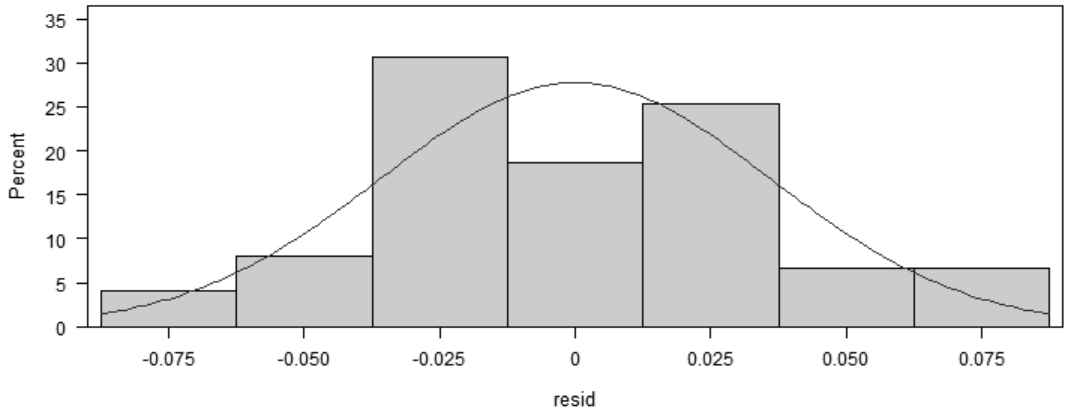

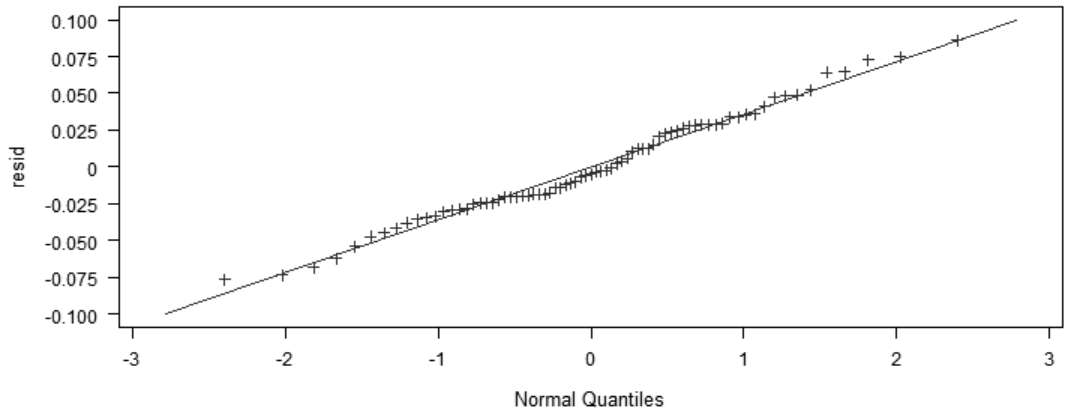

Histogram and QQ Plot for 5.8S rRNA

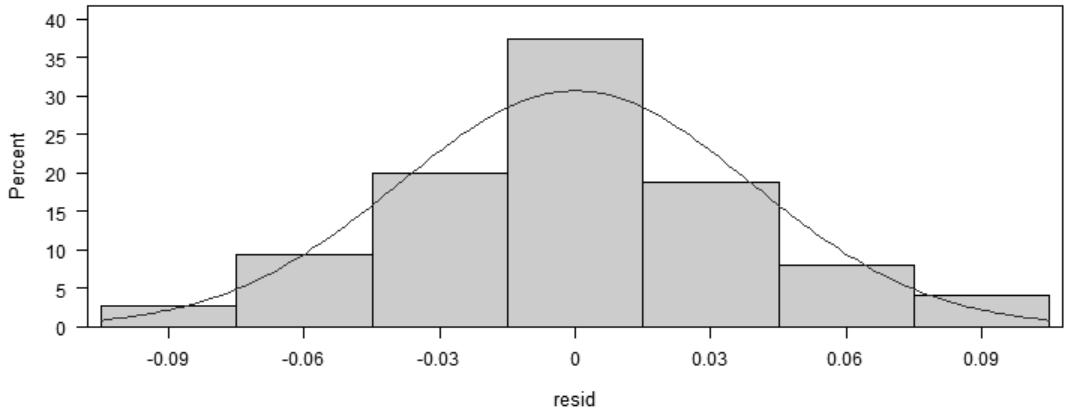

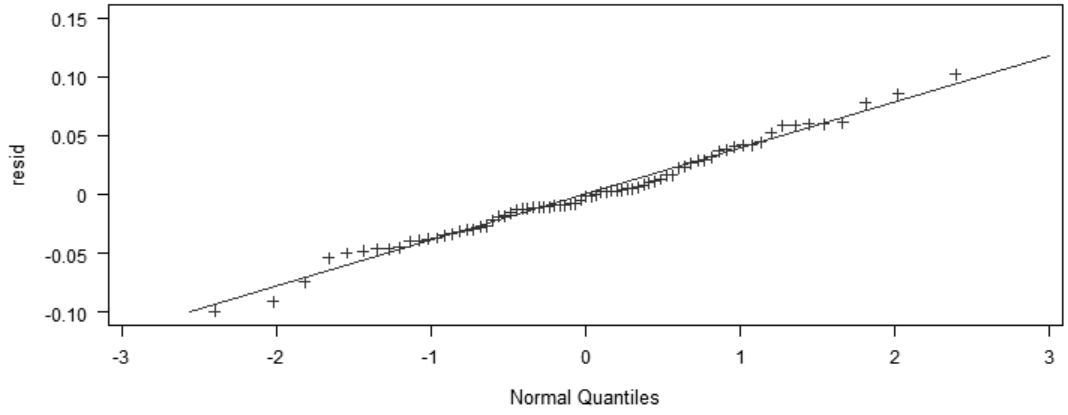

Histogram and QQ Plot for 4.5S RNA

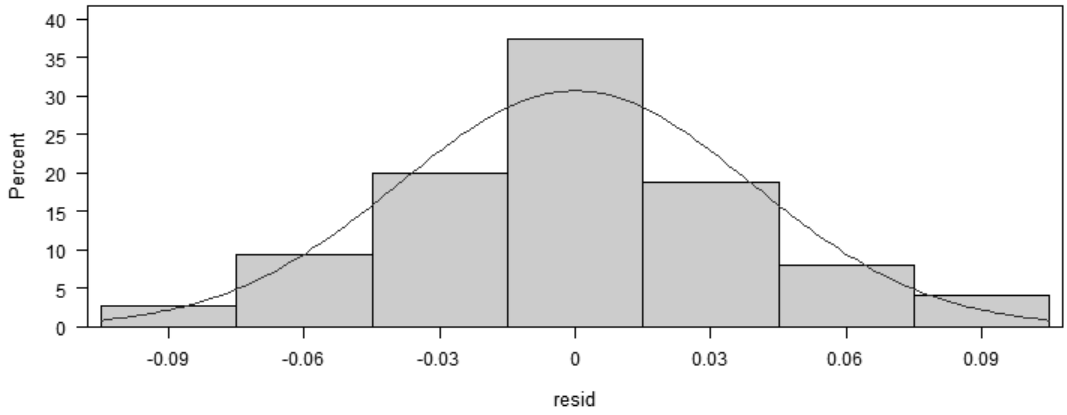

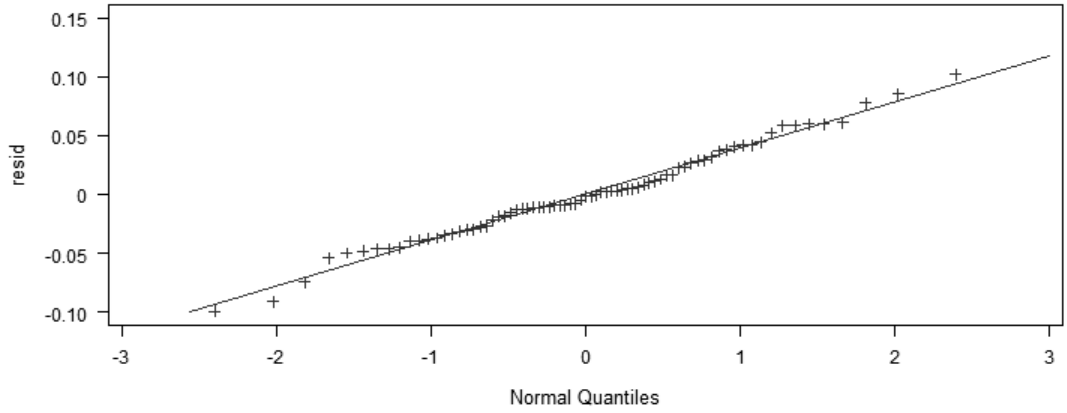

Residual Plot for 5S rRNA

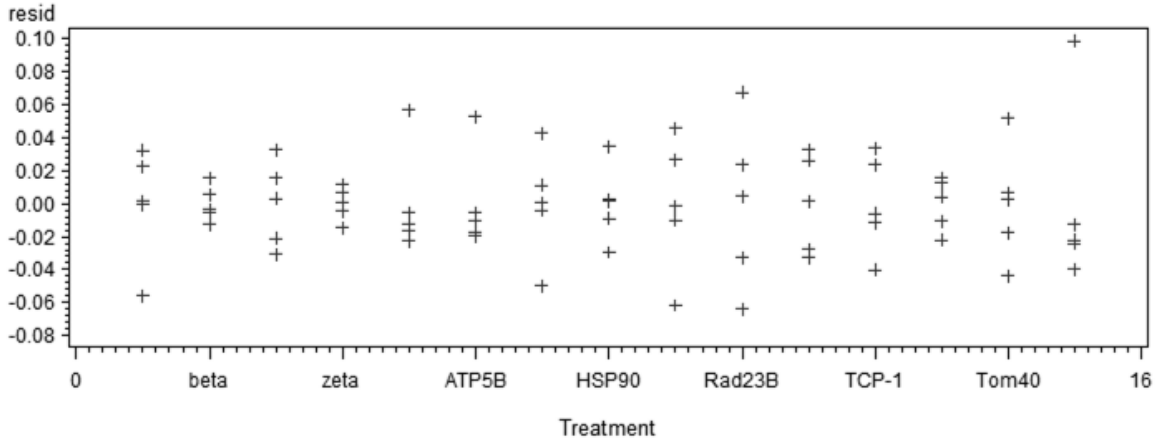

Residual Plot for MRP

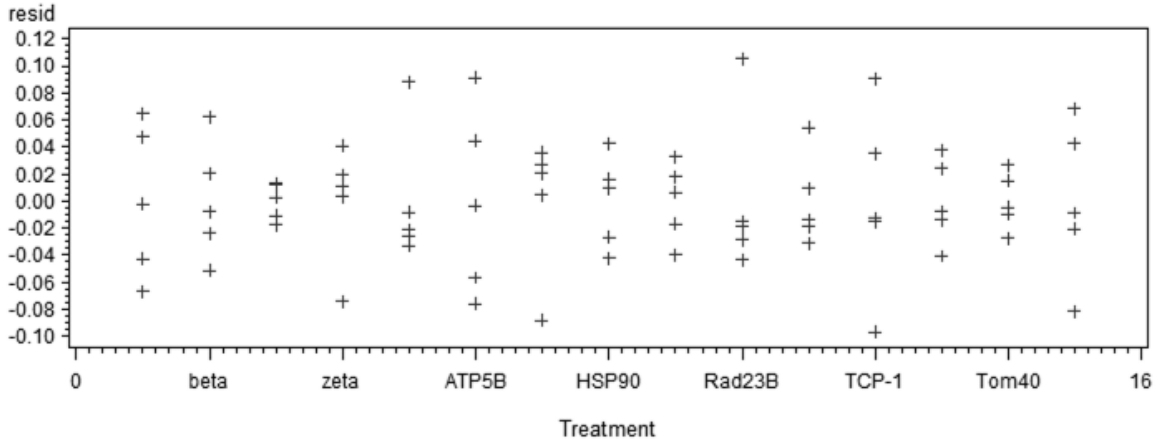

Residual Plot for RNASE P

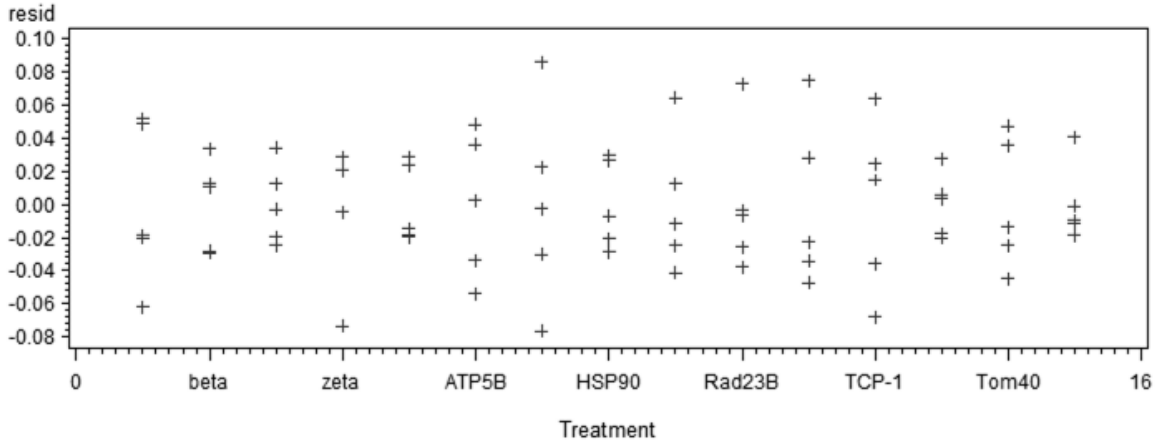

Residual Plot for 5.8S rRNA

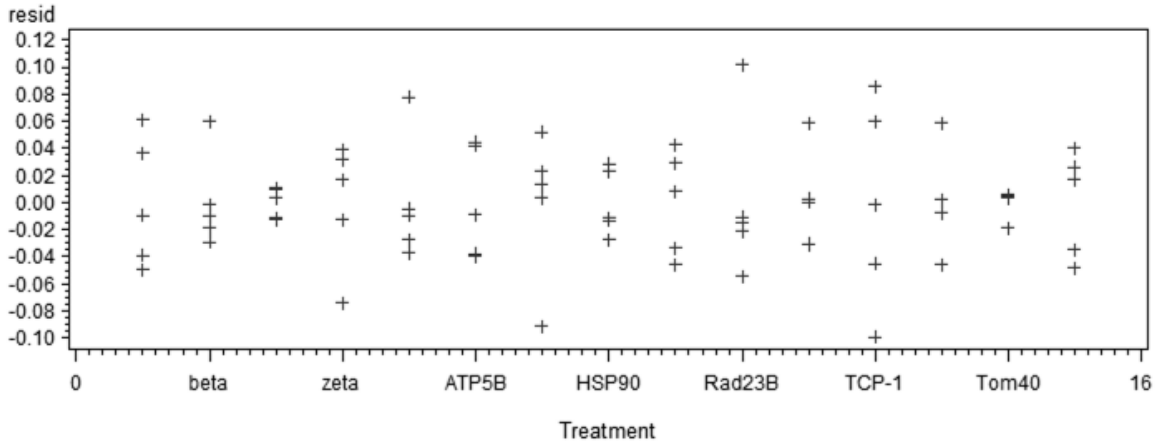

Residual Plot for 4.5S RNA

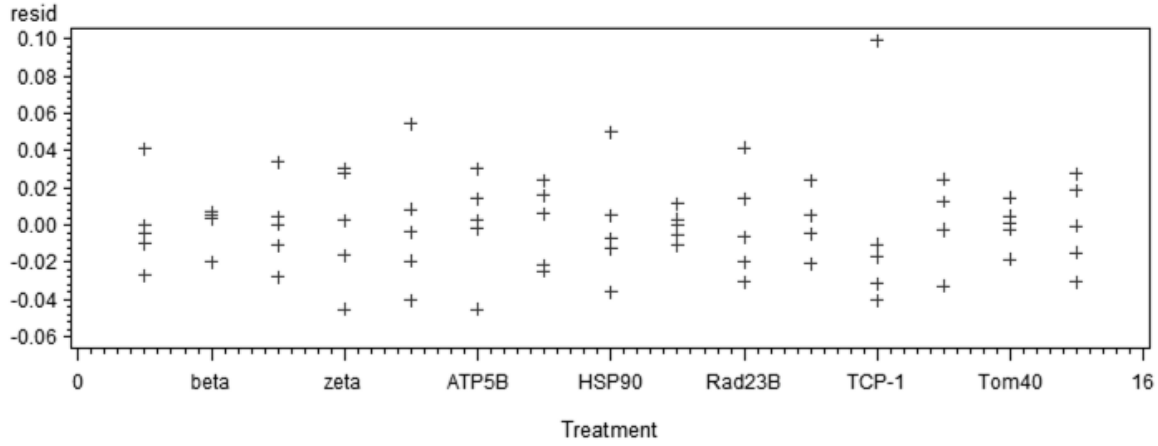

Residual Plot for 5S rRNA

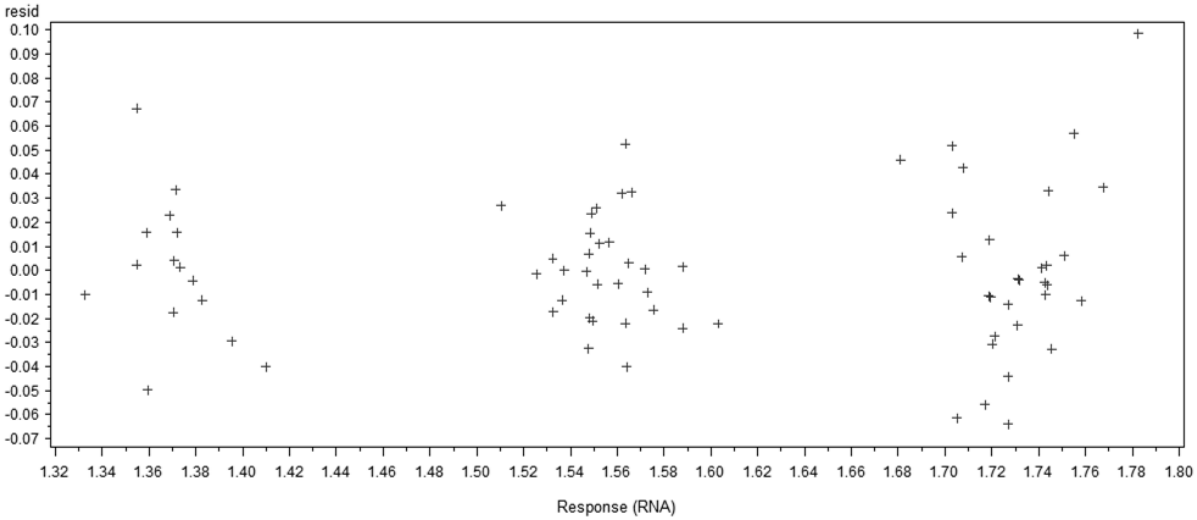

Residual Plot for MRP

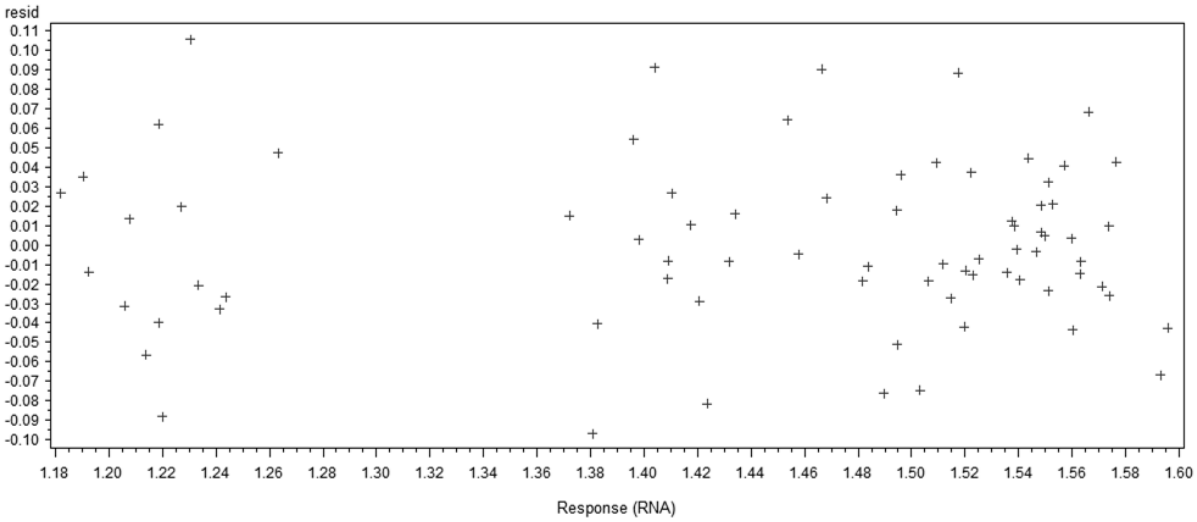

Residual Plot for RNASE P

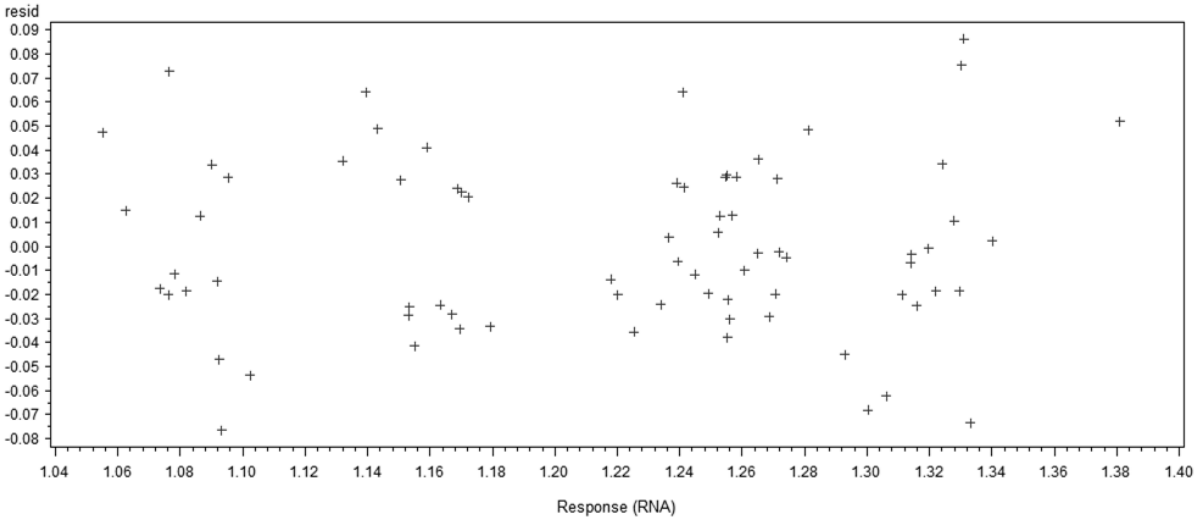

Residual Plot for 5.8S rRNA

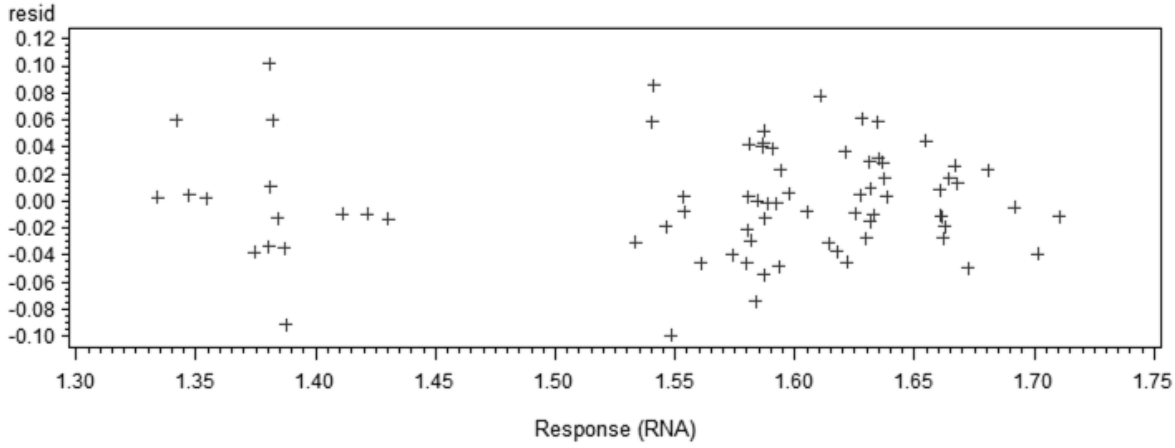

Residual Plot for 4.5S RNA